

Nucleation of Cavities in Gels

A DISSERTATION
SUBMITTED TO THE FACULTY OF THE GRADUATE SCHOOL
OF THE UNIVERSITY OF MINNESOTA
BY

Robert David Foldes

IN PARTIAL FULFILLMENT OF THE REQUIREMENTS
FOR THE DEGREE OF
Doctor of Philosophy

Prof. Ronald Siegel

August, 2017

© Robert David Foldes 2017
ALL RIGHTS RESERVED

Acknowledgements

I am thankful to many people who helped, supported and encouraged me throughout my years as a PhD student.

I would like to start by thanking my adviser, Prof. Ronald Siegel, for his mentorship on my thesis and for his support. His patience, motivation, knowledge and advice helped me through my research and in the writing of this thesis. I really enjoyed working with him and he was a great adviser to me.

I would like to thank the University of Minnesota and the School of Mathematics for the opportunity to conduct this research and for helping me grow in mathematics and beyond. I would like to extend a special thank you to Prof. Richard McGehee who believed in me since the start, to Dean Chris Cramer for his support and to Ms. Jan Morse for all her continuous help. I would also like to greatly thank the Luxembourg National Research Fund for supporting this project.

Finally, I would like to thank my family and my friends who have always been there for me, especially my parents.

Dedication

To Zsuzsi, Kati and Gyuri.

Abstract

Many implantable devices are made of synthetic polymers which upon insertion absorb water, causing the polymer to swell and form a gel (mixture of solid and fluid). Since the swelling leads to an expansion of the polymer, a gel is considered to be a compressible material. A high concentration of stress due to the swelling may lead to the nucleation and growth of cavities within the gel, which is likely to cause the debonding of the material from the support it is attached to. In this dissertation, we focus on the cavitation in a gel occupying a spherical domain, subject to either displacement boundary conditions or free swelling. We consider a total free energy of the gel accounting for the elasticity of the polymer and for the mixing between polymer and fluid, called the Flory-Huggins energy. In addition to penalizing gel deformation, the free energy represents competing effects of entropy that favours mixing, polymer-polymer and fluid-fluid interaction forces. We study the material properties necessary to allow for a nucleation of cavities and analyze radially symmetric deformations.

Contents

Acknowledgements	i
Dedication	ii
Abstract	iii
List of Tables	vii
List of Figures	viii
1 Introduction	1
1.1 Phenomenology	1
1.2 Literature Review	2
1.2.1 Gels	3
1.2.2 Cavitation	3
1.2.3 Debonding	5
1.3 Dissertation Overview	6
2 Mathematical Prerequisites	8
2.1 Nonlinear Elasticity	8
2.1.1 Kinematics	8
2.1.2 Mechanical Principles	11
2.2 Sobolev Spaces	14
2.3 Calculus of Variations	15
2.3.1 Variational approach	16

2.3.2	Existence of Minimizers	21
2.4	Cavitation in Nonlinear Elasticity	25
3	Gels	28
3.1	Introduction	28
3.1.1	Definition	28
3.1.2	Mixture Theory	29
3.2	Energy	32
3.2.1	Elastic Energy Potential	32
3.2.2	Flory-Huggins Energy	33
3.2.3	Dimensionless Energy Quantities	39
3.2.4	Total Energy	39
3.2.5	Cavity Surface Energy	40
4	Radial Energy Minimizers	42
4.1	Existence of Minimizer	42
4.2	Euler-Lagrange Equations	44
4.3	Minimizing Solutions	49
4.3.1	Boundary Conditions	49
4.3.2	Solution without Cavity	50
4.3.3	Solution with Cavity	52
5	Stress Fields	56
5.1	Configuration and Gel Model	56
5.2	Linearization	58
5.3	Linearized Solution	60
5.3.1	Displacement Boundary Conditions	60
5.3.2	Dead-load Traction Boundary Conditions	61
5.4	Reverse Linearization	61
5.4.1	Linearization	61
5.4.2	First Variation	63
5.5	Numerical Results	64
5.5.1	Problem Setup	64

5.5.2	Parameters	65
5.5.3	Results	66
5.6	Stresses in Spherical Caps	72
5.6.1	Configuration	73
5.6.2	Numerical Simulations	75
6	Conclusion and Discussion	78
6.1	Summary	78
6.2	Results	79
6.3	Outlook	80
6.3.1	Experiments	80
6.3.2	Total Free Energy	81
6.3.3	Geometry	81
6.3.4	Time-dependence	82
	References	83
	Appendix A.	86
A.1	Operations on Determinants and Traces	86
A.2	Deformation Mapping	88
A.2.1	Deformation Gradient	88
A.2.2	Operations in Spherical Coordinates	90
A.2.3	Computations in the Reference Configuration	91
A.3	Set of Parameters	94

List of Tables

5.1	Error between r and r_1 for Different $\delta_1 = 0.1$ and $\delta_2 = 0.01$	67
A.1	List of Essential Parameters in Thesis	94

List of Figures

2.1	Mapping between Reference and Deformed Configurations	9
3.1	Elastomer Gel [29]	29
3.2	Gel Mixture, Polymer Chains (Black) and Solvent Molecules (Gray) . .	29
3.3	Lattice Representation for Components and Mixture (Source: Wikipedia)	34
3.4	Interaction of Neighboring Molecules (Source: MIT OCW 3.012 Lect. 24)	36
4.1	Cavity Formation through Phase Separation	54
5.1	Reference Radial Deformations and Strains for Different Stretches . . .	66
5.2	Reference Radial Stresses for Different Stretches	67
5.3	Radial Stresses with Modified Material Parameters for Different Stretches	68
5.4	Radial Stresses with Modified Material Configuration for Different Stretches	68
5.5	Reference Radial Stress at Outer Boundary for Different Stretches . . .	69
5.6	Reference Energy-Stress Relation for Different Stretches	70
5.7	Reference Energy Compared to Initial and Radial Energies	70
5.8	Reference Relaxed State with Stress-Free Outer Boundary	71
5.9	Relaxed State with Stress-Free Outer Boundary for Increasing χ	72
5.10	Relaxed State with Stress-Free Outer Boundary for Decreasing δ	72
5.11	Spherical Cap (Source: geoweb.princeton.edu/people/simons/PIX) . . .	73
5.12	Spherical Cap Boundaries	74
5.13	Spherical Cap, Displacement Boundary Condition $r(1, \Psi) = 1.1$	76
5.14	Spherical Cap, Displacement Boundary Condition $r(1, \Psi) = 2$	76
5.15	Spherical Cap, Traction Boundary Condition $\mathbf{p}_1 \cdot \mathbf{N} = 0.01$	77
5.16	Spherical Cap, Traction Boundary Condition $\mathbf{p}_1 \cdot \mathbf{N} = 0.05$	77
A.1	General Constellation (Source: Wikiversity)	88

Chapter 1

Introduction

1.1 Phenomenology

This dissertation studies mathematical and physical aspects of cavitation in gels. We consider a gel to be a mixture of a nonlinear elastic solid, more specifically a polymer, and a fluid. We assume that each point in the domain is occupied by only solid and fluid, at respective volume fraction ratios ϕ_1 and ϕ_2 , with $0 \leq \phi_1, \phi_2 \leq 1$ and $\phi_1 + \phi_2 = 1$. Many implantable devices are made of synthetic polymers, which upon insertion absorb water, causing the polymer to swell and form a gel. Cavities in nonlinear elastic materials occur when the deformation map becomes singular, and such that, a point is mapped into a surface (cavity surface).

In this thesis, we consider the total free energy of a gel to account for the elasticity and compressibility of the polymer as well as for the mixing between polymer and fluid. We study equilibrium configurations, with and without cavity, by minimizing the energy, subject to appropriate boundary conditions.

On the one hand, we determine sufficient conditions on the energy to allow for singular solutions of the corresponding Euler-Lagrange equations. Namely, there are two competing minimizers to the total energy, one with and one without cavity. The cavity solution occurs when the associated energy is lower than that for the solution without cavity. We note that we use the term “energy” in this dissertation to refer to the free energy.

On the other hand, cavities form when there is a local concentration of extentional

stress that causes the material to break and form a cavity, so as to reach relaxation. This is especially true for gels as a critical stress may lead to the break of a polymer chain, which leads to phase separation. Therefore, we derive the stress fields associated to the minimizers of the energy in the case of a fixed, infinitesimal core at the center of the gel. We study the physically relevant parameters of the system and their impact on the stresses, especially around the aforementioned core.

Analysis of cavities in gels presents new opportunities and challenges compared to nonlinear elasticity. First, in nonlinear elastic materials, a cavity may occur when an applied displacement or traction on the boundary reaches a critical value. Whereas these may also cause cavitation in gels, the genuine phenomenon in gels is cavitation by swelling. An almost dry gel placed into water swells and increases volume, by as much as 500 times. At a given temperature, the gel in the presence of fluid is assumed to achieve equilibrium at a preferred volume fraction $0 < \phi_1^* < 1$. Hence, although an elastic, almost dry body may be at equilibrium away from the fluid, this state becomes unstable as soon as fluid is available. This means that the gel swells to relax the residual stress.

Second, the gel's permeability may allow the fluid to fill the cavity, in which case cavitation is a phase separation where solid and fluid completely separate. Mass balance provides additional information, which ultimately helps determine the cavity radius.

In either case, a cavity forms to release stress, hence lowering the energy of the material and causing the traction on the cavity boundary to be zero. In this dissertation, we focus on the cavitation in a gel occupying a spherical domain, with spherically symmetric displacement boundary conditions, as well as cavitation of a swelling gel.

1.2 Literature Review

We start with an in-depth review of previous research relevant for the topic of this dissertation. We review studies on gels, on the nucleation and growth of cavities in an elastic material and on the phenomena of debonding, both from a theoretical and an experimental point of view.

1.2.1 Gels

Previous research, as in [1], [2], [3] or [4], addresses the modeling of gel dynamics within a fluid environment. In particular, [1] determines sufficient conditions on the energy of a gel to ensure a global minimizer, and presents a mixed finite element method for a gel model. In contrast to the static analysis in [1], the authors in [2] address the gel dynamics. They discuss a hyperbolic free boundary problem of gel swelling and analyze the effects of the inertia terms. In addition, [3] develops a model for a polyelectrolyte gel to express the permeability properties of the interface between gel and surrounding fluid. Finally, [4] treats the linearization of the governing equations for a gel and studies the stability of equilibrium solutions for different boundary conditions.

From a more physical point of view, the authors in [5] study the kinematics of gel swelling. They determine the size of the gel after swelling in terms of the characteristic time of swelling, and compare the theoretical results to values obtained experimentally. In a more specific work, [6] addresses the swelling dynamics of a gel undergoing a volume transition. In particular, the authors perform both analytical and numerical computations, and determine the characteristic time for the swelling process in 1D.

From a different perspective, [7] directly links the network's change of shape, responsible for the time-dependent behavior, to viscoelasticity. The paper specifically studies the theory behind this material-specific property. For instance, it discusses some macroscopic observations due to material-specific time and length, and provides explicit conditions for the timing of viscoelastic relaxation.

In [8], the authors investigate pattern formations of a viscoelastic material, such as fingering or crack propagation, through tunable material properties, from a viscous liquid to an elastic solid. Their experiments explain instabilities observed in a material with viscoelastic properties, which determine the mechanism when the material is detached from a rigid substrate.

1.2.2 Cavitation

In an early work on cavitation, Gent and Tompkins experimentally investigate in [10] the nucleation and growth of gas bubbles in crosslinked elastomers. They determine the necessary condition for the formation of the bubble, namely that the gas supersaturation

pressure has to exceed a critical value. They also study the growth of the bubbles and look at the amount of bubbles possibly present. Modern studies of cavitation in solids started in 1982 with [9], based on the experiments in [10]. Ball studies three-dimensional radial deformations in nonlinear elasticity for homogeneous isotropic materials, both compressible and incompressible. Under specific growth conditions on the stored energy, he shows that a radial discontinuous minimizing deformation bifurcates from a uniform expansion at a critical value of boundary displacement or traction, leading to cavitation.

Following the work of Ball, the study on cavitation in nonlinear, elastic, spherical materials for radial deformations has been extended in several directions. Sivaloganathan and Spector postulate radial cavitating deformations with specific properties in [11], and construct equilibrium equations satisfied by them. These ordinary differential equations correspond to the variational problem of minimizing the material's energy. In [12] and [13], the authors consider incompressible composite elastic materials and study void nucleation for isotropic and anisotropic cases. Both studies use a uniform radial dead-load traction at the boundary, resulting in a bifurcation problem where a cavity forms once a critical value of the pressure is attained. They also analyze the effect of the cavity on possible debonding at the interface of the two composite materials. In [14], Pence and Tsai extend the research to an elastic body composed of a uniformly swelling compressible shell and of a non-swelling incompressible core. By prescribing traction continuity on the interface and traction-free conditions on the outer boundary, they observe two phenomena. One is the appearance of discontinuous solutions at the interface without cavitation in the core, and the other one is the formation of a cavity at the origin, meaning inside the incompressible material. In [15], Horgan studies only compressible materials by considering a special form for the energy. He determines the critical value of the displacement at the boundary for which the formation of a cavity is possible.

All of the above research focuses on cavitation in elastic materials with the restriction to radially symmetric deformation. The full three dimensional case was first addressed by Muller and Spector in [16], without the restriction to spherical domains and deformations. Moreover, they consider a surface penalizing term in the energy, accounting for both the total area cavities present and the area of the body's surface. In order to correctly account for these surfaces, for instance by preventing the cavity from being

filled up with material from another region of the body, they add an invertibility assumption. In [17], Henao and Mora-Corral take a slightly different approach to model the general case. They add a term to the total free energy of the body that accounts for the total area created by cavitation as well as fracture. This method has the advantage of not requiring the invertibility assumption of Muller and Spector in order to prove the existence of minimizers. Another relevant aspect of their work is the ability to treat two types of cavitation mechanisms: the one with cavities generating at locations with impurities or defects, and the more challenging case without the requirement of preexisting cavities.

This review has so far only focused on the analysis of cavitation in nonlinear elasticity. However, the deformation of gels, possibly resulting in the nucleation and the growth of cavities, is dependent on time. Unfortunately, time evolution studies of cavities are even more scarce than the static work before. In [18], Pericak-Spector and Spector study radial cavity growth in an elastic material, leading to a hyperbolic problem. More recently, Henao and Serfaty analyze the effect of a given deformation on an initial small hole in the domain in [19], mapping it into a macroscopically visible cavity.

1.2.3 Debonding

Detachment of a thin film, subject to an increase of internal stresses, from a substrate is known as debonding. A well accepted, although poorly understood point of view, is that cavities form at the onset of debonding, grow and merge, leading to fracture. In [20], Doi and Yamaguchi postulate that continuous stressing of a gel during the debonding process results in the nucleation of a cavity, once a critical pressure is reached. They propose a viscoelastic model to study its growth and evolution, as well as present simulations under strong simplifying assumptions. Moreover, [21] experimentally examines the growth dynamics of cavities during the early stages of debonding. The authors consider different materials, all of which exhibit viscoelastic properties. Their experiments examine, among other things, total projected size, average shape and growth rate of the cavities.

From a different perspective, [22] uses a variational approach to examine the formation of cracks and the phenomena of debonding. They consider an elastic film, bonded to a stiff substrate, and they impose displacement boundary conditions. By energy

minimization, they recreate certain experimental observations, such as the periodicity of transverse cracks or the peripheral debonding of each regular segment.

1.3 Dissertation Overview

This dissertation is structured as follows: In this chapter, Chapter 1, we gave an overview of the topics in this dissertation and a brief motivation for the importance of this research. We also reviewed past studies in the areas of gels and cavitation that are fundamental for this dissertation.

In Chapter 2, we review important mathematical notions, which serve as tools for the upcoming work, including the statement of important theorems and concepts. We start with a review on nonlinear elasticity, in particular the kinematics and mechanical principles such as balance laws. We continue with an introduction to Sobolev spaces, followed by fundamental results in the Calculus of Variations. This includes details on the variational approach and the existence results for minimizers of specific functionals. We conclude the chapter with an overview of cavitation in nonlinear elasticity by giving a mathematical summary on the work of John Ball in [9].

Chapter 3 is devoted to the development and analysis of the gel model used in this dissertation. First, we specify the definition of a gel and of its key features we aim to capture in our model. Then, we turn to describing the main characteristics of the gel through its energy, for instance elasticity, compressibility and interaction of polymer and solvent components in the gel. This latter property is given by the so called Flory-Huggins free energy of mixing, for which we provide a physical derivation. Finally, we discuss the importance for the right choice of a polymer volume fraction.

In Chapter 4, we focus on the study of deformations that minimize the total free energy of the gel described in Chapter 3. We give existence results for energy minimizers, with or without the presence of a cavity after deformation. We use the variational approach to derive the Euler-Lagrange equations for the gel, in particular for radially symmetric deformations. We define different types of boundary conditions that appropriately model both cavity and no-cavity scenarios. We first consider the case of pure expansion without cavity, before describing the concept we use to model the nucleation of a cavity.

In Chapter 5, we approach cavitation from a physical point of view. We investigate the stress fields across the material, in particular around the origin. We assume a fixed core in the center to avoid the singularity. We numerically solve the Euler-Lagrange equations for different boundary conditions to determine the stresses related to the minimizing solutions. The focus is on a stress-free boundary condition at the outside of the body, which corresponds to an equilibrium state after swelling. Furthermore, we analyze the impact of the main gel parameters on the stress field and the total free energy of the gel. Finally, we provide an analysis of the stress fields in a gel occupying a cap domain glued a substrate by its flat surface.

The last part of the dissertation, Chapter 6, is devoted to a discussion of the results from the thesis. In particular, we assess the outcomes of both the mathematical and the physical approaches to cavitation in gels. Finally, we propose an outlook on possible future directions.

Chapter 2

Mathematical Prerequisites

2.1 Nonlinear Elasticity

In this section, we present an outline of the main concepts in nonlinear elasticity, based on work by M. E. Gurtin, E. Fried and L. Anand in [23] as well as by E. Tadmor, R. Miller and R. Elliott in [24].

2.1.1 Kinematics

We start by introducing a general notation. Let $\{\mathbf{e}_1, \mathbf{e}_2, \dots, \mathbf{e}_n\}$ be the canonical basis in \mathbb{R}^n , for $n \in \mathbb{N}^*$. We define a body to be a set of points, called particles. Let $\Omega_0 \subset \mathbb{R}^n$ be the default or reference configuration of this given body, and let $\mathbf{X} = X_1\mathbf{e}_1 + X_2\mathbf{e}_2 + \dots + X_n\mathbf{e}_n \in \Omega_0$ be the position of a particle in this body, where (X_1, X_2, \dots, X_n) are its Cartesian coordinates.

In particular, we introduce special coordinates in \mathbb{R}^3 that are of relevance in the upcoming work. For $n = 3$, we define $\hat{\mathbf{X}} := (R, \Theta, \Psi)$ to be the set corresponding to the spherical coordinates of \mathbf{X} . We consider the radial coordinate $R \in (0, 1)$ to be a dimensionless variable. The corresponding radial coordinate with dimension will be denoted by $\tilde{R} := R_0 R$, where R_0 gives the dimension of the radius. Furthermore, we have that $\Theta \in (0, \pi)$ and $\Psi \in (0, 2\pi)$.

Let $\Phi : \Omega_0 \rightarrow \Omega$ be the deformation map which takes $\mathbf{X} \in \Omega_0$ to $\mathbf{x} \in \Omega$, with $\mathbf{x} = (x_1, \dots, x_n)$, where $\Omega \subset \mathbb{R}^n$ is called the deformed configuration. For $n = 3$, $\hat{\mathbf{x}} = (r, \theta, \psi)$ is the position of a particle in spherical coordinates in the deformed configuration. Let

$\Upsilon := \Phi^{-1} : \Omega \rightarrow \Omega_0$ be the inverse of the deformation map. For simplicity, we use $g := \Upsilon$, so we have $R = g(r)$ and $1 = g_{,r}r_{,R}$, presuming radial symmetry.

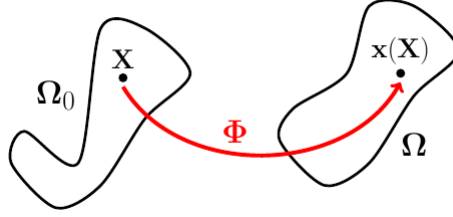


Figure 2.1: Mapping between Reference and Deformed Configurations

We speak about the Lagrangian or material description when we express the position and physical properties (e.g. velocity, acceleration, etc.) of a particle $\mathbf{x} = \mathbf{x}(\mathbf{X}) = \Phi(\mathbf{X})$ in terms of the reference coordinates $\mathbf{X} \in \Omega_0$. The Lagrangian view describes one single particle as it is affected by the deformation. On the other hand, the Eulerian or spatial description focuses on the properties of a particle at a given point in space $\mathbf{X} = \mathbf{X}(\mathbf{x}) = \Upsilon(\mathbf{x})$, regardless which particle in the reference configuration occupies that space after a given deformation.

Definition 2.1.1. We define the deformation tensor, also called the deformation gradient, by

$$\underline{\mathbf{F}} := \frac{\partial \Phi(\mathbf{X})}{\partial \mathbf{X}} = \frac{\partial \mathbf{x}(\mathbf{X})}{\partial \mathbf{X}}. \quad (2.1)$$

Explicit computations for the deformation gradient are found in the appendix for spherical coordinates. In this work, we use two different notations interchangeably for the deformation gradient, namely

$$\underline{\mathbf{F}} = \nabla \mathbf{x}.$$

We note that $\underline{\mathbf{F}}^T = \underline{\mathbf{F}}$ if $\underline{\mathbf{F}}$ is a diagonal matrix, where $\underline{\mathbf{F}}^T$ denotes the transpose of $\underline{\mathbf{F}}$. We are only looking at orientation-preserving deformations, meaning that we exclude inversion. By definition, this implies the orientation-preserving condition for the determinant of the deformation gradient:

$$\det \underline{\mathbf{F}} > 0, \quad \text{for all } \mathbf{X} \in \Omega_0. \quad (2.2)$$

The change of volume of the material from the reference to the deformed configuration is expressed by the *Jacobian*, denoted by J , of the deformation. It is derived from the local volume ratio of deformed volume to reference volume and is given by

$$J = \det \underline{\mathbf{F}}. \quad (2.3)$$

We say that the material is *incompressible* if and only if there is no change of volume occurring at any point during the deformation. Hence, material incompressibility implies that $\det \underline{\mathbf{F}} \equiv 1$, so that (2.3) yields

$$J \equiv 1. \quad (2.4)$$

Otherwise, the material is called compressible and we have that $J \neq 1$. Next, we can rewrite the deformation gradient as the product of two specific deformation tensors according to the following result:

Proposition 2.1.2. *Polar decomposition theorem*

$$\underline{\mathbf{F}} = \underline{\mathbf{R}} \underline{\mathbf{U}} = \underline{\mathbf{V}} \underline{\mathbf{R}}.$$

We have that the tensor $\underline{\mathbf{R}}$ describes a rotation and is orthogonal, that is $\underline{\mathbf{R}} \underline{\mathbf{R}}^{-1} = \underline{\mathbf{R}}^{-1} \underline{\mathbf{R}} = \underline{\mathbf{I}}$. Moreover, $\underline{\mathbf{U}}$ and $\underline{\mathbf{V}}$ are symmetric tensors and are called the right and left stretch tensors, respectively.

To see why $\underline{\mathbf{U}}$ and $\underline{\mathbf{V}}$ represent stretches, we have the following proposition.

Proposition 2.1.3. *Principal Stretches and Principal Directions*

$$\underline{\mathbf{U}} = \sum_{i=1}^n \kappa_i \mathbf{r}_i \otimes \mathbf{r}_i \quad \text{and} \quad \underline{\mathbf{V}} = \sum_{i=1}^n \kappa_i \mathbf{l}_i \otimes \mathbf{l}_i.$$

We have that κ_i are the eigenvalues of both $\underline{\mathbf{U}}$ and $\underline{\mathbf{V}}$, representing the principal stretches. The vectors \mathbf{r}_i and \mathbf{l}_i are the right and left principal directions, respectively, and correspond to the eigenvectors of $\underline{\mathbf{U}}$ and $\underline{\mathbf{V}}$, respectively.

Definition 2.1.4. We define the left Cauchy-Green tensor to be the matrix

$$\underline{\mathbf{B}} := \underline{\mathbf{F}} \underline{\mathbf{F}}^T. \quad (2.5)$$

We have that $\underline{\mathbf{B}} = \underline{\mathbf{F}}^2$ if $\underline{\mathbf{F}}$ is diagonal. Similarly, we define the right Cauchy-Green tensor to be $\underline{\mathbf{C}} := \underline{\mathbf{F}}^T \underline{\mathbf{F}}$. In the upcoming work, we only use the left Cauchy-Green tensor.

Definition 2.1.5. The first three invariants of a matrix $\underline{\mathbf{B}} \in \mathbb{M}^{n \times n}$ are defined as

$$I_1 = \text{tr} \underline{\mathbf{B}}, \quad I_2 = \frac{1}{2} [(\text{tr} \underline{\mathbf{B}})^2 - \text{tr} \underline{\mathbf{B}}^2], \quad I_3 = \det \underline{\mathbf{B}}. \quad (2.6)$$

These three invariants physically represent stretches exerted on the body during a deformation, where the index stands for the dimension. I_1 represents a linear stretch, I_2 stands for a surface stretch and I_3 invokes a volume stretch. We note that by definition of $\underline{\mathbf{B}}$ and $\underline{\mathbf{C}}$ and by the properties of the trace and the determinant, the left and right Cauchy-Green tensors have the same invariants.

2.1.2 Mechanical Principles

We continue by recalling certain fundamental principals such as balance laws.

Axiom 2.1.6. Balance of mass

Let $\rho_R = \rho_R(\mathbf{X})$ and $\rho_D = \rho_D(\mathbf{x})$ be the mass densities of a body in the reference and deformed configurations, respectively. Then the total mass of the body is conserved under deformation in a closed system, i.e.

$$\int_{\Omega_0} \rho_R(\mathbf{X}) d\mathbf{X} = \int_{\Omega} \rho_D(\mathbf{x}) d\mathbf{x}. \quad (2.7)$$

Next, we consider contact and body forces, which an environment exerts on the boundary and the interior of a body.

Definition 2.1.7. Let \mathcal{S} be a spatial surface, either in the interior of the body or on its boundary. Let $\mathbf{n} = \mathbf{n}(\mathbf{x})$ be the unit outer normal vector to \mathcal{S} at a point \mathbf{x} in the deformed configuration.

1. A contact force, denoted by $\mathbf{t} = \mathbf{t}(\mathbf{x}, \mathbf{n})$, is a force per unit area exerted across \mathcal{S} on the body on the 'negative' side of \mathcal{S} by the body on the 'positive' side.
2. A body force, denoted by $\mathbf{b} = \mathbf{b}(\mathbf{x})$, is a force per unit volume exerted by the environment on the body at the point \mathbf{x} .

We note that by Cauchy's lemma, the contact force satisfies the action-reaction principle, that is

$$\mathbf{t}(\mathbf{x}, -\mathbf{n}) = -\mathbf{t}(\mathbf{x}, \mathbf{n}). \quad (2.8)$$

These definitions allow us to define two further fundamental balance laws from continuum mechanics, namely

Axiom 2.1.8. Balance of Linear Momentum

$$\int_{\partial\Omega} \mathbf{t}(\mathbf{x}, \mathbf{n}) ds + \int_{\Omega} \mathbf{b}(\mathbf{x}) d\mathbf{x} = 0. \quad (2.9)$$

Axiom 2.1.9. Balance of Angular Momentum

$$\int_{\partial\Omega} \mathbf{r}(\mathbf{x}) \times \mathbf{t}(\mathbf{x}, \mathbf{n}) ds + \int_{\Omega} \mathbf{r}(\mathbf{x}) \times \mathbf{b}(\mathbf{x}) d\mathbf{x} = 0, \quad (2.10)$$

where $\mathbf{r} = \mathbf{r}(\mathbf{x})$ is the position vector of \mathbf{x} with respect to the origin.

An important result following these two balance laws is the theorem below.

Theorem 2.1.10. Cauchy's Theorem

There exists a spatial tensor field, denoted by $\underline{\mathbf{T}}$ and called the Cauchy stress, such that

$$\mathbf{t}(\mathbf{n}) = \underline{\mathbf{T}}\mathbf{n}. \quad (2.11)$$

This allows us to define the First Piola-Kirchhoff stress by

$$\underline{\mathbf{P}} = (\det \underline{\mathbf{F}}) \underline{\mathbf{T}} \underline{\mathbf{F}}^{-T}. \quad (2.12)$$

Finally, we also define the Second Piola-Kirchhoff stress by

$$\underline{\mathbf{S}} = \underline{\mathbf{F}}^{-1} \underline{\mathbf{P}}. \quad (2.13)$$

Remark 1. We note that the Second Piola-Kirchhoff stress is a force per unit area in the reference configuration, whereas the Cauchy stress is a force per unit area in the deformed configuration. On the other hand, the First-Piola Kirchhoff stress is defined as the force per unit reference area mapped back to the reference configuration.

Using Cauchy's theorem and the divergence theorem, we have that

$$\int_{\partial\Omega} \mathbf{t}(\mathbf{x}, \mathbf{n}) ds = \int_{\Omega} \operatorname{div} \underline{\mathbf{T}} d\mathbf{x}.$$

This identity leads to another important result, the local balance of linear momentum

$$\operatorname{div} \underline{\mathbf{T}} + \mathbf{b} = 0. \quad (2.14)$$

We can also derive a similar local form for the balance of angular momentum, given by

$$\underline{\mathbf{T}} = \underline{\mathbf{T}}^T. \quad (2.15)$$

We note that the first Piola-Kirchhoff stress is not necessarily symmetric, unlike the Cauchy stress, however the Second Piola-Kirchhoff stress is. Finally, we have that the Cauchy and Piola-Kirchhoff stresses are characterized by the deformation gradient $\underline{\mathbf{F}}$, a relation we call constitutive equations. Mathematically, we translate this as follows:

Proposition 2.1.11. Constitutive equations

$$\underline{\mathbf{T}} = \hat{\underline{\mathbf{T}}}(\underline{\mathbf{F}}), \quad \underline{\mathbf{P}} = \hat{\underline{\mathbf{P}}}(\underline{\mathbf{F}}), \quad \underline{\mathbf{S}} = \hat{\underline{\mathbf{S}}}(\underline{\mathbf{F}}), \quad (2.16)$$

where $\hat{\underline{\mathbf{T}}}$, $\hat{\underline{\mathbf{P}}}$ and $\hat{\underline{\mathbf{S}}}$ are called response functions defined in terms of the deformation gradient.

We say that a material in the reference configuration is homogeneous if its response function is independent of $\mathbf{X} \in \Omega_0$. We conclude this section by introducing the principle of material frame-indifference.

Definition 2.1.12. Let \mathcal{F} be a frame of reference in the observed space, i.e. in the deformed configuration, let $\underline{\mathbf{Q}}$ be an orthogonal linear tensor, i.e. $\underline{\mathbf{Q}} \underline{\mathbf{Q}}^T = \underline{\mathbf{Q}}^T \underline{\mathbf{Q}} = \underline{\mathbf{I}}$, and let \mathbf{l} be a translation. A change of frame $\mathcal{F} \rightarrow \mathcal{F}^*$ in the observed space transforms a spatial point $\mathbf{x} \in \Omega$ into another point $\mathbf{x}^* \in \Omega$ through

$$\mathbf{x}^* = \underline{\mathbf{Q}}\mathbf{x} + \mathbf{l}.$$

We now give the necessary conditions for tensors to remain the same after a change of frame, which we refer to as frame-indifferent or objective tensors.

Definition 2.1.13. Objective tensors

1. A zeroth-order tensor s , or scalar, is objective if $s^* = s$ for any change of frame.
2. A first-order tensor \mathbf{v} , or vector, is objective if $\mathbf{v}^* = \underline{\mathbf{Q}}\mathbf{v}$ for any change of frame.
3. A second-order tensor $\underline{\mathbf{M}}$, or vector, is objective if $\underline{\mathbf{M}}^* = \underline{\mathbf{Q}} \underline{\mathbf{M}} \underline{\mathbf{Q}}^T$ for any change of frame.

For instance, the Cauchy stress tensor is frame-indifferent, as we can show that $\underline{\mathbf{T}}^* = \underline{\mathbf{Q}} \underline{\mathbf{T}} \underline{\mathbf{Q}}$.

2.2 Sobolev Spaces

This section serves as a brief recall on the notion of Sobolev spaces and the main definitions relevant to the work later. They are based on the work by L. C. Evans in [25] where the reader can learn more about important theorems on Sobolev spaces. We introduce the following notation used throughout this section, unless stated otherwise. Let us assume Ω_0 to be an open subset of \mathbb{R}^n and let $1 \leq p \leq \infty$ be fixed. We start by recalling some basic definitions from functional analysis.

Definition 2.2.1. Banach Spaces

A Banach space X is a normed linear space that is complete.

Definition 2.2.2. Hilbert Spaces

A Hilbert space H is a Banach space equipped with an inner product that generates the norm.

Definition 2.2.3. L^p Spaces

We define a Lebesgue space, and denote it by L^p , as the space given by

$$L^p(\Omega_0) = \{f : \Omega_0 \rightarrow \mathbb{R} \text{ measurable} \mid \|f\|_{L^p(\Omega_0)} < \infty\},$$

where the associated norms to $L^p(\Omega_0)$ for $1 \leq p < \infty$ and $p = \infty$, respectively, are given by

$$\|f\|_{L^p(\Omega_0)} = \left(\int_{\Omega_0} |f|^p d\mathbf{X} \right)^{\frac{1}{p}}, \quad \|f\|_{L^\infty(\Omega_0)} = \text{ess sup}_{\Omega_0} |f|.$$

To define a Sobolev space, we proceed by recalling that a vector of the form $\alpha = (\alpha_1, \dots, \alpha_n)$, with $\alpha_i \in \mathbb{N}$ for $i = 1, \dots, n$, is called a multiindex of order $|\alpha| = \sum_{i=1}^n \alpha_i$. Given such an α , we define the partial derivative of order $|\alpha|$ for a function $x : \Omega_0 \rightarrow \mathbb{R}$ to be

$$D^\alpha x(\mathbf{X}) := \frac{\partial^{|\alpha|} x(\mathbf{X})}{\partial X_1^{\alpha_1} \dots \partial X_n^{\alpha_n}} = \partial_{X_1}^{\alpha_1} \dots \partial_{X_n}^{\alpha_n} x.$$

Definition 2.2.4. Sobolev Spaces

Let $x : \Omega_0 \rightarrow \mathbb{R}$, let $k \in \mathbb{N}$ and let α be a multiindex. We define a Sobolev space to be

$$W^{k,p}(\Omega_0) = \{x \in L^p(\Omega_0) \mid D^\alpha x \in L^p(\Omega_0) \quad \forall |\alpha| \leq k\},$$

and the associated norms to $W^{k,p}(\Omega_0)$ for $1 \leq p < \infty$ and $p = \infty$, respectively, are given by

$$\|x\|_{W^{k,p}(\Omega_0)} = \left(\sum_{|\alpha| \leq k} \|D^\alpha x\|_{L^p(\Omega_0)}^p \right)^{\frac{1}{p}}, \quad \|x\|_{W^{k,\infty}(\Omega_0)} = \max_{|\alpha| \leq k} \|D^\alpha x\|_{L^\infty(\Omega_0)}.$$

Definition 2.2.5. The closure of $C_c^\infty(\Omega_0)$ in $W^{k,p}(\Omega_0)$ is denoted by $W_0^{k,p}(\Omega_0)$.

We have that a Sobolev space is a Banach space. We see that Sobolev spaces are subspaces of Lebesgue spaces as we restrict the derivatives of L^p functions to L^p as well. We summarize this observation for $n = 1$, that is $\Omega_0 \subset \mathbb{R}$:

$$C_0^\infty(\Omega_0) \subset \dots \subset W^{2,p}(\Omega_0) \subset C^1(\bar{\Omega}_0) \subset W^{1,p}(\Omega_0) \subset C(\bar{\Omega}_0) \subset L^\infty(\Omega_0) \subset \dots \subset L^1(\Omega_0).$$

Next, we define convergence for Sobolev spaces.

Definition 2.2.6. Convergence in $W^{k,p}$

Let $\{x_m\}_{m=1}^\infty$ be a sequence in $W^{k,p}(\Omega_0)$ and let $x \in W^{k,p}(\Omega_0)$. We say that x_m converges to x in $W^{k,p}(\Omega_0)$, and denote it as $x_m \rightarrow x$ in $W^{k,p}(\Omega_0)$, if

$$\lim_{m \rightarrow \infty} \|x_m - x\|_{W^{k,p}(\Omega_0)} = 0.$$

2.3 Calculus of Variations

In this section, we introduce the variational approach to determine critical points of a functional $I[\cdot]$ in a given reference configuration $\Omega_0 \subset \mathbb{R}^n$. For instance, $I[\cdot]$ may

be the energy functional $E_{tot} = \int_{\Omega_0} \sum_i W_i d\mathbf{X}$, where W_i are different stored energy functions. We determine necessary and sufficient conditions on the functional $I[\cdot]$ to admit a minimizer. The definitions, theorems and methods in this section are based on the work by L. C. Evans in [25] as well as by C. Dacorogna in [26]. Let us assume $n < p < \infty$ for this section, unless otherwise stated.

2.3.1 Variational approach

In this section, we focus on using the principle of the “first variation” to find equations, called *Euler-Lagrange equations*, whose roots are critical points of the functional $I[\cdot]$. We define a smooth function f by

$$f : \Omega_0 \times \mathbb{R}^m \times \mathbb{M}^{m \times n} \rightarrow \mathbb{R}, \quad (2.17)$$

called the *Lagrangian*. An example for a Lagrangian is the energy function W_i . Hence, we consider the functional $I[\cdot]$ to be given by

$$I[\mathbf{x}] := \int_{\Omega_0} f(\mathbf{X}, \mathbf{x}(\mathbf{X}), \nabla \mathbf{x}(\mathbf{X})) d\mathbf{X}, \quad (2.18)$$

where $\mathbf{x} : \Omega_0 \rightarrow \mathbb{R}^m$ is the function we want to minimize for under given conditions. Therefore, we define an admissible set of solutions, denoted by \mathcal{A} . We have that \mathcal{A} is non-empty, and it is given by

$$\mathcal{A} := \{\mathbf{x} \in \mathcal{X} \mid \text{restrictions and boundary conditions}\}, \quad (2.19)$$

where \mathcal{X} is a normed vector space of functions to be determined. One restriction in the upcoming work is the orientation-preserving condition given in (2.2), i.e. $\det \nabla \mathbf{x} > 0$. An example for an admissible set would be

$$\mathcal{A}_1 = \{\mathbf{x} \in W^{1,p} \mid \det \nabla \mathbf{x} > 0, \mathbf{x} = \mathbf{x}_0 \text{ on } \partial\Omega_0\}.$$

Let $\mathbf{x} \in \mathcal{A}$ be a *critical point* of I , that is $\delta I[\mathbf{x}] = 0$ and let $\mathbf{y} \in \mathcal{A}$ be a test function.¹ We define the real valued function $i : \mathbb{R} \rightarrow \mathbb{R}$ by

$$i(t) := I[\mathbf{x} + t\mathbf{y}] = \int_{\Omega_0} f(\mathbf{X}, \mathbf{x} + t\mathbf{y}, \nabla(\mathbf{x} + t\mathbf{y})) d\mathbf{X}, \quad t \in \mathbb{R}. \quad (2.20)$$

¹ A detailed introduction on critical points and differentiability of I , i.e. I' , can be found in [25].

Since \mathbf{x} is a critical point of $I[\cdot]$, we have that $i(t)$ has a extremum at $t = 0$, i.e.

$$i'(0) = 0, \quad (2.21)$$

which we call the *first variation*. This extremum is a minimum, making \mathbf{x} a minimizer, if

$$i''(0) \geq 0, \quad (2.22)$$

called the *second variation*. For the remaining part of this work, we want to exclusively find minimizers of $I[\cdot]$ so that we need (2.22) to be fulfilled.

First variation

We start by computing the first variation (2.21), which will lead us to the Euler-Lagrange equation of the functional I , whose solutions are critical points of I . Recalling (2.20), it follows by linearity that

$$i'(t) = \frac{d}{dt} I[\mathbf{x} + t\mathbf{y}] = \int_{\Omega_0} \frac{d}{dt} (f(\mathbf{X}, \mathbf{x} + t\mathbf{y}, \nabla(\mathbf{x} + t\mathbf{y}))) \, d\mathbf{X}.$$

Let us compute the expression inside the integral explicitly at $t = 0$. First,

$$\begin{aligned} \left. \frac{d}{dt} \right|_{t=0} f(\mathbf{X}, \mathbf{x} + t\mathbf{y}, \nabla(\mathbf{x} + t\mathbf{y})) &= \left. \frac{d}{dt} \right|_{t=0} f(\mathbf{X}, x_i + ty_i, \nabla(x_i + ty_i)), \quad i = 1, \dots, m \\ &= \frac{\partial f}{\partial x_i} y_i + \frac{\partial f}{\partial x_{i,j}} y_{i,j}, \quad i = 1, \dots, m; \, j = 1, \dots, n \\ &= \nabla f \cdot \mathbf{y} + \frac{\partial f}{\partial(\nabla \mathbf{x})} : \nabla \mathbf{y}. \end{aligned}$$

Hence, the integral of $\frac{d}{dt} (f(\mathbf{X}, \mathbf{x} + t\mathbf{y}, \nabla(\mathbf{x} + t\mathbf{y})))$ at $t = 0$ gives $i'(0)$, that is

$$\begin{aligned} i'(0) &= \int_{\Omega_0} \left[\frac{\partial f}{\partial(\nabla \mathbf{x})} : \nabla \mathbf{y} + \nabla f \cdot \mathbf{y} \right] \, d\mathbf{X} \\ &= \int_{\Omega_0} \nabla \cdot \left(\frac{\partial f}{\partial(\nabla \mathbf{x})} \mathbf{y} \right) \, d\mathbf{X} - \int_{\Omega_0} \left(\nabla \cdot \frac{\partial f}{\partial(\nabla \mathbf{x})} \right) \cdot \mathbf{y} \, d\mathbf{X} + \int_{\Omega_0} \nabla f \cdot \mathbf{y} \, d\mathbf{X} \\ &= \int_{\partial\Omega_0} \frac{\partial f}{\partial(\nabla \mathbf{x})} \mathbf{y} \cdot \mathbf{n} \, dS + \int_{\Omega_0} \left[\nabla f - \nabla \cdot \frac{\partial f}{\partial(\nabla \mathbf{x})} \right] \cdot \mathbf{y} \, d\mathbf{X} \end{aligned}$$

where the last equality follows from the Divergence Theorem. As $i'(0) = 0$, we obtain

$$\underbrace{\int_{\partial\Omega_0} \frac{\partial f}{\partial(\nabla \mathbf{x})} \mathbf{y} \cdot \mathbf{n} \, dS}_{(*)} + \int_{\Omega_0} \left[\nabla f - \nabla \cdot \frac{\partial f}{\partial(\nabla \mathbf{x})} \right] \cdot \mathbf{y} \, d\mathbf{X} = 0. \quad (2.23)$$

We say that (2.23) is the *weak form* of the Euler-Lagrange equations. We have two possibilities for the boundary term (*) to vanish. On the one hand, we can impose essential boundary conditions through the definition of the admissible set \mathcal{A} to force (*) equal to zero. On the other hand, we can have natural boundary conditions which let (*) be zero. In either case, equation (2.23) becomes

$$\int_{\Omega_0} \left[\nabla f - \nabla \cdot \frac{\partial f}{\partial(\nabla \mathbf{x})} \right] \cdot \mathbf{y} \, d\mathbf{X} = 0. \quad (2.24)$$

Since equation (2.24) is true for all $\mathbf{y} \in \mathcal{A}$, we obtain that

$$\nabla \cdot \frac{\partial f}{\partial(\nabla \mathbf{x})} - \nabla f = 0 \quad \text{on } \Omega_0, \quad (2.25)$$

which is the *compact* or *strong form* of the Euler-Lagrange equations. If f only depends on $\nabla \mathbf{x}$, i.e. $f(\mathbf{X}, \mathbf{x}, \nabla \mathbf{x}) = f(\nabla \mathbf{x})$, we obtain that $\nabla f = 0$ and the Euler-Lagrange equations (2.25) become

$$\nabla \cdot \frac{\partial f}{\partial(\nabla \mathbf{x})} = 0 \quad \text{on } \Omega_0,$$

From this, we identify the response function of the first Piola-Kirchhoff stress tensor for a hyperelastic material as

$$\hat{\mathbf{P}}(\nabla \mathbf{x}) \equiv \frac{\partial f}{\partial(\nabla \mathbf{x})}.$$

We summarize our computations above through the following main result in calculus of variation.

Theorem 2.3.1. *Let $f = f(\mathbf{X}, \mathbf{x}, \underline{\xi})$, let \mathcal{A} be the admissible set, and*

$$(P) \quad \inf_{\mathbf{x} \in \mathcal{A}} \left\{ I(\mathbf{x}) = \int_{\Omega_0} f(\mathbf{X}, \mathbf{x}(\mathbf{X}), \nabla \mathbf{x}(\mathbf{X})) \, d\mathbf{X} \right\}.$$

If (P) admits a minimizer $\bar{\mathbf{x}} \in \mathcal{A}$, then necessarily

$$-\sum_{j=1}^n \left(f_{\xi_j^i}(\mathbf{X}, \bar{\mathbf{x}}, \nabla \bar{\mathbf{x}}) \right)_{\mathbf{X}_j} + f_{x^i}(\mathbf{X}, \bar{\mathbf{x}}, \nabla \bar{\mathbf{x}}) = 0, \quad \text{in } \Omega_0 \text{ for } i = 1, \dots, m. \quad (2.26)$$

The equations (2.26) are the weak form of the Euler-Lagrange equations, as seen in (2.25). Let us finish by expressing this fundamental theorem explicitly in 1D.

Theorem 2.3.2. *Let $m = n = 1$. Let $\Omega_0 = C^2([a, b])$, $f = f(X, x, \xi)$, $\mathcal{A} = \{x \in C^1([a, b]) \mid x(a) = \alpha, x(b) = \beta\}$, and*

$$(P) \quad \inf_{x \in \mathcal{A}} \left\{ I(x) = \int_a^b f(X, x(X), x'(X)) dX \right\}.$$

If (P) admits a minimizer $\bar{x} \in \mathcal{A} \cap C^2([a, b])$, then necessarily

$$\frac{d}{dX} (f_\xi(X, \bar{x}(X), \bar{x}'(X))) = f_x(X, \bar{x}(X), \bar{x}'(X)), \quad X \in (a, b).$$

Second Variation

We saw that the first variation leads to finding the critical points \mathbf{x} of our functional $I[\cdot]$. Next, we determine if these critical points are also minimizers of I by invoking the concept of second variation given in (2.22). Consequently, for $\mathbf{x} \in \mathcal{A}$ to be a minimizer, it has to satisfy

$$i''(0) = \frac{d^2}{dt^2} \Big|_{t=0} I[\mathbf{x} + t\mathbf{y}] \geq 0, \quad (2.27)$$

for any test function $\mathbf{y} \in \mathcal{A}$. As before for the first variation, we start by computing $\frac{d^2}{dt^2} (f(\mathbf{X}, \mathbf{x} + t\mathbf{y}, \nabla(\mathbf{x} + t\mathbf{y})))$, since $\frac{d^2}{dt^2} I[\mathbf{x} + t\mathbf{y}] = \int_{\Omega_0} \frac{d^2}{dt^2} (f(\mathbf{X}, \mathbf{x} + t\mathbf{y}, \nabla(\mathbf{x} + t\mathbf{y}))) d\mathbf{X}$.

$$\begin{aligned} & \frac{d^2}{dt^2} \Big|_{t=0} f(\mathbf{X}, \mathbf{x} + t\mathbf{y}, \nabla(\mathbf{x} + t\mathbf{y})) \\ &= \frac{d^2}{dt^2} \Big|_{t=0} f(\mathbf{X}, x_i + ty_i, \nabla(x_i + ty_i)), \quad i = 1, \dots, m \\ &= \sum_{i,j=1}^m \frac{\partial^2 f}{\partial x_i \partial x_j} y_i y_j + 2 \sum_{i,j=1}^m \sum_{k=1}^n \frac{\partial^2 f}{\partial x_i \partial x_{j,k}} y_i y_{j,k} + \sum_{i,j=1}^m \sum_{k,l=1}^n \frac{\partial^2 f}{\partial x_{i,k} \partial x_{j,l}} y_{i,k} y_{j,l}, \end{aligned}$$

Since the integral of $\frac{d^2}{dt^2} (f(\mathbf{X}, \mathbf{x} + t\mathbf{y}, \nabla(\mathbf{x} + t\mathbf{y})))$ at $t = 0$ yields $i''(0)$, we must have

$$i''(0) = \int_{\Omega_0} \sum_{i,j=1}^m \frac{\partial^2 f}{\partial x_i \partial x_j} y_i y_j + 2 \sum_{i,j=1}^m \sum_{k=1}^n \frac{\partial^2 f}{\partial x_i \partial x_{j,k}} y_i y_{j,k} + \sum_{i,j=1}^m \sum_{k,l=1}^n \frac{\partial^2 f}{\partial x_{i,k} \partial x_{j,l}} y_{i,k} y_{j,l} d\mathbf{X} \geq 0. \quad (2.28)$$

We obviously have that (2.28) is satisfied if the integrand is positive for any $\mathbf{X} \in \Omega_0$ for some non-zero test function \mathbf{y} . However, it is in general non-trivial to show the positiveness of the integrand in the multidimensional case. Indeed, we would need to prove that (2.28) holds at any $\mathbf{X} \in \Omega_0$ and for any \mathbf{y} . Moreover, as opposed to the first variation, we cannot use the divergence theorem to eliminate the derivative terms in \mathbf{y} .

Fortunately, the analysis related to the thesis is considerably simplified by working with a spherical domain of radius $R \in (0, 1)$ and a purely symmetric radial deformation $r(R) \in (0, r(1))$, reducing the 3D problem to 1D. Even though the derivative terms would still not vanish using integration by parts, there exist general results on the second variation in 1D, which we briefly summarize following the work in [27] and [28].

We start by defining the Lagrangian in 1D to be a smooth function f given by

$$f : \Omega_0 \times \mathbb{R} \times \mathbb{R} \rightarrow \mathbb{R}, \quad (2.29)$$

where $\Omega_0 = [X_0, X_1]$, with $X_0, X_1 \in \mathbb{R}$. It follows that the energy functional is given by

$$I[x] := \int_{\Omega_0} f(X, x(X), x'(X)) dX, \quad (2.30)$$

where $x : \Omega_0 \rightarrow \mathbb{R}$ is the function we want to minimize for under given conditions. The set of admissible solutions is still denoted by \mathcal{A} . As before, a critical point x of the functional I is also a minimizer if the second variation (2.22) is satisfied. Following the above steps for the general case, we retrieve the condition (2.28), which becomes

$$\int_{\Omega_0} \frac{\partial^2 f}{\partial x^2} y^2 + 2 \frac{\partial^2 f}{\partial x \partial x'} y y' + \frac{\partial^2 f}{\partial x'^2} (y')^2 dX \geq 0, \quad (2.31)$$

where $y \in \mathcal{A}$. As already mentioned for 3D case, it is usually very hard or even impossible to show that (2.31) holds pointwise for every $X \in \Omega_0$. We can instead rely on some results that help with the analysis, the main one being as follows:

Theorem 2.3.3. *Let $x(X)$ be a critical point of $I[\cdot]$. Let $\frac{\partial^2 f}{\partial x^2}$, $\frac{\partial^2 f}{\partial x \partial x'}$ and $\frac{\partial^2 f}{\partial x'^2}$ be continuous functions on Ω_0 . The functional*

$$i''(0) = \int_{\Omega_0} \frac{\partial^2 f}{\partial x^2} y^2 + 2 \frac{\partial^2 f}{\partial x \partial x'} y y' + \frac{\partial^2 f}{\partial x'^2} (y')^2 dX$$

is strictly positive for any $y \not\equiv 0$ such that $y(X_0) = y(X_1) = 0$, assuming that the following conditions are satisfied:

1. *Legendre condition: $\frac{\partial^2 f}{\partial x'^2} > 0$ for all $X \in \Omega_0$.*
2. *Conjugate point condition: For any $X_0 < \tilde{X} \leq X_1$, the linear Euler-Lagrange problem related to the functional $i''(0)$, given by*

$$-\frac{d}{dX} \left(\frac{\partial^2 f}{\partial x'^2} y' \right) + \left[\frac{\partial^2 f}{\partial x^2} - \frac{d}{dX} \left(\frac{\partial^2 f}{\partial x \partial x'} \right) \right] y = 0, \quad y(X_0) = y(\tilde{X}) = 0,$$

has as only solution the trivial one, that is $y(X) \equiv 0$.

We note that \tilde{X} is called the conjugate point to X_0 if the Lagrange problem in the second condition has a non-trivial solution y .

2.3.2 Existence of Minimizers

We just saw that we can find critical points of a functional $I[\cdot]$, and determine if these critical points are minimizers through the first and second variations, respectively. We would next like to obtain the necessary conditions for the existence of a minimizer to our functional $I[\cdot]$ without the variational approach. Let us assume that the space for the admissible set \mathcal{A} is the Sobolev space $\mathcal{X} = W^{1,p}(\Omega_0)$ for the remaining part of this section. First, we look at the most basic case in \mathbb{R} , and then extend the results to higher dimensions m .

Introduction

In this subsection, we assume that $m = 1$. We start by stating a growth condition on our functional $I[\cdot]$, also defined as a coercivity condition.

Definition 2.3.4. Coercivity

We say that a function f satisfies the *coercivity inequality* if

$$\exists \alpha > 0, \beta \geq 0 \text{ such that } f(\mathbf{X}, x, \xi) \geq \alpha |\xi|^p - \beta \quad \forall \mathbf{X} \in \Omega_0, x \in \mathbb{R}, \xi \in \mathbb{R}^n. \quad (2.32)$$

Then we define the *coercivity condition* on $I[\cdot]$ by

$$I[x] \geq \delta \|\nabla x\|_{L^p(\Omega_0)}^p - \gamma, \quad (2.33)$$

for $\gamma = \beta|\Omega_0|$ and some strictly positive constant δ .

Next, we recall two definitions from functional analysis in the field of Banach spaces.

Definition 2.3.5. Let B be a Banach space. A bounded linear operator $\phi : B \rightarrow \mathbb{R}$ is called a *bounded linear functional* on \mathbb{R} . We denote the set of all bounded linear functionals by B' , and B' is the dual of B . If $x \in B$, $\phi \in B'$, then we write $\langle \phi, x \rangle$ to denote the real number $\phi(x)$. We define the norm on B' by $\|\phi\| := \sup\{\langle \phi, x \rangle \mid \|x\| \leq 1\}$.

Definition 2.3.6. Let B be a Banach space. We say that a sequence $\{x_k\}_{k=1}^{\infty} \subset B$ *converges weakly* to $x \in B$, written

$$x_k \rightharpoonup x,$$

if $\langle \phi, x_k \rangle \rightarrow \langle \phi, x \rangle$ for each bounded linear functional $\phi \in B'$.

For instance, if $B = L^p$, then a sequence x_k converges weakly to x in L^p if $x_k, x \in L^p$ and if $\lim_{k \rightarrow \infty} \int_{\Omega_0} (x_k(\mathbf{X}) - x(\mathbf{X})) \phi(\mathbf{X}) d\mathbf{X} = 0$, $\phi \in L^{p'}(\Omega_0)$, where $\Omega_0 \in \mathbb{R}^n$ an open set. The notion of weak convergence allows us to define our second condition, namely the weak lower semicontinuity condition.

Definition 2.3.7. Weak Lower Semicontinuity

A functional I is (sequentially) *weakly lower semicontinuous* on $W^{1,p}(\Omega_0)$, provided

$$I[x] \leq \liminf_{k \rightarrow \infty} I[x_k]$$

whenever

$$x_k \rightharpoonup x \text{ weakly in } W^{1,p}(\Omega_0).$$

The third and last condition is the property of convexity for the function f .

Definition 2.3.8. Convexity

A function $f : \mathbb{R}^m \rightarrow \mathbb{R}$ is called *convex* provided

$$f(\tau x + (1 - \tau)y) \leq \tau f(x) + (1 - \tau)f(y), \quad (2.34)$$

for all $x, y \in \mathbb{R}^m$ and each $0 \leq \tau \leq 1$.

We have that the property of convexity, under certain conditions, can imply weak lower semicontinuity of the functional $I[.]$, as shown in the following theorem.

Theorem 2.3.9. *Let f be smooth and bounded from below. Let $\xi \mapsto f(\mathbf{X}, x, \xi)$ be convex for all $x \in \mathbb{R}$ and $\mathbf{X} \in \Omega_0$. Then $I[.]$ is weakly lower semicontinuous on $W^{1,p}(\Omega_0)$.*

The existence of a minimizer for the functional $I[.]$, such as for Theorem 2.3.2, is guaranteed through the following result:

Theorem 2.3.10. Existence of Minimizers

Let us assume that f satisfies the coercivity inequality (2.32) and that f is convex in the variable ξ . Suppose also that the admissible set \mathcal{A} is non-empty. Then there exists at least one function $\bar{x} \in \mathcal{A}$ solving $I[\bar{x}] = \min_{y \in \mathcal{A}} I[y]$.

Finally, we define conditions under which this minimizer is also unique. Let us assume that

$$(C1) \quad f = f(\mathbf{X}, \xi),$$

that is f does not depend on x . Moreover, we assume there exists $\theta > 0$ such that

$$(C2) \quad \sum_{i=1}^n \sum_{j=1}^n f_{,\xi_i \xi_j}(\mathbf{X}, \xi) \gamma_i \gamma_j \geq \theta |\gamma|^2, \quad \gamma \in \mathbb{R}^n.$$

This inequality assumption ensures uniform convexity of the mapping $\xi \mapsto f(\mathbf{X}, \xi)$ for any $\mathbf{X} \in \Omega_0$. We refer to [25] for the explicit derivation of a convexity inequality, similar to (C2), from the inequality (2.28) found in the section on second variation.

With this, we can state the following uniqueness result.

Theorem 2.3.11. Uniqueness of Minimizers

Suppose that conditions (C1) and (C2) hold. Then a minimizer $\bar{x} \in \mathcal{A}$ of $I[\cdot]$ is unique.

Higher dimensions

In a next step, we state necessary conditions and results for the existence of minimizers for any m . First, the initial inequality (2.32) can be reformulated as follows: We say that the function f satisfies the *coercivity inequality* if there exist constants $\alpha > 0$ and $\beta \geq 0$ such that

$$f(\mathbf{X}, \mathbf{x}, \underline{\xi}) \geq \alpha |\underline{\xi}|^p - \beta, \tag{2.35}$$

for all $\mathbf{X} \in \Omega_0$, $\mathbf{x} \in \mathbb{R}^m$, $\underline{\xi} \in \mathbb{M}^{m \times n}$, and for constants $\alpha > 0$, $\beta \geq 0$. The generalized existence theorem for minimizer is stated as follows:

Theorem 2.3.12. General Existence of Minimizers

Let f satisfy the coercivity inequality (2.35) and let f be convex in the variable $\underline{\xi}$. Suppose also that the admissible set \mathcal{A} is non-empty. Then there exists $\bar{\mathbf{x}} \in \mathcal{A}$ solving $I[\bar{\mathbf{x}}] = \min_{\mathbf{y} \in \mathcal{A}} I[\mathbf{y}]$.

Theorem 2.3.13. General Uniqueness of Minimizers

Let us assume that f does not depend on \mathbf{x} . Moreover, let the mapping $\underline{\xi} \mapsto f(\mathbf{X}, \underline{\xi})$ be uniformly convex. Then a minimizer $\bar{\mathbf{x}} \in \mathcal{A}$ of $I[\cdot]$ is unique.

However, the function f is in many problems not convex so that we can not apply Theorem 2.3.12 to guarantee the existence of a minimizer. Therefore, we introduce a weaker condition, called polyconvexity, which is more frequently satisfied by f and which allows to conclude on the existence of minimizers. For the remaining part of this section, let us assume that $m = n$ and let us assume that f depends explicitly on the determinant of $\nabla \mathbf{x}$, i.e.

$$f(\mathbf{X}, \mathbf{x}, \nabla \mathbf{x}) = g(\mathbf{X}, \mathbf{x}, \nabla \mathbf{x}, \det \nabla \mathbf{x}), \quad (2.36)$$

for $\mathbf{X} \in \Omega_0$, $\mathbf{x} \in \mathbb{R}^n$, $\nabla \mathbf{x} \in \mathbb{M}^{n \times n}$ and where $g : \bar{\Omega}_0 \times \mathbb{R}^n \times \mathbb{M}^{n \times n} \times \mathbb{R} \rightarrow \mathbb{R}$ is smooth.

Definition 2.3.14. Polyconvexity

Let f satisfy (2.36). f is called *polyconvex* if for each fixed $\mathbf{x} \in \mathbb{R}^n$, $\mathbf{X} \in \Omega_0$, the joint mapping given by

$$(\underline{\xi}, r) \mapsto g(\mathbf{X}, \mathbf{x}, \underline{\xi}, r)$$

is convex.

Lemma 2.3.15. Weak Continuity of Determinants

Let us assume that $x_k \rightharpoonup \mathbf{x}$ weakly in $W^{1,p}(\Omega_0, \mathbb{R}^n)$. Then

$$\det \nabla x_k \rightharpoonup \det \nabla \mathbf{x} \text{ weakly in } L^{\frac{p}{n}}(\Omega_0).$$

At this point, we can also recall a related result on convergence between Sobolev and Lebesgue spaces, which is a Corollary of the Rellich-Kondrachov Theorem.

Proposition 2.3.16. *Let Ω_0 be a bounded open set with Lipschitz boundary and $1 \leq p < \infty$. If $x_k \rightharpoonup \mathbf{x}$ in $W^{1,p}(\Omega_0)$, then*

$$x_k \rightarrow \mathbf{x} \text{ in } L^p(\Omega_0).$$

We conclude this section with two important results for polyconvex functions.

Proposition 2.3.17. Lower Semicontinuity for Polyconvex Functionals

Let f be bounded from below and polyconvex. Then $I[\cdot]$ is weakly lower semicontinuous on $W^{1,p}(\Omega_0, \mathbb{R}^n)$.

Theorem 2.3.18. Existence of Minimizers for Polyconvex Functionals

Let f satisfy the coercivity inequalities (2.35) and let f be polyconvex. Furthermore, suppose that the admissible set \mathcal{A} is non-empty. Then there exists $\bar{\mathbf{x}} \in \mathcal{A}$ solving $I[\bar{\mathbf{x}}] = \min_{\mathbf{y} \in \mathcal{A}} I[\mathbf{y}]$.

Remark 2. We note that, for many physical problems, certain constraints restrictions on the function \mathbf{x} , for example what normed function space \mathcal{X} we use, or what admissible set \mathcal{A} we prescribe. Similarly as for the previous results, we can show the existence of minimizers for certain constraints. We do not discuss the details of these results here, however we revisit the concept of constraints in calculus of variations for the purpose of this thesis at a later stage.

2.4 Cavitation in Nonlinear Elasticity

The nucleation and growth of cavities in an elastic body with different material properties has been the scope of experimental and mathematical research for the past few decades. This section is devoted to a mathematical summary of the fundamental work by John Ball in [9] on the static analysis of cavitation.

Notation

Let a body occupy a unit spherical domain $\Omega_0 = \{\mathbf{X} \in \mathbb{R}^3 \mid |\mathbf{X}| \leq 1\}$ in the reference configuration and let $\Phi : \Omega_0 \rightarrow \Omega$ be the deformation map taking $\mathbf{X} \in \Omega_0$ to $\mathbf{x} \in \Omega$, where Ω is the domain in the deformed configuration. We assume a purely radial deformation

$$\mathbf{x}(\mathbf{X}) = \frac{r(R)}{R} \mathbf{X},$$

with $R = |\mathbf{X}|$, so that Ω is a spherical domain as well. The deformation gradient $\underline{\mathbf{F}} = \frac{\partial \mathbf{x}(\mathbf{X})}{\partial \mathbf{X}}$ from (2.1) in spherical coordinates, explicitly computed in the appendix, is given by

$$\underline{\mathbf{F}} = \text{diag} \left(r, r, \frac{r}{R}, \frac{r}{R} \right). \quad (2.37)$$

We define the stored energy function of an isotropic body by

$$W = \hat{W}(I_1, I_2, I_3),$$

where I_i are the invariants of $\underline{\mathbf{B}} = \underline{\mathbf{F}} \underline{\mathbf{F}}^T$ for $i = 1, 2, 3$, as defined in (2.6). Alternatively, we may also define the energy density W as

$$W = \tilde{W}(\kappa_1, \kappa_2, \kappa_3), \quad (2.38)$$

where κ_i are the eigenvalues of $\underline{\mathbf{B}}$, for $i = 1, 2, 3$, and are called the principle stretches from Proposition 2.1.3. We assume that W is frame-indifferent, namely $W(\underline{\mathbf{Q}} \underline{\mathbf{F}}) = W(\underline{\mathbf{F}})$ for any $\underline{\mathbf{Q}} \in SO(3)$ (Definition 2.1.13). The total free energy of the body is given by $E_{tot} = \int_{\Omega_0} W d\mathbf{X}$. The Cauchy stress tensor is given by $\underline{\mathbf{T}} = \hat{\underline{\mathbf{T}}}(\underline{\mathbf{F}})$, which we express in spherical coordinates. The boundary conditions will be of two types:

1. Displacement boundary conditions: $r(1) = \lambda$ for $\lambda > 0$.
2. Traction boundary conditions in terms of the Cauchy stress tensor: $T_{rr}(r(1)) = p_0$ where $p_0 \geq 0$ is an applied pressure on the boundary.

In the presence of a cavity, we also have a traction-free condition for the cavity, meaning that there is no radial stress at the surface of the cavity, mathematically translating into

$$T_{rr}(0^+) = 0. \quad (2.39)$$

We follow [9] for the mathematical summary, which is the first major work on cavitation in elastic materials.

Incompressible Case

Let us start by assuming that the body is incompressible: We recall (2.4) which states that a material is incompressible if and only if $\det \underline{\mathbf{F}} = 1$. This, together with (2.37), gives $r, R \frac{r^2}{R^2} = 1$ which implies that

$$r(R) = (R^3 + \rho^3)^{\frac{1}{3}},$$

where $\rho \geq 0$. If $\rho = 0$, we obtain the trivial solution $r(R) = R$ when there is no deformation. If $\rho > 0$, we have a deformation with a cavity of radius ρ . The author determines necessary conditions for the existence of finite energy and the conditions for the radial deformation to be a weak equilibrium solution of the Euler-Lagrange equations. Moreover, the main result determines the critical stretch λ_{cr} or the critical pressure p_{0cr} at which the deformation $r(R)$ with cavity radius $\rho > 0$ bifurcates from the trivial solution, for the displacement and traction boundary conditions, respectively.

Compressible Case

Let us now turn to the more general case where the material is compressible, that is when $\det \underline{\mathbf{F}} \neq 1$. We consider the stored energy function W expressed in terms of the principal stretches of $\underline{\mathbf{F}}$ as in (2.38). The goal is to find radial minimizers for the energy and determine conditions under which these minimizers are discontinuous, that is $r(0) \neq 0$. We start by defining the admissible set \mathcal{A} for the radial deformation by

$$\mathcal{A} = \left\{ \mathbf{x} = \frac{r(R)}{R} \mathbf{X} : \Omega_0 \rightarrow \Omega \mid r_{,R} > 0, r(0) \geq 0, E(\Omega_0) < \infty, \text{ boundary conditions} \right\}.$$

Then, we derive the Euler-Lagrange equations for the system and we obtain the result that radial deformations are weak equilibrium solutions. Assuming displacement boundary conditions, the trivial solution for the Euler-Lagrange equation is given by $r(R) = \lambda R$, which is the uniform radial expansion. We have a similar trivial solution for the traction problem. We aim to find necessary conditions for which a solution with cavity, i.e. $r(0) > 0$, bifurcates from this trivial one. Under certain hypothesis on the deformation and the energy, we have the traction-free condition (2.39) on the boundary of a cavity. This leads us to the following important results: For sufficiently large λ or p_0 , any radial deformation that is a minimizer of the energy E on \mathcal{A} satisfies $r(0) > 0$. Such solution with cavity only exists once a critical displacement λ_{cr} or pressure p_{0cr} are attained. Otherwise, the trivial solution is the unique minimizer and is stable.

Chapter 3

Gels

In this chapter, we define the notion of a gel and describe its material properties. We introduce and discuss the energy terms to best describe these characteristics. Finally, we elaborate on the phenomenon of cavitation within a gel.

3.1 Introduction

3.1.1 Definition

We define a gel as an distinguishable and compressible mixture of an elastic solid, polymer in our study, and a viscous fluid, which we refer to as solvent. We assume the polymer to be hyperelastic and incompressible, a characteristic we elaborate on further in the upcoming section on mixture theory. Our system underlies equations of balance of mass and linear momentum for both the solid and the fluid components. The connection between these components is realized through the Flory-Huggins energy of mixing and the boundary conditions. The latter are either displacement or swelling conditions, and are described at a later point.

We model the total free energy of a gel as a sum of an elastic energy, a volume energy accounting for compressibility, and the Flory-Huggins mixing energy, all of them described in detail below. We note that the mechanics of the gel are described by the elastic and volume energies, whereas the chemical composition is accounted for by the Flory-Huggins mixing energy.

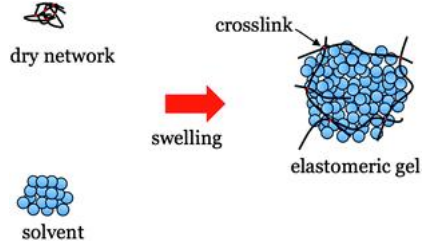


Figure 3.1: Elastomer Gel [29]

3.1.2 Mixture Theory

We defined the gel as a binary mixture of two different components, namely a polymer and a solvent. We start by introducing some basic concepts for our work, following [1], [30] or [31].

Notation

We use a lattice method to describe the polymer and solvent mixture. Polymer molecules are assumed to be chains of a fixed number of monomer molecules, and the solvent molecules are represented in black and gray, respectively, in the figure below. Each

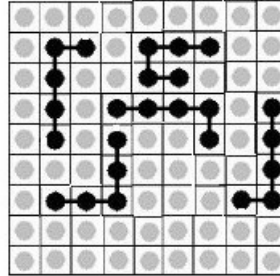


Figure 3.2: Gel Mixture, Polymer Chains (Black) and Solvent Molecules (Gray)

configuration yields a different total free energy for the system. We therefore calculate the ensemble average of these energies. Next, we define the following quantities in our lattice system:

v_0 - Volume of one lattice site,

n_1 - Number of lattice sites occupied by one monomer molecule,

n_2 - Number of lattice sites occupied by one solvent molecule,

n - Number of monomers in a polymer chain,

N_1 - Number of polymers in the mixture,

N_2 - Number of solvent molecules in the mixture.

The volume v_1 of one polymer molecule and the volume v_2 of one solvent molecule are given by

$$v_1 := nn_1v_0, \quad v_2 := n_2v_0,$$

respectively. The total volume V_1 of polymer and the total volume V_2 of solvent in the mixture are defined by

$$V_1 := N_1v_1, \quad V_2 := N_2v_2,$$

respectively. The total volume V of the mixture and the total number N of lattice sites are given by

$$V = V_1 + V_2, \quad N = \frac{V_1 + V_2}{v_0} = nn_1N_1 + n_2N_2.$$

Let us now describe some of main properties of the gel mixture.

Mixture Distinguishability

A mixture is said to be indistinguishable if the governing equations do not distinguish between the different components in the mixture, that is if they do not depend on the respective volume fractions. A gel, however, is distinguishable since we distinguish between polymer and solvent components, which are connected through the Flory-Huggins energy of mixing. We explicitly define and derive this mixing energy in the next section. We define the volume fractions of polymer and fluid in the deformed configuration for the gel by

$$\phi_1 = \frac{V_1}{V} \quad \text{and} \quad \phi_2 = \frac{V_2}{V},$$

respectively, with $0 \leq \phi_1, \phi_2 \leq 1$. We have that the volume fractions also depend explicitly on the position within the domain of the deformed configuration Ω , that is

$$\phi_1 = \phi_1(\mathbf{x}) \quad \text{and} \quad \phi_2 = \phi_2(\mathbf{x}).$$

Moreover, since we have a binary mixture, we assume that no component other than polymer or solvent is present in the gel, which mathematically translates to

$$\phi_1 + \phi_2 = 1. \quad (3.1)$$

Mixture Incompressibility

The mass densities ρ_i and the volume fractions ϕ_i are related through the intrinsic densities γ_i through

$$\rho_i = \gamma_i \phi_i,$$

where $i = 1$ for the polymer and $i = 2$ for the solvent. The intrinsic density is the mass of one molecule per the volume it occupies, denoted by v_i above. We call a molecule of the component i incompressible if v_i is constant, that is if n_i is constant. This incompressibility also implies that γ_i is constant.

We say that the mixture is incompressible if each component in the mixture is incompressible. In this work, we assume the polymer to be incompressible. Hence, v_1 is constant and so is γ_1 . Without loss of generality, we may assume $\gamma_1 = 1$, so that

$$\rho_1 = \phi_1. \quad (3.2)$$

Moreover, in the case of an isolated system, an incompressible solvent would imply mixture incompressibility being material incompressibility, as defined by (2.4), since the total volume V of the mixture could not change. Hence, we will have

1. Solvent compressibility if system is isolated, yielding a non-constant v_2 .
2. Solvent incompressibility otherwise, and, without loss of generality, $\gamma_2 = 1$.

In the latter case, when the system is not isolated, the solvent can be incompressible. However, the mixture may remain compressible and allow for volume changes. Indeed, in the case of a non-isolated system, we consider the gel to be immersed in an infinite medium consisting of its solvent component. Hence, the gel may expand its volume by absorbing more solvent, and increasing the number N_2 of solvent molecules within the mixture.

The volume fraction and the density of the polymer in the reference configuration Ω_0 are given by

$$\phi_0 = \phi_0(\mathbf{X}) \quad \text{and} \quad \rho_0,$$

respectively. We say that the material is homogeneous if ϕ_0 does not depend on \mathbf{X} , i.e. if ϕ_0 is constant. Next, we can relate the volume fraction of the polymer in the reference configuration, ϕ_0 , to the one in the deformed configuration, ϕ_1 , using balance of mass.

Proposition 3.1.1. $\phi_0 = \phi_1 \det \underline{\mathbf{F}}$.

Proof. By the balance of mass equation (2.7) and by (3.2), we have that

$$\int_{\Omega_0} \phi_0(\mathbf{X}) d\mathbf{X} = \int_{\Omega_0} \rho_0(\mathbf{X}) d\mathbf{X} = \int_{\Omega} \rho_1(\mathbf{x}) d\mathbf{x} = \int_{\Omega} \phi_1(\mathbf{x}) d\mathbf{x} = \int_{\Omega_0} \phi_1(\mathbf{x}(\mathbf{X})) \det \underline{\mathbf{F}} d\mathbf{X},$$

and the result follows. \square

3.2 Energy

In this part, we define the total free energy of the gel with its different components that describe the main physical characteristics key to our work. Our model for the thesis is based on the model described in [1].

3.2.1 Elastic Energy Potential

The first property in a gel we account for is the elasticity of the polymer component. In general, the stored elastic energy W is defined in terms of either the invariants (2.6) or the eigenvalues, also called principal stretches (Proposition 2.1.3), of the left Cauchy-Green tensor $\underline{\mathbf{B}} = \underline{\mathbf{F}} \underline{\mathbf{F}}^T$: $W = f(I_1, I_2, I_3)$ or $W = f(\lambda_1, \lambda_2, \lambda_3)$. For instance, we consider a stored elastic energy potential of the form

$$W_E(\underline{\mathbf{F}}) = \frac{\mu}{2s} I_1^s + h(I_3), \tag{3.3}$$

where h is a convex function accounting for volume changes of the material due to compression or expansion. We choose h to be of the form

$$h(\det \underline{\mathbf{F}}) = \zeta_1 (\det \underline{\mathbf{F}})^{-\beta_1} + \zeta_2 (\det \underline{\mathbf{F}})^{\beta_2}.$$

Here, the elastic energy potential encompasses the following material properties: the elastic stiffness modulus, denoted by $\mu > 0$ and defined by $\mu = \frac{k_B T}{v_0} \nu$, $\zeta_1 \geq 0$ and $\zeta_2 \geq 0$ which are material coefficients, as well as $\beta_1 > 0$ and $\beta_2 > 0$ which are related to the mixture compressibility.

Furthermore, we have that k_B is the Boltzmann constant, T is the temperature of the gel and ν is the crosslink number density in the reference configuration. We note that in general, the exponent s satisfies $s > 1$. In particular, we consider the special case of $s = 1$ which corresponds to a Neo-Hookean material, i.e. a material where the stress-strain curve is not linear.

Remark 3. We assume that the elastic energy density is given by W_E in (3.3). This implies that the material has an initial energy, which is not zero, in the reference configuration, since $\underline{\mathbf{F}} = \underline{\mathbf{I}}$ in this case and $W_E(\underline{\mathbf{I}}) \neq 0$. However, the physics require the elastic energy to be zero when the body is not exposed to any deformation. Therefore, the elastic energy is usually given by

$$\hat{W}_E(\underline{\mathbf{F}}) = \frac{\mu}{2s} (I_1^s - \|\underline{\mathbf{I}}\|^{2s}) + \hat{h}(I_3),$$

with $\hat{h} = 0$ for $\underline{\mathbf{F}} = \underline{\mathbf{I}}$. This approach is taken in other works on gels, as for instance in [1]. The inclusion of the constant terms, that is the identity terms, does not have an effect on the energy minimization as the constant terms vanish in the variational approach. Furthermore, we almost exclusively focus on the difference of energies in the result section of this thesis, so that the constant terms vanish again. Hence, we proceed by using the simplified energy density W_E given in (3.3) instead of the more accurate \hat{W}_E .

3.2.2 Flory-Huggins Energy

Secondly, the remaining main property we account for in our gel model is the polymer-solvent mixture. The corresponding binding energy between the two components in the gel is called the Flory-Huggins energy of mixing.

Definition

We first define the Flory-Huggins energy density in terms of the polymer and fluid fractions as

$$W_{FH}(\phi_1, \phi_2) = a\phi_1 \ln \phi_1 + b\phi_2 \ln \phi_2 + c\phi_1\phi_2, \quad (3.4)$$

with a, b, c being constants which we will identify in the derivation of the Flory-Huggins energy below.

Derivation

There are two components that determine the free energy of mixing, namely entropy and enthalpy. We need to look at the mixture on a molecular level to determine these two quantities. Let us start by deriving the entropy for the gel.

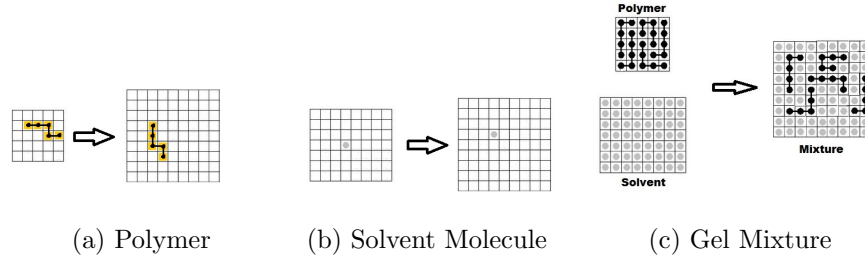


Figure 3.3: Lattice Representation for Components and Mixture (Source: Wikipedia)

1. Entropy

The entropy, denoted by S , measures the disorder in the system:

$$S := k_B \ln \Sigma, \quad (3.5)$$

with Σ the number of ways to arrange molecules on the lattice. Let us determine how many ways there are to arrange molecules in the lattice: Before mixture, $\Sigma_1 = N\phi_1$ for each polymer and $\Sigma_2 = N\phi_2$ for each solvent molecule and, in mixture, $\Sigma_{12} = N$ for each molecule, i.e. either polymer or solvent.

The entropy changes for one polymer and one solvent molecule, respectively, when going from its original state to the mixing state, are given by

$$\Delta S_1 = k_B \ln \Sigma_{12} - k \ln \Sigma_1 = -k_B \ln \phi_1, \quad \Delta S_2 = k_B \ln \Sigma_{12} - k \ln \Sigma_2 = -k_B \ln \phi_2.$$

Hence, the total entropy change in the mixing is given by

$$\Delta S = N_1 \Delta S_1 + N_2 \Delta S_2 = -k_B N \left(\frac{\phi_1}{nn_1} \ln \phi_1 + \frac{\phi_2}{n_2} \ln \phi_2 \right),$$

and therefore the total entropy change per lattice site becomes

$$\Delta \bar{S} = \frac{\Delta S}{N} = -k_B \left(\frac{\phi_1}{nn_1} \ln \phi_1 + \frac{\phi_2}{n_2} \ln \phi_2 \right).$$

The total entropy change per unit volume is $\frac{\Delta \bar{S}}{v_0}$. Therefore, the energy associated with the entropy change per lattice site and per unit volume is

$$\Delta \bar{F} = -T \Delta \bar{S} = \frac{k_B T}{v_0} \left(\frac{\phi_1}{nn_1} \ln \phi_1 + \frac{\phi_2}{n_2} \ln \phi_2 \right). \quad (3.6)$$

The higher the entropy change, the lower the energy so the more favorable the mixing. There is a second part of the mixing energy, called enthalpy, which we will derive next.

2. Enthalpy

The enthalpy, denoted by U , is the internal energy of the system. This energy originates from interactions between molecules in the mixtures. There are three types of such interactions: the interaction u_{11} between two monomers, the interaction u_{22} between two solvent molecules as well as the interaction u_{12} between monomer and solvent molecule. The average interaction of a molecule with its neighboring molecules is given by

$$U_1 = \phi_1 u_{11} + \phi_2 u_{12}, \quad U_2 = \phi_1 u_{12} + \phi_2 u_{22},$$

for monomer and solvent molecules, respectively. This assumption of average molecule interaction is part of the *mean field approximation* theory.

If a molecule has z neighbors, e.g. $z = 4$ in for a square lattice, then the total interaction energy with all neighboring molecules before mixture is zu_{11} for a monomer and zu_{22} for a solvent molecule. In the mixture, this total interaction energy becomes zU_1 for a monomer and zU_2 for a solvent molecule. Hence the total interaction energies between molecules before and in the mixture are given by

$$U_0 = \frac{zN}{2} (\phi_1 u_{11} + \phi_2 u_{22}), \quad U = \frac{zN}{2} (\phi_1 U_1 + \phi_2 U_2),$$

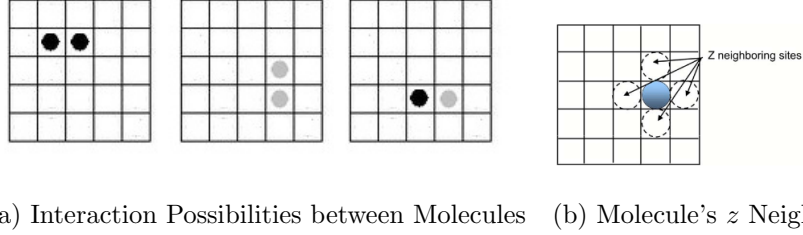


Figure 3.4: Interaction of Neighboring Molecules (Source: MIT OCW 3.012 Lect. 24)

respectively. Then, the total interaction energy change for the mixing process becomes

$$\Delta U = U - U_0 = \frac{zN}{2} \phi_1 \phi_2 (2u_{12} - u_{11} - u_{22}).$$

Similarly as before for the entropy, the total free energy density change on mixing per lattice site is

$$\Delta \bar{U} = \frac{\Delta U}{N} = \frac{z}{2} \phi_1 \phi_2 (2u_{12} - u_{11} - u_{22}).$$

The total free energy change on mixing per unit volume is then $\frac{\Delta \bar{U}}{v_0}$. We define the Flory interaction parameter by

$$\chi \equiv \frac{z(2u_{12} - u_{11} - u_{22})}{2k_B T} = \frac{\Delta w}{2k_B T},$$

where Δw is the change in the energy per monomer-solvent interaction. Therefore the total enthalpy of the system is written as

$$\Delta \bar{U} = k_B T \chi \phi_1 \phi_2.$$

We are left to summarize that the Flory-Huggins energy of mixing is the total free energy of mixing per lattice site and per unit volume, resulting from the sum of enthalpy and entropy energy terms:

$$W_{FH}(\phi_1, \phi_2) := \frac{1}{v_0} (\Delta \bar{U} - T \Delta \bar{S}),$$

We can finally identify the coefficients a , b and c defined above as

$$a = \frac{k_B T}{n n_1 v_0}, \quad b = \frac{k_B T}{n_2 v_0}, \quad c = \frac{k_B T}{v_0} \chi.$$

We may continue assuming that n_1 and n_2 are constant for remainder of this chapter, unless otherwise stated, and without loss of generality, $n_1 = n_2 = 1$.

Remark 4. The case when n_1 or n_2 are non-constant refers to the compressibility of either the polymer or the solvent, respectively. This may occur when imposing displacement boundary conditions, e.g. $r(1) = \lambda$ for $\lambda > 1$, for an isolated system. If so, we may express n_i in terms of λ through the balance of mass, for $i = 1, 2$.

Indeed, let us assume that n_1 is constant, for instance $n_1 = 1$ without loss of generality, and that n_2 is non-constant. Let the reference configuration Ω_0 be a unit sphere, and the deformed configuration Ω be a sphere of radius λ . The volumes of Ω are given by

$$V = \frac{4\pi\lambda^3}{3}.$$

Moreover, we have that $V = V_1 + V_2$, where $V_1 = N_1 n n_1 v_0$ and $V_2 = N_2 n_2 v_0$ are the volumes of polymer and solvent in Ω , as defined before. Hence, we obtain by simple algebra that

$$n_2 = \frac{\frac{4\pi\lambda^3}{3} - N_1 n n_1}{N_2}. \quad (3.7)$$

where we assumed $v_0 = 0$.

Analysis of Flory-Huggins Energy

We want to express the Flory-Huggins energy (3.4) in a more compact form. By the binary mixture property given by (3.1), we can also write (3.4) in terms of ϕ_1 only:

$$W_{FH}(\phi_1) = a\phi \ln \phi_1 + b(1 - \phi_1) \ln(1 - \phi_1) + c\phi_1(1 - \phi_1). \quad (3.8)$$

We can also express the Flory-Huggins energy in terms of the deformation gradient $\underline{\mathbf{F}}$. We recall that Proposition 3.1.1 gives $\phi_1 = \frac{\phi_0}{\det \underline{\mathbf{F}}}$, which immediately implies $W_{FH}(\phi_1) = W_{FH}(\underline{\mathbf{F}})$, i.e.

$$W_{FH}(\underline{\mathbf{F}}) = \frac{a\phi_0}{\det \underline{\mathbf{F}}} \ln \frac{\phi_0}{\det \underline{\mathbf{F}}} + \frac{b(\det \underline{\mathbf{F}} - \phi_0)}{\det \underline{\mathbf{F}}} \ln \left(1 - \frac{\phi_0}{\det \underline{\mathbf{F}}}\right) + \frac{c\phi_0}{\det \underline{\mathbf{F}}} \left(1 - \frac{\phi_0}{\det \underline{\mathbf{F}}}\right). \quad (3.9)$$

We note that $n \gg 1$, which suggests that the first term has the least contribution. Next, let us analyze each of the three terms' behavior in (3.9).

$$1. \ A(\det \underline{\mathbf{F}}) := \left(a \frac{\phi_0}{\det \underline{\mathbf{F}}} \ln \frac{\phi_0}{\det \underline{\mathbf{F}}}\right) \det \underline{\mathbf{F}} = a\phi_0 \ln \frac{\phi_0}{\det \underline{\mathbf{F}}}.$$

- We have that the domain is $\text{dom } A = (0, \infty)$. Furthermore, the function A has a single root at $\det \underline{\mathbf{F}} = \phi_0$, and we get that $\lim_{\det \underline{\mathbf{F}} \rightarrow +\infty} A(\det \underline{\mathbf{F}}) = -\infty$ as well as $\lim_{\det \underline{\mathbf{F}} \rightarrow 0^+} A(\det \underline{\mathbf{F}}) = +\infty$.
 - Since $\frac{\partial A}{\partial \det \underline{\mathbf{F}}} = \frac{-a\phi_0}{\det \underline{\mathbf{F}}}$, we get that $\frac{\partial A}{\partial \det \underline{\mathbf{F}}} < 0$ for $\det \underline{\mathbf{F}} \in \text{dom } A$. Moreover, we have $\lim_{\det \underline{\mathbf{F}} \rightarrow +\infty} \frac{\partial A}{\partial \det \underline{\mathbf{F}}} = 0^-$ and $\lim_{\det \underline{\mathbf{F}} \rightarrow 0^+} \frac{\partial A}{\partial \det \underline{\mathbf{F}}} = -\infty$.
 - Finally, as $\frac{\partial^2 A}{\partial (\det \underline{\mathbf{F}})^2} = \frac{a\phi_0}{(\det \underline{\mathbf{F}})^2} > 0$.
2. $B(\det \underline{\mathbf{F}}) := \left[b \left(1 - \frac{\phi_0}{\det \underline{\mathbf{F}}} \right) \ln \left(1 - \frac{\phi_0}{\det \underline{\mathbf{F}}} \right) \right] \det \underline{\mathbf{F}} = b(\det \underline{\mathbf{F}} - \phi_0) \ln \left(1 - \frac{\phi_0}{\det \underline{\mathbf{F}}} \right)$.
- Since $\lim_{\det \underline{\mathbf{F}} \rightarrow \phi_0} B(\det \underline{\mathbf{F}}) = 0$, we see that the domain of B is $\text{dom } B = [\phi_0, \infty)$. Also, we have that $\lim_{\det \underline{\mathbf{F}} \rightarrow \infty} B(\det \underline{\mathbf{F}}) = -b\phi_0$.
 - $\frac{\partial B}{\partial \det \underline{\mathbf{F}}} = b \left[\frac{\phi_0}{\det \underline{\mathbf{F}}} + \ln \left(1 - \frac{\phi_0}{\det \underline{\mathbf{F}}} \right) \right]$ implies that $\frac{\partial B}{\partial \det \underline{\mathbf{F}}} < 0$ for $\det \underline{\mathbf{F}} \in \text{dom } B$. We also get that $\lim_{\det \underline{\mathbf{F}} \rightarrow +\infty} \frac{\partial B}{\partial \det \underline{\mathbf{F}}} = 0^-$ and $\lim_{\det \underline{\mathbf{F}} \rightarrow \phi_0} \frac{\partial B}{\partial \det \underline{\mathbf{F}}} = -\infty$.
 - Furthermore, we have $\frac{\partial^2 B}{\partial (\det \underline{\mathbf{F}})^2} = \frac{b\phi_0^2}{(\det \underline{\mathbf{F}})^2(\det \underline{\mathbf{F}} - \phi_0)}$, so that $\frac{\partial^2 B}{\partial (\det \underline{\mathbf{F}})^2} > 0$ for $\det \underline{\mathbf{F}} \in (\phi_0, \infty)$.
3. $C(\det \underline{\mathbf{F}}) := \left[c \frac{\phi_0}{\det \underline{\mathbf{F}}} \left(1 - \frac{\phi_0}{\det \underline{\mathbf{F}}} \right) \right] \det \underline{\mathbf{F}} = c\phi_0 \left(1 - \frac{\phi_0}{\det \underline{\mathbf{F}}} \right)$.
- We note that $\text{dom } C = (0, \infty)$ and that the function C has a single root at $\det \underline{\mathbf{F}} = \phi_0$. Moreover, we get that $\lim_{\det \underline{\mathbf{F}} \rightarrow +\infty} C(\det \underline{\mathbf{F}}) = c\phi_0$ as well as that $\lim_{\det \underline{\mathbf{F}} \rightarrow 0^+} C(\det \underline{\mathbf{F}}) = -\infty$.
 - As $\frac{\partial C}{\partial \det \underline{\mathbf{F}}} = \frac{c\phi_0^2}{(\det \underline{\mathbf{F}})^2}$, we obtain that $\frac{\partial C}{\partial \det \underline{\mathbf{F}}} > 0$ for $\det \underline{\mathbf{F}} \in \text{dom } C$.
 - Finally, as $\frac{\partial^2 C}{\partial (\det \underline{\mathbf{F}})^2} = \frac{-2c\phi_0^2}{(\det \underline{\mathbf{F}})^3}$, we have that $\frac{\partial^2 C}{\partial (\det \underline{\mathbf{F}})^2} < 0$ on $\text{dom } C$.

Let us recall that a hydrophilic interaction describes an attraction between polymer and solvent, enhancing the mixing and the growth of the gel. On the other hand, a hydrophobic interaction implies a repulsion between polymer and solvent, causing a collapse of the gel. Based the observation on the functions A , B and C above, we conclude that A and B are hydrophilic terms and hence welcome expansion. On the other hand, C opposes expansion and hence is hydrophobic.

Finally, a gel phase transition occurs for some critical parameters of the system, in which case the gel separates into phases. A gel phase transition is mathematically given by a convexity transition of the total free energy. We have that the Flory-Huggins

energy accounts for such phase transitions in a gel, given that the parameters a , b and c have certain critical values.

3.2.3 Dimensionless Energy Quantities

Since the value $\frac{k_B T}{v_0}$ appears in the elastic stiffness modulus as well as in each coefficient of the Flory-Huggins, it is natural to define the constant η as

$$\eta := \frac{k_B T}{v_0},$$

In order to have dimensionless quantities in our energy, we make use of η to get

$$\bar{a} = \frac{a}{\eta} = \frac{1}{n}, \bar{b} = \frac{b}{\eta} = 1, \bar{c} = \frac{c}{\eta} = \chi, \bar{\mu} = \frac{\mu}{\eta} = \nu, \bar{\zeta}_1 = \frac{\zeta_1}{\eta}, \bar{\zeta}_2 = \frac{\zeta_2}{\eta}. \quad (3.10)$$

3.2.4 Total Energy

Finally, the total free energy of a gel is given by

$$E_{\text{tot}} = \int_{\Omega_0} \phi_0 W_E \, d\mathbf{X} + \int_{\Omega} W_{FH} \, d\mathbf{x},$$

or equivalently, we may express the total free energy all together in the reference configuration by

$$\begin{aligned} E_{\text{tot}} &= \int_{\Omega_0} \phi_0 W_E + (\det \mathbf{F}) W_{FH} \, d\mathbf{X} \\ &= \int_{\Omega_0} W(\mathbf{X}, \mathbf{F}) \, d\mathbf{X}. \end{aligned}$$

where we define the total stored energy density function W by

$$W(\mathbf{X}, \mathbf{x}, \mathbf{F}) := \phi_0 W_E + (\det \mathbf{F}) W_{FH}. \quad (3.11)$$

The dimensionless stored energy is denoted by \bar{W} , with \bar{W}_E and \bar{W}_{FH} being the dimensionless quantities for W_E and W_{FH} , respectively. The dimensionless total free energy is given by

$$\bar{E}_{\text{tot}} = \int_{\Omega_0} \bar{W}(\mathbf{X}, \mathbf{F}) \, d\mathbf{X}.$$

Remark 5. We note that, by abuse of notation, we may use E and \bar{E} interchangeably to refer to dimensionless quantities during the remainder of this thesis if the context is clear. This is also true for W and \bar{W} .

We can finally express the total free energy in radial components for a radially symmetric deformation in 3D, as given by (2.37), by

$$\begin{aligned} \bar{E}_{\text{tot}} = 4\pi \int_0^1 \phi_0 \left[\frac{\nu}{2s} \left(r_{,R}^2 + 2\frac{r^2}{R^2} \right)^s + \bar{\zeta}_1 \left(\frac{R^2}{r_{,R}r^2} \right)^{\beta_1} + \bar{\zeta}_2 \left(\frac{r_{,R}r^2}{R^2} \right)^{\beta_2} \right. \\ \left. + \frac{1}{n} \ln \frac{\phi_0 R^2}{r_{,R}r^2} + \left(\frac{r_{,R}r^2}{\phi_0 R^2} - 1 \right) \ln \left(1 - \frac{\phi_0 R^2}{r_{,R}r^2} \right) + \chi \left(1 - \frac{\phi_0 R^2}{r_{,R}r^2} \right) \right] R^2 dR. \end{aligned}$$

In the next chapter, we investigate the critical points of the total free energy of a gel occupying a spherical domain in the reference configuration, and in which circumstances these critical points are minimizers. These minimizers belong to a set of radial deformations which includes continuous and discontinuous deformations, the latter being one where a cavity forms. In a first step, we need to guarantee the existence of such minimizers and one main condition to be satisfied is the boundedness of the total free energy. However, it is important to note that for radial deformations in the presence of a cavity,

$$\lim_{R \rightarrow 0^+} \bar{E}_{\text{tot}} = +\infty.$$

We may impose a *defect* to obtain a finite energy at the origin through

$$\phi_0(0) = 0.$$

This defect at the origin of the body corresponds to only having solvent, and hence no polymer, at the origin. We can make several choices on the polymer fraction to achieve this type of defect.

For this work, we assume the polymer fraction ϕ_0 to be piecewise constant, namely $\phi_0 = 0$ at the origin and $\phi_0 = k$ with $k \in (0, 1]$ elsewhere in the domain. In this case, the polymer fraction would not depend on the radius R and it would have a discontinuity at or around zero rather than being smooth.

3.2.5 Cavity Surface Energy

We primarily focus the study on the total free energy of the gel defined above. However, in the case of a spherical cavity of radius ρ within the gel, we may want to quantify the energy required for its nucleation. First, we denote the energy per unit area by σ_{gel} .

This quantity is material specific and is a constant value for the material in question. Hence, the total free energy of cavity nucleation for a gel is given by

$$E_\rho = \int_{\Gamma_\rho} \sigma_{gel} dS,$$

where Γ_ρ denotes the cavity surface. In particular, the nucleation energy is given by $E_\rho = 4\pi\rho^2\sigma_{gel}$ for a spherical domain Ω_0 and a purely radial deformation acting on it.

Remark 6. If we could not give a specific value for σ_{gel} in some cases, we may alternatively determine an upper bound for it, denoted by σ_{gel}^* : If a deformation with cavity occurs, it means that under the same boundary conditions such deformation yields a lower total free energy than a deformation without cavity under the same boundary conditions. The upper bound σ_{gel}^* is then determined by the difference of these two energies.

Chapter 4

Radial Energy Minimizers

4.1 Existence of Minimizer

We start this section by recalling the general existence theorem of minimizers for a deformation, given in Theorem 2.3.18. Let

$$f : \Omega_0 \times \mathbb{R}^m \times \mathbb{R}^{m \times n}$$

be a smooth function and let us define the functional

$$I[\mathbf{x}] = \int_{\Omega_0} f(\mathbf{X}, \mathbf{x}(\mathbf{X}), \nabla \mathbf{x}(\mathbf{X})) d\mathbf{X},$$

with $\mathbf{x} : \Omega_0 \rightarrow \mathbb{R}^m$. Let f satisfy the coercivity inequality (2.35), that is $\exists A_1 > 0, A_2 \geq 0$ such that $f(\mathbf{X}, \mathbf{x}, \underline{\xi}) \geq A_1 |\underline{\xi}|^p - A_2$, $\forall \mathbf{X} \in \Omega_0, \mathbf{x} \in \mathbb{R}^m, \underline{\xi} \in \mathbb{R}^{m \times n}$ and $p \geq 1$. Moreover, let f be polyconvex, as defined in (2.3.14), namely that if for each fixed $\mathbf{x} \in \mathbb{R}^m, \mathbf{X} \in \Omega_0$, the joint mapping $(\underline{\xi}, \Upsilon) \mapsto f(\mathbf{X}, \mathbf{x}, \underline{\xi}, \Upsilon)$ is convex. Finally, let us define an admissible set by

$$\mathcal{A} = \{\mathbf{x} \in \mathcal{X} \mid \text{restrictions and boundary conditions}\},$$

with \mathcal{A} non-empty, where \mathcal{X} is a normed vector space to be determined. An example for an admissible set would be $\mathcal{A}_1 = \{\mathbf{x} \in W^{1,p} \mid \det \nabla \mathbf{x} > 0, \mathbf{x} = \mathbf{x}_0 \text{ on } \partial\Omega_0\}$.

Theorem 4.1.1. *Let f satisfy the coercivity inequality and let f be polyconvex. Furthermore, suppose that the admissible set \mathcal{A} is non-empty. Then there exists $\bar{\mathbf{x}} \in \mathcal{A}$ solving $I[\bar{\mathbf{x}}] = \min_{\mathbf{y} \in \mathcal{A}} I[\mathbf{y}]$.*

Proof. The proof is based on [32], and we only highlight the major steps here. A lower bound for I follows from the coercivity inequality, which then implies that there exists a subsequence of infimizing sequence that converges weakly to $\bar{\mathbf{x}}$. It remains to show that $\bar{\mathbf{x}} \in \mathcal{A}$, which is done in two steps: first, the weak lower-semicontinuity of the determinant and the polyconvexity of I imply that I is lower semi-continuous. Using this and Mazur's lemma, the result follows. \square

We note that in our study, the function f represents a stored energy function W and the functional I is the total free energy of the material, denoted E_{tot} .

In [9], the author proves the existence of radial minimizers for a specific class of energies of the form $\sum_{i=1}^3 \bar{W}_1(\kappa_i) + \bar{W}_2(\kappa_1\kappa_2\kappa_3)$, where κ_i are the principal stretches of the deformation, namely $\kappa_1 = r, \kappa_2 = \kappa_3 = \frac{r}{R}$. The admissible set is

$$\mathcal{A}_\lambda = \{r \in W^{1,1}(0,1) \mid r(0) \geq 0, r, r_R(R) > 0 \text{ a.e.}, r(1) = \lambda \text{ and } \bar{E}_{tot} < \infty\},$$

for the radial displacement boundary value problem, $\lambda > 0$, and the theorem is as follows:

Theorem 4.1.2. *Let us assume that $\bar{W}_1 : (0, \infty) \rightarrow [0, \infty)$ is C^1 and convex (H1), $\lim_{\kappa \rightarrow \infty} \bar{W}_1(\kappa) = \infty$ (H2), $\bar{W}_2 : (0, \infty) \rightarrow \mathbb{R}$ is C^1 and strictly convex (H3), and $\lim_{\kappa \rightarrow 0^+} \bar{W}_2(\kappa) = \lim_{\kappa \rightarrow \infty} \frac{\bar{W}_2(\kappa)}{\kappa} = \infty$. Then \bar{E}_{tot} attains an absolute minimum on \mathcal{A}_λ .*

The author proves the existence of a radial minimizer for a traction boundary value problem as well, by replacing (H2) with $\bar{W}_1(\kappa) \geq K\kappa^\gamma$, for all κ , with $K > 0$ and $\gamma > 1$ (H2') and a corresponding set of admissible minimizers. For $s = 1$, we can decompose \bar{W} in such a way, namely $\bar{W}_1 := \frac{\nu}{2} |\mathbf{F}|^2$ and $\bar{W}_2 := \bar{W} - \bar{W}_1$. Indeed, we have that (H1), (H2), (H2'), (H3) and (H4) are verified, where we require $\phi_0 < \det \mathbf{F}$ and $\frac{1}{n\phi_1} + \frac{1}{\phi_2} \geq 2\chi$ (with $>$ if $\bar{\zeta}_1 = \bar{\zeta}_2 = 0$) to satisfy (H3). We note that this existence result of radial minimizers is not restricted to solid materials, and hence applies to our gel mixture.

4.2 Euler-Lagrange Equations

The existence theorem for solutions to Euler-Lagrange equations is for instance given in [25]. Assuming the same notation as above, we have that

Theorem 4.2.1. *Let Ω_0 be a bounded open set with Lipschitz boundary. Let $f : \Omega_0 \times \mathbb{R}^m \times \mathbb{M}^{m \times n}$ be as above and satisfy the following growth conditions*

1. $|f(\mathbf{X}, \mathbf{x}, \underline{\xi})| \leq \beta (1 + |\mathbf{x}|^p + |\underline{\xi}|^p)$
2. $|f_{,\mathbf{x}}(\mathbf{X}, \mathbf{x}, \underline{\xi})| \leq \beta (1 + |\mathbf{x}|^{p-1} + |\underline{\xi}|^{p-1})$
3. $|f_{,\underline{\xi}}(\mathbf{X}, \mathbf{x}, \underline{\xi})| \leq \beta (1 + |\mathbf{x}|^{p-1} + |\underline{\xi}|^{p-1})$

for some $\beta \geq 0$ and for all $\mathbf{X} \in \Omega_0$, $\mathbf{x} \in \mathbb{R}^m$ and $\underline{\xi} \in \mathbb{M}^{m \times n}$. Let $\bar{\mathbf{x}}$ be a minimizer of $\inf_{\bar{\mathbf{y}} \in \mathcal{A}} I[\bar{\mathbf{y}}]$. Then \bar{x} satisfies the weak form of the Euler-Lagrange equations

$$-\sum_{i=1}^n \left(f_{\xi_i^k}(\mathbf{X}, \mathbf{x}, \underline{\xi}) \right)_{X_i} + f_{x^k}(\mathbf{X}, \mathbf{x}, \underline{\xi}) = 0 \quad (4.1)$$

on Ω_0 and $x^k = g^k$ on $\partial\Omega_0$ for $k = 1, \dots, m$.

Remark 7. We say that \bar{x} is a weak solution of (4.1) if it satisfies

$$\sum_{k=1}^m \int_{\Omega_0} \sum_{i=1}^n f_{\xi_i^k}(\mathbf{X}, \mathbf{x}, \underline{\xi}) y_{X_i}^k + f_{x^k}(\mathbf{X}, \mathbf{x}, \underline{\xi}) y^k d\mathbf{x} = 0,$$

for all $\mathbf{y} \in W_0^{1,p}(\Omega_0, \mathbb{R}^m)$, with $\mathbf{y} = (y^1, \dots, y^m)$.

Given the existence of a minimizer, we derive the Euler-Lagrange equations for the energy, as described in the Chapter on Mathematical Prerequisites, under the section on Calculus of Variations. Let $\mathbf{x} \in \mathcal{A}$ be a critical point of E_{tot} , and let $\mathbf{y} \in \mathcal{A}$ be arbitrary. Let us define the real valued function by

$$i : \mathbb{R} \rightarrow \mathbb{R}; t \mapsto i(t) := E_{tot}[\mathbf{x} + t\mathbf{y}], \quad (4.2)$$

for $t \in \mathbb{R}$. Since \mathbf{x} is a critical point of $E_{tot}[\cdot]$, we have that $i(t)$ has an extremum at $t = 0$, i.e. $i'(0) = 0$, which is the first variation. This extremum is a minimum, making \mathbf{x} a minimizer, if $i''(0) \geq 0$, which is the second variation. For the remaining part of

this work, we want to find the minimizer exclusively, so that the second variation needs to be fulfilled. To obtain the Euler-Lagrange equation, we explicitly compute $i'(0) = 0$. We work with dimensionless quantities as it facilitates the analysis, and we note that the results above for W and E_{tot} also apply to \bar{W} and \bar{E}_{tot} . We have

$$\begin{aligned} \bar{E}_{tot} = \int_{\Omega_0} \phi_0 \left[\frac{\nu}{2s} |\underline{\mathbf{F}}|^{2s} + \bar{\zeta}_1 (\det \underline{\mathbf{F}})^{-\beta_1} + \bar{\zeta}_2 (\det \underline{\mathbf{F}})^{\beta_2} \right. \\ \left. + \frac{1}{n} \ln \frac{\phi_0}{\det \underline{\mathbf{F}}} + \left(\frac{\det \underline{\mathbf{F}}}{\phi_0} - 1 \right) \ln \left(1 - \frac{\phi_0}{\det \underline{\mathbf{F}}} \right) + \chi \left(1 - \frac{\phi_0}{\det \underline{\mathbf{F}}} \right) \right] d\mathbf{X}. \end{aligned} \quad (4.3)$$

We compute the derivative of $i(t) = \bar{E}_{tot}[\mathbf{x} + t\mathbf{y}] = \int_{\Omega_0} \bar{W}(\mathbf{X}, \mathbf{x} + t\mathbf{y}, \nabla(\mathbf{x} + t\mathbf{y})) d\mathbf{X}$ with respect to t at $t = 0$, with $\mathbf{x}, \mathbf{y} \in \Omega$ and \mathbf{x} an extremum of I :

$$\begin{aligned} 0 = i'(0) \\ = \int_{\Omega_0} \left\{ \nu \phi_0 |\nabla \mathbf{x}|^{2(s-1)} \nabla \mathbf{x} - \phi_0 \left[\bar{\zeta}_1 \beta_1 (\det \nabla \mathbf{x})^{-\beta_1} - \bar{\zeta}_2 \beta_2 (\det \nabla \mathbf{x})^{\beta_2} \right] (\nabla \mathbf{x})^{-1} \right. \\ \left. - \left[\frac{1}{n} \phi_0 - \left(\phi_0 + \det \nabla \mathbf{x} \ln \frac{\det \nabla \mathbf{x} - \phi_0}{\det \nabla \mathbf{x}} \right) - \frac{\chi \phi_0^2}{\det \nabla \mathbf{x}} \right] (\nabla \mathbf{x})^{-1} \right\} : \nabla \mathbf{y}^T d\mathbf{X}, \end{aligned}$$

where we used the definition $\text{tr}(\nabla \mathbf{y}(\nabla \mathbf{x})^{-1}) = (\nabla \mathbf{x})^{-1} : \nabla \mathbf{y}$. This is the weak formulation of the Euler-Lagrange equations corresponding to the minimization problem of the total free energy \bar{E}_{tot} . We determine the strong form as before by defining $P(\nabla \mathbf{x})$ to be the expression within the brackets.

$$\begin{aligned} P(\nabla \mathbf{x}) := \nu \phi_0 |\nabla \mathbf{x}|^{2(s-1)} \nabla \mathbf{x} - \phi_0 \left[\bar{\zeta}_1 \beta_1 (\det \nabla \mathbf{x})^{-\beta_1} - \bar{\zeta}_2 \beta_2 (\det \nabla \mathbf{x})^{\beta_2} \right] (\nabla \mathbf{x})^{-1} \\ - \left[\frac{1}{n} \phi_0 - \left(\phi_0 + \det \nabla \mathbf{x} \ln \frac{\det \nabla \mathbf{x} - \phi_0}{\det \nabla \mathbf{x}} \right) - \frac{\chi \phi_0^2}{\det \nabla \mathbf{x}} \right] (\nabla \mathbf{x})^{-1} \end{aligned}$$

We recall that by invoking the Divergence Theorem, we get

$$0 = \int_{\Omega_0} P(\nabla \mathbf{x}) : \nabla \mathbf{y}^T d\mathbf{X} = \int_{\partial\Omega_0} [P(\nabla \mathbf{x})^T \mathbf{n}] \cdot \mathbf{y}^T dS - \int_{\Omega_0} [\nabla \cdot P(\nabla \mathbf{x})] \cdot \mathbf{y}^T d\mathbf{X}. \quad (4.4)$$

Since this equation is true for any \mathbf{y} , we get the Euler-Lagrange equations to be

$$\nabla \cdot P(\nabla \mathbf{x}) = 0. \quad (4.5)$$

Also, we note that the natural boundary conditions are given by $0 = P(\nabla \mathbf{x})^T \mathbf{n}$.

Assuming radial symmetry for the volume fracture function, i.e. $\phi_0(\mathbf{X}) = \phi_0(R)$, we use the computations in the appendix to obtain (4.5) explicitly:

$$\begin{aligned}
0 = & \nu \left(r_{,R}^2 + 2 \frac{r^2}{R^2} \right)^{s-1} \\
& \cdot \left[2(s-1)\phi_0 \frac{r_{,RR}r_{,R}^2 R^3 + 2r_{,R}r(r_{,R}R - r)}{R(r_{,R}^2 R^2 + 2r^2)} + \phi_0 \left(r_{,RR} + 2 \frac{r_{,R}}{R} - 2 \frac{r}{R^2} \right) + \phi_{0,R}r_{,R} \right] \\
& + \bar{\zeta}_1 \beta_1 \left(r_{,R} \frac{r^2}{R^2} \right)^{-\beta_1} \left\{ \frac{\phi_0 \left[(r_{,RR}r + 2r_{,R}^2)R - 2r_{,R}r \right] (\beta_1 + 1)}{r_{,R}^2 r R} - \frac{\phi_{0,R}}{r_{,R}} \right\} \\
& + \bar{\zeta}_2 \beta_2 \left(r_{,R} \frac{r^2}{R^2} \right)^{\beta_2} \left\{ \frac{\phi_0 \left[(r_{,RR}r + 2r_{,R}^2)R - 2r_{,R}r \right] (\beta_2 - 1)}{r_{,R}^2 r R} + \frac{\phi_{0,R}}{r_{,R}} \right\} \\
& + \frac{\phi_0 \left[(r_{,RR}r + 2r_{,R}^2)R - 2r_{,R}r \right] - \phi_{0,R}r_{,R}r R}{r_{,R}^2 r} \left(\frac{1}{nR} + \frac{\phi_0 R}{r_{,R}r^2 - \phi_0 R^2} - \frac{2\chi\phi_0 R}{r_{,R}r^2} \right).
\end{aligned} \tag{4.6}$$

We note that the purely radial deformation $r = \lambda R$, for $\lambda > 0$, together with $\phi_0(R)$ constant, is always a trivial solution as $r_{,R} = \lambda$, $r_{,RR} = 0$, and (4.6) becomes $0 = 0$.

On the other hand, we may consider a purely radial deformation $r = \lambda R$, but assume $\phi_0(R)$ to be non-constant. Then the explicit Euler-Lagrange equation (4.6) gives that

$$\frac{\phi_{0,R}}{\lambda} \left[\nu \lambda^2 (2\lambda^2)^{s-1} - \bar{\zeta}_1 \beta_1 \lambda^{-2\beta_1} + \bar{\zeta}_2 \beta_2 \lambda^{2\beta_2} - \frac{1}{n} - \frac{\phi_0}{\lambda^2 - \phi_0} + \chi \frac{2\phi_0}{\lambda^2} \right] = 0.$$

Since the first term is non-zero, the second must be zero. However, we see that ϕ_0 does not depend on the radial variable R when isolating and expressing it as a function of the other terms, since none of the coefficients do. Hence, the polymer volume fraction in the reference configuration must be constant for a purely radial deformation.

In a first step, we assumed that the total free energy of the gel only depends on the deformation gradient $\underline{\mathbf{F}}$, and carried out the energy minimization by using the balance of mass to substitute for the polymer fraction ϕ_1 . In a second attempt, we may omit this substitution so that the total free energy depends explicitly on both the deformation gradient $\underline{\mathbf{F}}$ and the polymer volume fraction ϕ_1 . Therefore, we start by expressing the total stored energy density W in terms of $\underline{\mathbf{F}}$ and ϕ_1 .

$$W(\underline{\mathbf{F}}, \phi_1) = \frac{\phi_0 \nu}{2s} |\underline{\mathbf{F}}|^{2s} + \phi_0 \left[\bar{\zeta}_1 (\det \underline{\mathbf{F}})^{-\beta_1} + \bar{\zeta}_2 (\det \underline{\mathbf{F}})^{\beta_2} \right] \\ + \det \underline{\mathbf{F}} \left[\frac{1}{n} \phi_1 \ln \phi_1 + (1 - \phi_1) \ln(1 - \phi_1) + \chi \phi_1 (1 - \phi_1) \right].$$

Hence, the total free energy of the gel E_{tot} in terms of $\underline{\mathbf{F}}$ and ϕ_1 becomes

$$E_{tot} = E_{tot}(\underline{\mathbf{F}}, \phi_1) = \int_{\Omega_0} W(\underline{\mathbf{F}}, \phi_1) d\mathbf{X}. \quad (4.7)$$

We relate the two variables $\underline{\mathbf{F}}$ and ϕ_1 by introducing the concept of constraints, a notion we mentioned in Remark 2, and we follow [33] for the work below. In our case, it is appropriate to introduce the integral constraint of the form

$$C_1(\underline{\mathbf{F}}, \phi_1) := \int_{\Omega_0} c_1(\mathbf{X}, \mathbf{x}, \underline{\mathbf{F}}, \phi_1) d\mathbf{X} = C_0, \quad (4.8)$$

where c_1 is a smooth function relating the variables $\underline{\mathbf{F}}$ and ϕ_1 , and prescribes the constraint. C_0 is a constant depending on the parameters of the problem. We seek for minimizers $\mathbf{x} \in \mathcal{A}$ of the total free energy E_{tot} given by (4.7), subject to the constraint (4.8), and such that \mathbf{x} is not an extremum of the constrain function C_1 itself. Then, there exists a constant $\Lambda > 0$, called the Lagrange Multiplier, such that \mathbf{x} is the critical point of the constrained energy E_{cstr} given by

$$E_{cstr}(\underline{\mathbf{F}}, \phi_1) = E_{tot}(\underline{\mathbf{F}}, \phi_1) + \Lambda [C(\underline{\mathbf{F}}, \phi_1) - C_0] \\ = \int_{\Omega_0} W(\underline{\mathbf{F}}, \phi_1) + \Lambda c(\underline{\mathbf{F}}, \phi_1) d\mathbf{X} - \Lambda C_0. \quad (4.9)$$

The constraint in our case is the balance of mass from Proposition 3.1.1, so that we get

$$C_1(\underline{\mathbf{F}}, \phi_1) = \int_{\Omega_0} \phi_1 \det \underline{\mathbf{F}} d\mathbf{X}, \quad C_0 = \int_{\Omega_0} \phi_0 d\mathbf{X}.$$

In case we were to impose multiple constraints, the above arguments would be still valid using multiple Lagrange multipliers.

Remark 8. We may also impose a non-integral constraint of the form $C_2(\underline{\mathbf{F}}, \phi_1) = 0$, where C_2 is a function describing the constraint between $\underline{\mathbf{F}}$ and ϕ_1 . We note that this constraint is local as it applies point by point, whereas the integral (4.8) was global as it

applied to the whole of the deformation \mathbf{x} . This implies that the Langrange multiplier for the non-constrained problem would depend on each position, that is $\Lambda = \Lambda(\mathbf{X})$. Hence, the constrained energy E_{cstr} to be minimized would be given by $E_{cstr}(\underline{\mathbf{F}}, \phi_1) = \int_{\Omega_0} W(\underline{\mathbf{F}}, \phi_1) + \Lambda(\mathbf{X})C_2 \, d\mathbf{X}$

Finally, we carry out the variational steps to find the extremum of the total free energy E_{tot} as we did before in the absence of a constraint. For $\underline{\mathbf{F}} = \nabla \mathbf{x}$, we define

$$f(\mathbf{X}, \mathbf{x}, \nabla \mathbf{x}) := W(\nabla \mathbf{x}, \phi_1(\mathbf{x})) + \Lambda C_1(\nabla \mathbf{x}, \phi_1(\mathbf{x})).$$

Then, we express the first variation as

$$i(t) = I[\mathbf{x} + t\mathbf{y}] = \int_{\Omega_0} f(\mathbf{X}, \mathbf{x} + t\mathbf{y}, \nabla(\mathbf{x} + t\mathbf{y})),$$

and we compute the derivative of $i(t)$ with respect to t at $t = 0$, where $\mathbf{x}, \mathbf{y} \in \Omega$ and \mathbf{x} an extremum of I . Hence, we obtain that

$$\begin{aligned} i'(0) &= \int_{\Omega_0} \left\{ \phi_0 \nu |\nabla \mathbf{x}|^{2(s-1)} \nabla \mathbf{x} + \phi_0 \left[-\bar{\zeta}_1 \beta_1 (\det \nabla \mathbf{x})^{-\beta_1} + \bar{\zeta}_2 \beta_2 (\det \nabla \mathbf{x})^{\beta_2} \right] (\nabla \mathbf{x})^{-1} \right. \\ &\quad \left. + \det \nabla \mathbf{x} \left[\frac{1}{n} \phi_1 \ln \phi_1 + (1 - \phi_1) \ln(1 - \phi_1) + \chi \phi_1 (1 - \phi_1) + \Lambda \phi_1 \right] (\nabla \mathbf{x})^{-1} \right\} : \nabla \mathbf{y}^T d\mathbf{X} \\ &\quad + \int_{\Omega_0} \left\{ \det \nabla \mathbf{x} \left[\frac{1}{n} (1 + \ln \phi_1) - (1 + \ln(1 - \phi_1)) + \chi(1 - 2\phi_1) + \Lambda \right] \frac{d}{d\mathbf{x}} \phi_1 \right\} \cdot \mathbf{y}^T d\mathbf{X}. \end{aligned}$$

We apply the Divergence Theorem, as seen in (4.4), to the first integral, and obtain

$$\begin{aligned} i'(0) &= \int_{\partial\Omega_0} \left\{ \phi_0 \nu |\nabla \mathbf{x}|^{2(s-1)} \nabla \mathbf{x} + \phi_0 \left[-\bar{\zeta}_1 \beta_1 (\det \nabla \mathbf{x})^{-\beta_1} + \bar{\zeta}_2 \beta_2 (\det \nabla \mathbf{x})^{\beta_2} \right] (\nabla \mathbf{x})^{-1} \right. \\ &\quad \left. + \det \nabla \mathbf{x} \left[\frac{1}{n} \phi_1 \ln \phi_1 + (1 - \phi_1) \ln(1 - \phi_1) + \chi \phi_1 (1 - \phi_1) + \Lambda \phi_1 \right] (\nabla \mathbf{x})^{-1} \right\} \mathbf{n} \cdot \mathbf{y}^T dS \\ &\quad - \int_{\Omega_0} \left\{ \nabla \cdot \left[\phi_0 \nu |\nabla \mathbf{x}|^{2(s-1)} \nabla \mathbf{x} + \phi_0 \left[-\bar{\zeta}_1 \beta_1 (\det \nabla \mathbf{x})^{-\beta_1} + \bar{\zeta}_2 \beta_2 (\det \nabla \mathbf{x})^{\beta_2} \right] (\nabla \mathbf{x})^{-1} \right. \right. \\ &\quad \left. \left. + \det \nabla \mathbf{x} \left[\frac{1}{n} \phi_1 \ln \phi_1 + (1 - \phi_1) \ln(1 - \phi_1) + \chi \phi_1 (1 - \phi_1) + \Lambda \phi_1 \right] (\nabla \mathbf{x})^{-1} \right] \right. \\ &\quad \left. - \det \nabla \mathbf{x} \left[\frac{1}{n} (1 + \ln \phi_1) - (1 + \ln(1 - \phi_1)) + \chi(1 - 2\phi_1) + \Lambda \right] \frac{d}{d\mathbf{x}} \phi_1 \right\} \cdot \mathbf{y}^T d\mathbf{X}. \end{aligned}$$

Since both surface and volume integrals are true for any test function y , we obtain that the surface integral yields the natural boundary conditions and that the volume integral yields the strong form of the Euler-Lagrange equations.

4.3 Minimizing Solutions

4.3.1 Boundary Conditions

Let the binary mixture of polymer and solvent occupy a unit spherical body Ω_0 in the reference configuration. Let the surrounding environment be an infinite space of the solvent composing the gel. We start by defining three different types of boundaries $\partial\Omega_0$ of the body.

1. Permeable: both polymer and solvent can cross the boundary;
2. Impermeable: neither polymer nor solvent can cross the boundary;
3. Semi-permeable: only solvent can cross the boundary, not polymer.

The case of a semi-permeable boundary gives rise to the definition of a thermodynamic force, called the osmotic pressure:

Definition 4.3.1. The osmotic pressure, denoted by Π , is the minimum force per unit area on the boundary $\partial\Omega_0$ required to prevent the solvent from moving across the semi-permeable boundary.

As previously observed, we consider a traction-free condition on the boundary of the cavity, that is the radial component of the Cauchy stress tensor at the cavity boundary ρ is zero:

$$T_{rr}(\rho) = 0.$$

In particular, we need to determine the response function \hat{T} . We recall that for a hyperelastic body, T is given by

$$\underline{\mathbf{T}}(\underline{\mathbf{F}}) := \frac{1}{\det \underline{\mathbf{F}}} \frac{\partial W}{\partial \underline{\mathbf{F}}} \underline{\mathbf{F}}^T. \quad (4.10)$$

Given the total stored energy density W for a gel above, we obtain that the Cauchy stress tensor is

$$\underline{\mathbf{T}} = \left\{ \frac{\nu\phi_0}{\det \underline{\mathbf{F}}} |\underline{\mathbf{F}}|^{2(s-1)} \underline{\mathbf{F}} \underline{\mathbf{F}}^T + \phi_0 \dot{h} - \frac{\phi_0}{n \det \underline{\mathbf{F}}} + \left[\frac{\phi_0}{\det \underline{\mathbf{F}}} + \ln \left(1 - \frac{\phi_0}{\det \underline{\mathbf{F}}} \right) \right] + \frac{\chi\phi_0^2}{(\det \underline{\mathbf{F}})^2} \right\} \mathbf{I}. \quad (4.11)$$

For $\mathbf{n} = \begin{bmatrix} 1 & 0 \end{bmatrix}^T$ being a normal radial vector, we have that the outward pressures at the outer and inner boundaries are given by

$$\mathbf{t}_1 = \underline{\mathbf{T}}\mathbf{n}, \quad \text{and} \quad \mathbf{t}_2 = -\underline{\mathbf{T}}\mathbf{n},$$

respectively. Equivalently, we can reformulate this condition in terms of the reference configuration by using the radial component of First Piola-Kirchhoff stress tensor $\underline{\mathbf{P}}$:

$$\lim_{R \rightarrow 0^+} P_{RR}(R) = 0.$$

We consider two types of boundary conditions at the outer boundary $\partial\Omega_0$, namely at $R = 1$, which we have seen in [9].

1. Displacement boundary condition: $r(1) = \lambda$, where $\lambda > 0$ is a uniform and symmetric expansion on the boundary of the body.
2. Traction-free boundary condition: $T_{rr}(1) = 0$, corresponding to a free swelling of the gel upon insertion to a fluid environnement consisting of the gel's solvent component.

We note that for $\lambda = 1$, we have no deformation, for $\lambda < 1$ we have compression and for $\lambda > 1$ we have expansion, and we consider the latter case.

4.3.2 Solution without Cavity

Let Ω_0 be the unit spherical domain of the gel in the reference configuration and let us consider of a deformation with no cavity. We recall that the principal stretches of the deformation are κ_1, κ_2 and κ_3 , the square roots of the eigenvalues of $\underline{\mathbf{B}} = \underline{\mathbf{F}} \underline{\mathbf{F}}^T$. We may have two approaches for the deformation: On the one hand, the gel may be immersed in a fluid environment and swell by absorbing water. It expands symmetrically in all directions when $\kappa_1 = \kappa_2 = \kappa_3 = \kappa$, if no forces are acting on it, until it reaches an equilibrium. On the other hand, we may apply a uniform symmetric displacement $\lambda > 1$ at $\partial\Omega_0$, that is $r(1) = \lambda$. We can combine the two approaches by stating that $\kappa = \lambda$.

Swelling Equilibrium

In both cases, we want to determine the optimal state of mixing, that is the equilibrium state of the gel with respect to the polymer fraction ϕ_1 . Therefore, we consider the total free energy in terms of the polymer volume fraction as

$$E_{tot} = E_{tot}(\phi_1) = \int_{\Omega_0} W(\phi_1) d\mathbf{X}.$$

where $W(\phi_1)$ is the total stored energy density in terms of ϕ_1 . To find the optimal value, denoted by ϕ_1^* , we need to find the minimum of E_{tot} , that is the smallest $\frac{d}{d\phi_1} E_{tot} = 0$ such that $\frac{d^2}{d\phi_1^2} E_{tot} > 0$. This relation is equivalent to finding the smallest root of

$$\frac{d}{d\phi_1} W = 0. \quad (4.12)$$

Since $W(\phi_1) = \det \underline{\mathbf{F}} \{ \phi_1 W_E + W_{FH} \}$ and $\underline{\mathbf{F}} = \text{diag}(\lambda, \lambda, \lambda)$, as we consider a pure expansion, we obtain that

$$\begin{aligned} W(\phi_1) = \lambda^3 \left\{ \phi_1 \left[\frac{\mu}{2s} (3\lambda^2)^s + \zeta_1 \lambda^{-3\beta_1} + \zeta_2 \lambda^{3\beta_2} \right] \right. \\ \left. + a\phi_1 \ln \phi_1 + b(1 - \phi_1) \ln(1 - \phi_1) + c\phi_1(1 - \phi_1) \right\}, \end{aligned}$$

so that the solution to Equation (4.12) is given by

$$a \ln \phi_1^* - b \ln(1 - \phi_1^*) - 2c\phi_1^* = - \left[\frac{\mu}{2s} (3\lambda^2)^s + \zeta_1 \lambda^{-3\beta_1} + \zeta_2 \lambda^{3\beta_2} + a - b + c \right].$$

Remark 9. Swelling is an important phenomena for gels: we may assume the reference configuration to be a dry gel occupying a spherical domain, possibly even very dry with $\phi_0 = 1 - \epsilon$, where $\epsilon \ll 1$. The body, even though at equilibrium away from the fluid, becomes unstable upon insertion into a fluid medium: it starts absorbing the surrounding fluid and swells in order to release the residual stress. It continues swelling until it has swollen sufficiently to be in a stress-free state with the surrounding fluid with zero radial stress at the boundary $T_{rr}(r(1)) = 0$.

Minimizing Expansion without Cavity

For both displacement or swelling boundary conditions, we recall the case of a homogeneous gel with polymer fraction ϕ_0 constant. In this case, the deformation minimizing the total free energy of the gel is a purely homogeneous expansion $r(R) = \lambda R$, $\lambda > 0$, so that $\underline{\mathbf{F}} = \lambda I$. This implies that $\det \underline{\mathbf{F}} = \lambda^3$, so that $\phi_0 = \lambda^3 \phi_1$ by the balance of mass.

4.3.3 Solution with Cavity

We look for radially symmetric deformations $r(R)$, with $r(0) > 0$, which minimize our total free energy and are solutions of the Euler-Lagrange equations. In a dimensionless environment, the domain in the reference configuration is a unit ball.

We aim to find necessary conditions for which a solution with cavity, i.e. $r(0) > 0$ bifurcates from this trivial one. This leads us to the result based on Theorem 4.1.2: For sufficiently large λ , any radial deformation that is a minimizer of the energy $\bar{E}_{tot} = \int_{\Omega_0} \bar{W}(\mathbf{F}) d\mathbf{X}$ on \mathcal{A} satisfies $r(0) > 0$. A solution with a cavity of radius $0 < \rho := r(0)$ has formed. Such a solution with cavity only exists once a critical displacement λ_{cr} is attained, otherwise the trivial solution is the unique minimizer and is stable. At this point, we note that the cavity radius ρ will depend on λ , i.e. $\rho = \rho(\lambda)$.

The focus of this section is to determine how the theorem is compatible with the cavitation phenomena in gels. This leads us to the notion of phase separation.

Phase Separation

A mixture, such as a gel, may separate into high and low concentrated regions of its components upon the change of parameters of the system, such as temperature or pressure. These regions are called the concentrated and diluted phases, respectively, and this phenomenon is called phase separation. In particular, we invoke this concept to allow for the nucleation of a cavity. Our setup of a binary mixture requires the gel to partially separate into its two components as the cavity is composed of solvent component only.

We note that the deformation can occur under two different scenarios, corresponding the two boundary conditions seen previously. On the one hand, we may have a uniform radial stretch applied to the boundary, yielding the displacement boundary condition $r(1) = \lambda$, for $\lambda > 1$. On the other hand, we may encounter the more typical phenomenon for gels, namely free swelling, when the gel is immersed in an environment entirely composed of its fluid component. It absorbs the fluid until saturation, causing the gel to swell and to eventually relax, which yields a radially stress free boundary, expressed by $T_{rr}(1) = 0$.

We can distinguish between two scenarios of phase separation, characterized by the

type of deformation we consider.

Discontinuous Deformation

We have seen that, mathematically, cavitation is the result of a non-injective, and hence non-invertible, radial deformation $r(R)$, as the origin maps into a sphere of radius $r(0) = \rho > 0$. We recall that in the framework of nonlinear elasticity, the solid material within the ball Ω_0 deforms into a spherical shell Ω around the spherical cavity which remains empty. In a gel, however, the cavity is filled up with the solvent component of the gel, and the origin of the solvent depends on the outer boundary condition. We do not consider the solvent-filled cavity to be part of the deformed domain of the gel. This is a necessary hypothesis to reconcile cavity nucleation in gels with the mathematical framework of cavitation developed by Ball.

In the case of the displacement boundary condition, we assume that the solvent component in the cavity, after deformation, originates from the gel in the reference configuration. Mathematically, the mass of solvent component required to fill a cavity of radius $\rho > 0$ is given by

$$m_\rho = 4\pi^2 \int_0^\rho 1 \cdot r^2 dr = \frac{4\pi^3}{3} \rho^2. \quad (4.13)$$

Once we isolate m_ρ which is required to fill up the cavity, we deform the remaining gel which now has less solvent and hence more polymer. Hence, we use balance of mass (2.7) to determine the new solvent fraction which excludes m_ρ , and we get

$$4\pi^2 \int_0^1 \Gamma_2 [1 - \bar{\phi}_0(R)] R^2 dR = 4\pi^2 \int_0^1 \Gamma_2 [1 - \phi_0(R)] R^2 dR - m_\rho, \quad (4.14)$$

where Γ_2 is the intrinsic density of the solvent in the reference configuration. Here, $\bar{\phi}_0$ is the polymer fraction of the gel obtained from the original polymer fraction ϕ_0 , and excluding the solvent fraction that amounts to m_ρ . Explicitely, we have

$$\bar{\phi}_0 = \phi_0 + \rho^3. \quad (4.15)$$

We conclude that if a cavity of radius ρ forms after deformation, the solvent filling up the cavity is extracted from the gel of polymer fraction ϕ_0 in the reference configuration. Therefore, only the remaining gel, which now has polymer fraction $\bar{\phi}_0$ is deformed to the shell surrounding the cavity.

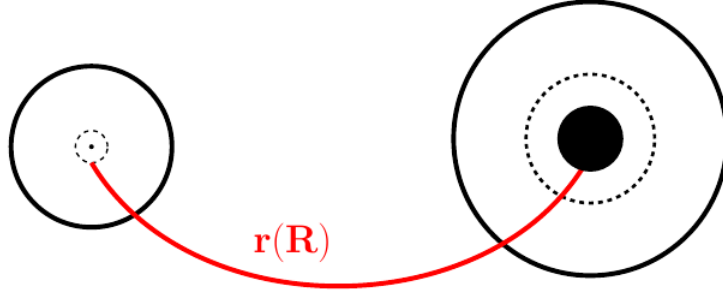


Figure 4.1: Cavity Formation through Phase Separation

From a different perspective, the free-swelling of the gel follows from a gel with initially low polymer fraction ϕ_0 being placed in an infinite environment of solvent component. The gel absorbs solvent component until it attains an equilibrium state. If a cavity forms, we assume it to be filled with the solvent component originating from the environment the gel is immersed into, and not from the gel itself. Hence, this method does not require balance of mass to account for the solvent in the cavity.

Continuous Deformation

There is a second approach for looking at the formation of a cavity within a gel, assuming balance of mass (2.7). We assume the gel in the reference configuration to have a polymer volume fraction $\phi_0 > 0$ for $R \in \Omega_0 \setminus \{0\}$ and $\phi_0(0) = 0$. As previously mentioned, when a cavity forms in a gel, it is filled up with its solvent component as we don't allow for any other material to be present through the condition (3.1). Hence, a cavity could form in a gel in case of a continuous deformation, with $r(0) = 0$ and $\phi_2 \equiv 1$ for $0 \leq r \leq \rho$ for $\rho > 0$ being the cavity radius. This occurs in the case, if there is a phase separation that occurs.

In the case of an isolated system as noted above, we recall that solvent density in the mixture is given by $\rho_2 = \gamma_2 \phi_2$, and we have γ_2 non-constant. Therefore, the statement of balance of mass yields

$$\int_0^1 \phi_0(R) R^2 dR = \int_\rho^\lambda \phi_1(r) r^2 dr, \quad (4.16)$$

$$\int_0^1 \Gamma_2 [1 - \phi_0(R)] R^2 dR = \int_0^\rho 1 \cdot r^2 dr + \int_\rho^\lambda \gamma_2 \phi_2(r) r^2 dr, \quad (4.17)$$

where Γ_2 is the intrinsic density of the solvent component in the reference configuration Ω_0 . We may simplify these relations by considering a non-isolated system, such as the free swelling of the gel.

In the latter case, where the gel of initially low polymer fraction ϕ_0 is placed in an infinite environment of solvent component, we are no longer in an isolated system. Therefore, as previously observed, we may assume the intrinsic density of the solvent to be constant, for instance $\gamma_2 = 1$, and hence $\rho_2 = \phi_2$. Hence, by the balance of mass, we get

$$\int_0^1 \phi_0(R) R^2 dR = \int_\rho^\lambda \phi_1(r) r^2 dr, \quad (4.18)$$

$$\int_0^1 [1 - \phi_0(R)] R^2 dR = \int_0^\rho 1 \cdot r^2 dr + \int_\rho^\lambda \phi_2(r) r^2 dr. \quad (4.19)$$

At this point, we note that we may not explicitly determine the critical displacement λ_{cr} at which the cavitating solution bifurcates from the pure expansion. The research in the literature review, such as the review paper [13], focuses on stored energy densities of special types that implicitly allowed to determine λ_{cr} . Indeed, their method avoids to explicitly solve the Euler-Lagrange equations to obtain the minimizing deformation. Instead, they solve for the critical displacement by directly applying the problem constraints, a method only applicable for certain types of stored energy densities. They consequently do not need to address the singularity at the origin. Since our stored energy functional for a gel is of a different type, due to the Neo-Hookean elastic energy, we may not invoke their method. Therefore, we proceed with an alternative approach, which we describe in the next chapter.

Chapter 5

Stress Fields

In this final chapter, we approach the cavitation phenomenon from a physical point of view. Having the previously obtained insight that the cavity forms in the center of the sphere, we focus on assessing the stresses in the gel. More specifically, we analyze the stress at the center of the sphere and observe how it is impacted by changes in key parameters.

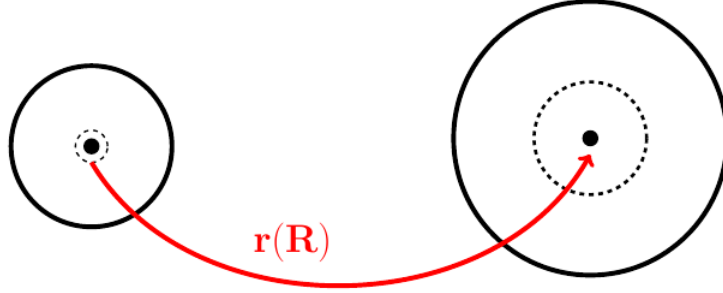
5.1 Configuration and Gel Model

To address the singularity at the origin during the numerical simulations, we assume a core of radius $0 < \delta \ll 1$ which does not change under any deformation. Therefore, in this chapter, the gel occupies a unit spherical domain $\Omega_0 = \{\mathbf{X} \in \mathbb{R}^3 \mid \delta \leq |\mathbf{X}| \leq 1\}$ in the reference configuration. We again denote the deformation map by $\Phi : \Omega_0 \rightarrow \Omega; \mathbf{X} \mapsto \mathbf{x}(\mathbf{X})$, which is purely radial so that $\mathbf{x}(\mathbf{X}) = \frac{r(R)}{R} \mathbf{X}$, with $R = |\mathbf{X}|$. We recall that the deformation gradient $\underline{\mathbf{F}}$ in spherical coordinates is given by

$$\underline{\mathbf{F}} = \nabla \mathbf{x} = \frac{\partial \mathbf{x}(\mathbf{X})}{\partial \mathbf{X}} = \text{diag} \left(r_{,R}, \frac{r}{R}, \frac{r}{R} \right).$$

We assume the same total free energy as previously defined in (3.11), namely

$$\begin{aligned} E_{tot} = \phi_0 \int_{\Omega_0} \frac{\mu}{2s} |\underline{\mathbf{F}}|^{2s} + \zeta_1 (\det \underline{\mathbf{F}})^{-\beta_1} + \zeta_2 (\det \underline{\mathbf{F}})^{\beta_2} \\ + a \ln \frac{\phi_0}{\det \underline{\mathbf{F}}} + b \left(\frac{\det \underline{\mathbf{F}}}{\phi_0} - 1 \right) \ln \left(1 - \frac{\phi_0}{\det \underline{\mathbf{F}}} \right) + c \left(1 - \frac{\phi_0}{\det \underline{\mathbf{F}}} \right) d\mathbf{X}. \end{aligned}$$



Contrary to the general form before, we focus in this chapter on the most significant parameters within a gel and their effects of the stress fields across the body. Therefore, we simplify the total free energy by making the following key assumptions. First, we only consider the Neo-Hookean case, that is when $s = 1$. Next, as described in the analysis of the Flory-Huggins energy, we have that $n \gg 1$. This implies that $a \ll b$, and hence shall be omitted for our analysis. Moreover, we also omit the compression and expansion parameters ζ_1 and ζ_2 in this step as the determinant is implicit in the Flory-Huggins energy of mixing.

We undimensionalize the total free energy according to (3.10), where we divided each parameter by $\frac{k_B T}{v_0}$, with k_B the Boltzman constant, T the temperature of the gel and v_0 the volume of one lattice site. Taking all these simplifying steps into account, the total free energy simplifies to

$$\bar{E}_{tot} = \phi_0 \int_{\Omega_0} \frac{\nu}{2} |\mathbf{F}|^2 + \ln \left(1 - \frac{\phi_0}{\det \mathbf{F}} \right) + \chi \left(1 - \frac{\phi_0}{\det \mathbf{F}} \right) d\mathbf{X}. \quad (5.1)$$

We recall that ϕ_0 is the polymer volume fraction, ν the polymer crosslink number density and χ is the Flory interaction parameter.

The Cauchy stress tensor is given by $\mathbf{T} = \hat{\mathbf{T}}(\mathbf{F}) := \frac{1}{\det \mathbf{F}} \frac{\partial W}{\partial \mathbf{F}} \mathbf{F}^T$, which we express in spherical coordinates. The boundary conditions will be of two types:

1. Fixed boundary condition at the core: $r(\delta) = \delta$ for $\delta > 0$ being the core radius.
2. Either radial displacement boundary condition, namely $r(1) = \lambda$ for $\lambda > 0$, or traction boundary conditions in terms of the Cauchy stress tensor, that is $T_{rr}(r(1)) = p_0$ with $p_0 \geq 0$, at the outer boundary.

We derived the Euler-Lagrange equations for the total reduced free energy \bar{E}_{tot} in the previous chapter. The strong form in radially symmetric coordinates is given in

(4.5), which for the simplified total free energy (5.1) becomes

$$0 = \nu\phi_0 \left(r_{,RR} + 2\frac{r_{,R}}{R} - 2\frac{r}{R^2} \right) + \frac{\phi_0 \left[(r_{,RR}r + 2r_{,R}^2)R - 2r_{,R}r \right]}{r_{,R}^2 r} \left(\frac{\phi_0 R}{r_{,R}r^2 - \phi_0 R^2} - \frac{2\chi\phi_0 R}{r_{,R}r^2} \right). \quad (5.2)$$

The radial component of the Cauchy stress tensor for (5.1) is given by

$$T_{rr}(r(R)) = \phi_0 \left\{ \frac{\nu R^2 r'}{r^2} + \left[\frac{R^2}{r^2 r'} + \frac{\ln \left(1 - \frac{\phi_0 R^2}{r^2 r'} \right)}{\phi_0} \right] + \frac{\chi\phi_0 R^4}{r^4 r'^2} \right\}. \quad (5.3)$$

5.2 Linearization

It is easy to see that the radial Euler-Lagrange equation (4.5) is highly nonlinear and only solvable numerically. In order to generate an analytical solution, we first need to linearize the equation. By doing so, we also need to linearize the Cauchy stress tensor. Therefore, we define

$$r = r_0 + \epsilon r_1 + \mathcal{O}(\epsilon^2), \quad (5.4)$$

where r_0 is a particular solution of (4.5) we want to linearize around, and r_1 a function to be determined. By (5.4), we have that

$$r' = r'_0 + \epsilon r'_1 + \mathcal{O}(\epsilon^2) \quad \text{and} \quad r'' = r''_0 + \epsilon r''_1 + \mathcal{O}(\epsilon^2).$$

We start by explicitly computing the linearized form of each term in (4.5), and we get

1. Trace term

$$r'^2 + 2\frac{r^2}{R^2} \rightarrow r_0'^2 + 2\frac{r_0^2}{R^2} + 2\epsilon \left(r'_0 r'_1 + 2\frac{r_0 r_1}{R^2} \right) + \mathcal{O}(\epsilon^2).$$

2. Determinant terms

$$\begin{aligned} \frac{r' r^2}{R^2} &\rightarrow \frac{r'_0 r_0^2}{R^2} \left(1 + \epsilon \frac{2r'_0 r_0 r_1 + r_0^2 r'_1}{r_0' r_0^2} \right) + \mathcal{O}(\epsilon^2), \\ \frac{R^2}{r' r^2} &\rightarrow \frac{R^2}{r'_0 r_0^2} \left(1 - \epsilon \frac{2r'_0 r_0 r_1 + r_0^2 r'_1}{r_0' r_0^2} \right) + \mathcal{O}(\epsilon^2). \end{aligned}$$

3. Laplace term (already linear)

$$R^2 r'' + 2Rr' - 2r \rightarrow R^2 r_0'' + 2Rr_0' - 2r_0 + \epsilon (R^2 r_1'' + 2Rr_1' - 2r_1) + \mathcal{O}(\epsilon^2).$$

4. Determinant “divergence” term

$$\begin{aligned} \frac{(r''r + 2r'^2)R - 2r'r}{r'^2 r} &\rightarrow \frac{(r_0''r_0 + 2r_0'^2)R - 2r_0'r_0}{r_0'^2 r_0} \\ &+ \epsilon \frac{(r_0' r_0^2 r_1'' - 2r_0'' r_0^2 r_1' - 2r_0'^3 r_1)R + 2r_0' r_0^2 r_1'}{r_0'^3 r_0^2} + \mathcal{O}(\epsilon^2). \end{aligned}$$

5. Flory-Huggins coefficient terms

$$\frac{\chi}{r'r^2} \rightarrow \frac{\chi}{r_0' r_0^2} \left(1 - \epsilon \frac{2r_0' r_0 r_1 + r_0^2 r_1'}{r_0' r_0^2} \right) + \mathcal{O}(\epsilon^2),$$

$$\frac{1}{r'r^2 - \phi_0 R^2} \rightarrow \frac{1}{r_0' r_0^2 - \phi_0 R^2} \left(1 - \epsilon \frac{2r_0' r_0 r_1 + r_0^2 r_1' - \phi_1 R^2}{r_0' r_0^2 - \phi_0 R^2} \right) + \mathcal{O}(\epsilon^2).$$

6. Finally, we have that $\frac{1}{r'} \rightarrow \frac{1}{r_0'} \left(1 - \epsilon \frac{r_1'}{r_0'} \right)$. Moreover, since we consider the Neo-Hookean case when $s = 1$, the divergence of the trace term $\frac{r'' r'^2 R^3 + 2r' r (r' R - r)}{R(r'^2 R^2 + 2r^2)}$ drops out automatically. Hence, it is not necessary to linearize it.

Combining the above linearizations of the individual terms, we can give the fully linearized version of (4.5) as follows

$$0 = \mathcal{F}_0(r_0, r_0', r_0'') + \epsilon \mathcal{F}_1(r_0, r_0', r_0'', r_1, r_1', r_1'') + \mathcal{O}(\epsilon^2). \quad (5.5)$$

Next, we choose r_0 to be the state at rest, that is $r_0 = R$. We have that $\mathcal{F}_0 = 0$ since \mathcal{F}_0 is the right hand side of (4.5) with $r = r_0$, which is a trivial solution (as the rest state) of the Euler-Lagrange equation. Hence, (5.5) implies that the first order term \mathcal{F}_1 is zero:

$$0 = \phi_0 (R^2 r_1'' + 2Rr_1' - 2r_1) \left(\nu + \frac{\phi_0}{1 - \phi_0} - 2\chi\phi_0 \right). \quad (5.6)$$

5.3 Linearized Solution

Finally, we want to determine the solution r_1 to the linearized Euler-Lagrange equations (5.6), subject to the boundary conditions mentioned above, namely $r_1(\delta) = \delta$ for $\delta > 0$ and $T_{rr}(r_1(1)) = p_0$. We have that the second order differential equation

$$R^2 r_1'' + 2R r_1' - 2r_1 = 0 \quad (5.7)$$

in (5.6) is called the “Euler equation”. Let us assume that $r_1 = R^\alpha$ for some constant α is a solution of (5.7). Substituting into (5.7) gives us

$$\alpha^2 + \alpha - 2 = 0. \quad (5.8)$$

If the roots of (5.8) are distinct and real, which is the case with $\alpha_1 = -2$ and $\alpha_2 = 1$, the solution of the differential equation (5.7) is a linear combination of R^{α_1} and R^{α_2} . Hence, we get that

$$r_1(R) = c_1 R^{-2} + c_2 R \quad (5.9)$$

is the solution to (5.7), with c_1 and c_2 are constants determined by the boundary conditions.

5.3.1 Displacement Boundary Conditions

On the one hand, we have that $r_1(\delta) = \delta$, which gives us $\delta = c_1 \delta^{-2} + c_2 \delta$. This implies that

$$c_2 = 1 - \frac{c_1}{\delta^3}.$$

On the other hand, let us assume a displacement boundary condition at $R = 1$, i.e $r(1) = \lambda$ for $\lambda > 0$, which implies $\lambda = c_1 + c_2 = c_1 + \left(1 - \frac{c_1}{\delta^3}\right)$. By solving for c_1 in terms of δ and λ , we get

$$c_1 = \frac{\delta^3(\lambda - 1)}{\delta^3 - 1}.$$

Consequently, we also obtain $c_2 = \frac{\delta^3 - \lambda}{\delta^3 - 1}$ and finally the solution critical deformation to energy E_{tot} subject to the boundary conditions $r(\delta) = \delta$ and $r(1) = \lambda$ is

$$r_1(R) = \frac{\delta^3(\lambda - 1)}{\delta^3 - 1} R^{-2} + \frac{\delta^3 - \lambda}{\delta^3 - 1} R. \quad (5.10)$$

5.3.2 Dead-load Traction Boundary Conditions

Alternatively, we may define free boundary conditions using the Cauchy stress tensor, namely by

$$T_{rr}(r(\delta)) = p_1, \quad T_{rr}(r(1)) = p_2.$$

where p_1 and p_2 represent pressures imposed on the boundary. We make the following observations:

1. We say that the outer boundary is free if $p_2 = 0$.
2. If $p_1 = p_2$, it immediately follows from (5.9) and the Cauchy stress tensor that $c_1 = 0$. Hence, $r_1(R) = c_2 R$, which corresponds to a uniform expansion.

5.4 Reverse Linearization

We may use a different approach to determine the minimizing radial deformation to the total free energy. Namely, we may first linearize the total free energy of the gel and then do the variational approach to obtain the Euler-Lagrange equations.

5.4.1 Linearization

The energy (5.1) is highly nonlinear, which originates from the determinant term. We linearize similarly as before, however we invoke a top-down approach. We define $\underline{\mathbf{F}} = \underline{\mathbf{F}}_0 + \epsilon \underline{\mathbf{F}}_1$ and obtain

$$\det \underline{\mathbf{F}} = \det(\underline{\mathbf{F}}_0 + \epsilon \underline{\mathbf{F}}_1) = \det \underline{\mathbf{F}}_0 \det(\underline{\mathbf{I}} + \epsilon \underline{\mathbf{F}}_0^{-1} \underline{\mathbf{F}}_1) \quad (5.11)$$

Moreover, we recall that for a square matrix $\underline{\mathbf{G}}$ of order n and for an orthonormal basis $\{\mathbf{e}_i\}_{i=1,\dots,n}$ of \mathbb{R}^n , we have

$$\begin{aligned} \det(\underline{\mathbf{I}} + \epsilon \underline{\mathbf{G}}) &= \det(\mathbf{e}_1 + \epsilon \mathbf{G}_1, \dots, \mathbf{e}_n + \epsilon \mathbf{G}_n) \\ &= \det(\mathbf{e}_1, \dots, \mathbf{e}_n) + \epsilon [\det(\mathbf{G}_1, \mathbf{e}_2, \dots, \mathbf{e}_n) + \dots + \det(\mathbf{e}_1, \dots, \mathbf{G}_n)] + \mathcal{O}(\epsilon^2) \\ &= 1 + \epsilon \sum_{i=1}^n G_{ii} + \mathcal{O}(\epsilon^2) \\ &= 1 + \epsilon \text{tr} \underline{\mathbf{G}} + \mathcal{O}(\epsilon^2), \end{aligned} \quad (5.12)$$

where $\underline{\mathbf{G}}_i$ are the column vectors of $\underline{\mathbf{G}}$, for $i = 1, \dots, n$. The first equality follows from the definition of the determinant and the second one from the linearity of the determinant. Finally, (5.11) and (5.12) imply that the linearization of the determinant is given by

$$\det(\underline{\mathbf{F}}_0 + \epsilon \underline{\mathbf{F}}_1) = \det \underline{\mathbf{F}}_0 [1 + \epsilon \text{tr}(\underline{\mathbf{F}}_0^{-1} \underline{\mathbf{F}}_1)]. \quad (5.13)$$

For instance, we may again consider the undeformed configuration around which we linearize, that is $\underline{\mathbf{F}}_0 = \underline{\mathbf{I}}$. Now, we may explicitly compute the linearized form of each term in (5.1), and we get

1. The trace term $\text{tr}(\underline{\mathbf{F}} \underline{\mathbf{F}}^T)$ is already linear, however we may still write

$$\begin{aligned} [\text{tr}(\underline{\mathbf{F}} \underline{\mathbf{F}}^T)]^s &\rightarrow [\text{tr}(\underline{\mathbf{F}}_0 \underline{\mathbf{F}}_0^T)]^s + \binom{s}{1} [\text{tr}(\underline{\mathbf{F}}_0 \underline{\mathbf{F}}_0^T)]^{s-1} [2\epsilon \text{tr}(\underline{\mathbf{F}}_0 \underline{\mathbf{F}}_1^T) + \epsilon^2 \text{tr}(\underline{\mathbf{F}}_1 \underline{\mathbf{F}}_1^T)] \\ &\quad + \binom{s}{2} [\text{tr}(\underline{\mathbf{F}}_0 \underline{\mathbf{F}}_0^T)]^{s-2} 4\epsilon^2 \text{tr}^2(\underline{\mathbf{F}}_0 \underline{\mathbf{F}}_1^T). \end{aligned}$$

2. Determinant terms alternative

$$\begin{aligned} (\det \underline{\mathbf{F}})^{-\beta_1} &\rightarrow (\det \underline{\mathbf{F}}_0)^{-\beta_1} \left[1 - \epsilon \beta_1 \text{tr}(\underline{\mathbf{F}}_0^{-1} \underline{\mathbf{F}}_1^T) + \epsilon^2 \frac{\beta_1(\beta_1 + 1)}{2} \text{tr}^2(\underline{\mathbf{F}}_0^{-1} \underline{\mathbf{F}}_1^T) \right], \\ (\det \underline{\mathbf{F}})^{\beta_2} &\rightarrow (\det \underline{\mathbf{F}}_0)^{\beta_2} \left[1 + \epsilon \beta_2 \text{tr}(\underline{\mathbf{F}}_0^{-1} \underline{\mathbf{F}}_1^T) + \epsilon^2 \frac{\beta_2(\beta_2 - 1)}{2} \text{tr}^2(\underline{\mathbf{F}}_0^{-1} \underline{\mathbf{F}}_1^T) \right]. \end{aligned}$$

3. Flory-Huggins coefficient terms Alternative

$$\ln \left(\frac{\phi_0}{\det \underline{\mathbf{F}}} \right) \rightarrow \ln \left(\frac{\phi_0}{\det \underline{\mathbf{F}}_0} \right) - \epsilon \text{tr}(\underline{\mathbf{F}}_0^{-1} \underline{\mathbf{F}}_1^T) + \epsilon^2 \frac{\text{tr}^2(\underline{\mathbf{F}}_0^{-1} \underline{\mathbf{F}}_1^T)}{2},$$

$$\begin{aligned} \ln \left(1 - \frac{\phi_0}{\det \underline{\mathbf{F}}} \right) &\rightarrow \ln \left(1 - \frac{\phi_0}{\det \underline{\mathbf{F}}_0} \right) + \frac{\phi_0}{\det \underline{\mathbf{F}}_0 - \phi_0} [\epsilon \text{tr}(\underline{\mathbf{F}}_0^{-1} \underline{\mathbf{F}}_1^T) - \epsilon^2 \text{tr}^2(\underline{\mathbf{F}}_0^{-1} \underline{\mathbf{F}}_1^T)] \\ &\quad - \frac{\phi_0^2}{2(\det \underline{\mathbf{F}}_0 - \phi_0)^2} \epsilon^2 \text{tr}^2(\underline{\mathbf{F}}_0^{-1} \underline{\mathbf{F}}_1^T), \end{aligned}$$

where we have used the Taylor expansion for the natural logarithm, which we recall to be $\ln(x) = \sum_{n=1}^{\infty} \frac{(-1)^{n+1}}{n} (x-1)^n$.

Combining the above linearizations of the individual terms, we can give the fully linearized version of the total radial energy (5.1) as follows

$$E_{tot}(\underline{\mathbf{F}}) = \mathcal{E}_0(\underline{\mathbf{F}}_0) + \epsilon \mathcal{E}_1(\underline{\mathbf{F}}_0, \underline{\mathbf{F}}_1) + \epsilon^2 \mathcal{E}_2(\underline{\mathbf{F}}_0, \underline{\mathbf{F}}_1). \quad (5.14)$$

We note that $\mathcal{E}_0 = E(\underline{\mathbf{F}}_0)$, which is a constant term and hence independent on $\underline{\mathbf{F}}_1$ so that it does not appear in the variation below.

5.4.2 First Variation

Finally, we perform a first variation on the total free energy, similarly as before. to derive the linearized Euler-Lagrange equations. Let $\underline{\mathbf{F}}_1$ such that $\underline{\mathbf{F}}_1 = \nabla \mathbf{x}_1$ for \mathbf{x}_1 a critical point of E_{tot} , and let $\underline{\mathbf{G}}_1 = \nabla \mathbf{y}_1$ with $\mathbf{y}_1 \in \mathcal{A}$, where \mathcal{A} is the admissible set of solutions. Let

$$i(t) := E_{tot}[\mathbf{x}_1 + t\mathbf{y}_1] = \mathcal{E}_0(\underline{\mathbf{F}}_0) + \epsilon \mathcal{E}_1(\underline{\mathbf{F}}_0, \underline{\mathbf{F}}_1 + t\underline{\mathbf{G}}_1) + \epsilon^2 \mathcal{E}_2(\underline{\mathbf{F}}_0, \underline{\mathbf{F}}_1 + t\underline{\mathbf{G}}_1)$$

for $t \in \mathbb{R}$ be as before. Since $\underline{\mathbf{F}}_1$ is a critical point of $\mathcal{E}_1 + \mathcal{E}_2$ and hence $E_{tot}[\cdot]$, we have that $i(t)$ has an extremum at $t = 0$, i.e. $i'(0) = 0$. To obtain the Euler-Lagrange equation, we explicitly compute $i'(0) = 0$. We obtain

$$\begin{aligned} 0 &= i'(0) \\ &= \int_{\Omega_0} \phi_0 \underline{\mathbf{F}}_0^{-1} \left\{ \nu [\text{tr}(\underline{\mathbf{F}}_0 \underline{\mathbf{F}}_0^T)]^{s-1} \left[\epsilon \underline{\mathbf{F}}_0^2 + \epsilon^2 \underline{\mathbf{F}}_0 \underline{\mathbf{F}}_1^T + 2(s-1) \epsilon^2 \frac{\text{tr}(\underline{\mathbf{F}}_0^{-1} \underline{\mathbf{F}}_1^T)}{\text{tr}(\underline{\mathbf{F}}_0 \underline{\mathbf{F}}_0^T)} \right] \right. \\ &\quad \left. - \chi \frac{\phi_0}{\det \underline{\mathbf{F}}_0} [-\epsilon + 2\epsilon^2 \text{tr}(\underline{\mathbf{F}}_0^{-1} \underline{\mathbf{F}}_1^T)] \right. \\ &\quad \left. \left[\epsilon \left(1 + \frac{\det \underline{\mathbf{F}}_0}{\phi_0} \ln \left(1 - \frac{\phi_0}{\det \underline{\mathbf{F}}_0} \right) \right) + \epsilon^2 \text{tr}(\underline{\mathbf{F}}_0^{-1} \underline{\mathbf{F}}_1^T) \frac{\phi_0}{\det \underline{\mathbf{F}}_0 - \phi_0} \right] \right\} : \underline{\mathbf{G}}_1^T d\mathbf{X}, \end{aligned}$$

which is the weak formulation of the Euler-Lagrange equations. We determine the strong form by defining $P(\underline{\mathbf{F}}_0, \underline{\mathbf{F}}_1)$ to be the expression within the brackets.

$$0 = \int_{\Omega_0} P(\underline{\mathbf{F}}_0, \underline{\mathbf{F}}_1) : \underline{\mathbf{G}}_1^T d\mathbf{X} = \int_{\partial\Omega_0} [P(\underline{\mathbf{F}}_0, \underline{\mathbf{F}}_1)^T N] \cdot \mathbf{y}_1^T dS - \int_{\Omega_0} [\nabla \cdot P(\underline{\mathbf{F}}_0, \underline{\mathbf{F}}_1)] \cdot \mathbf{y}_1^T d\mathbf{X}.$$

Since this equation is true for any \mathbf{y}_1 , we immediately get the Euler-Lagrange equations to be

$$\nabla \cdot P(\underline{\mathbf{F}}_0, \underline{\mathbf{F}}_1) = 0.$$

This can be explicitly rewritten as

$$0 = \epsilon^2 \phi_0 \mathbf{F}_0^{-1} \nabla \cdot \left\{ \nu [\text{tr}(\mathbf{F}_0 \mathbf{F}_0^T)]^{s-1} \left[\mathbf{F}_0 \mathbf{F}_1^T + 2(s-1) \frac{\text{tr}(\mathbf{F}_0^{-1} \mathbf{F}_1^T)}{\text{tr}(\mathbf{F}_0 \mathbf{F}_0^T)} \right] \right. \\ \left. + \left(\frac{\phi_0}{\det \mathbf{F}_0 - \phi_0} - \chi \frac{2\phi_0}{\det \mathbf{F}_0} \right) \text{tr}(\mathbf{F}_0^{-1} \mathbf{F}_1^T) \right\}, \quad (5.15)$$

where all the ϵ terms are omitted since they are constant and would drop out after derivation. Finally, for $s = 1$, for $\mathbf{F}_0 = \mathbf{I}$, and hence $\det \mathbf{F}_0 = 1$, as well as $\mathbf{F}_1 = \nabla \mathbf{x}_1$, we compute (5.15) in radial coordinates and we obtain

$$0 = \phi_0 (R^2 r_1'' + 2Rr_1 - 2r_1) \left(\nu + \frac{\phi_0}{1 - \phi_0} - 2\chi\phi_0 \right),$$

which is the same linearized Euler-Lagrange equation we previously obtained, as expected.

5.5 Numerical Results

In this section, we focus on solving the Euler-Lagrange equation (4.5) to determine the deformation r and the radial Cauchy stress profile. Here, a special focus is directed to the stress at the inner boundary and how it relates to the problem parameters.

5.5.1 Problem Setup

Since the equation (4.5) is highly nonlinear, we need to solve it numerically in order to obtain accurate results. This follows the previous approximations we obtained from the linearized equation (5.5). We proceed as follows: the nonlinear equation is of the form

$$\mathcal{F}(R, r, r', r'') = 0. \quad (5.16)$$

This is a second-order, nonlinear ordinary differential equation to be solved for r in terms of R . We solve (5.16) by reducing it to a system of two first order differential equations. Indeed, we define $u = r'$ and hence we get that $u' = r''$. We can extract r'' explicitly from (5.16) to obtain $r'' = \mathcal{G}(R, r, r')$ and we get

$$r' = u, \quad u' = \mathcal{G}(R, r, r'). \quad (5.17)$$

We can now implement (5.17) in MATLAB using the inbuilt ODE solver called `bvp4c`.

We recall that the boundary conditions are as mentioned above: The inner boundary of radius δ is fixed under the deformation r , namely $r(\delta) = \delta$. On the outer boundary, due to the constraints of the bvp4c, we impose displacement boundary conditions, that is $r(1) = \lambda$ for $\lambda > 0$.

Remark 10. We are interested in zero-stress boundary conditions on the outer boundary of the form $T_{rr}(r(1)) = 0$ as well. In order to impose this condition, we consider an initial guess for λ and optimize it by solving the differential equations until $T_{rr}(\lambda) = 0$.

Indeed, we obtain an initial guess by assuming that $r(R) = \lambda R$ near $R = 1$. This implies a simplified expression of T_{rr} at $r(1)$ which does only depend on λ , and no longer depend on r' as $r'(1) = \lambda$. Hence $T_{rr}(r(1))$ yields the initial λ_0 . We have that λ_0 is not the actual displacement at the outer boundary for which $T_{rr}(r(1)) = 0$ as we made the crude assumption of $r(R) = \lambda R$ at $R = 1$. Therefore, we optimize λ_0 by solving the Euler-Lagrange equations without this assumption until we obtain a λ for which $T_{rr}(r(1)) = 0$.

5.5.2 Parameters

In our upcoming simulations, we are investigating the gel's behavior based on certain material parameters and boundary conditions.

We start by defining the ranges for the material parameters. We aim to consider both fairly dry and wet gels as well as mixtures in between. Therefore, we consider the initial polymer volume fraction in ϕ_0 in the range $[0.1, 0.9]$. As described in [34], the polymer crosslink density number ν ranges between orders of magnitude 10^{-2} to 10^0 . We suppose a range of one order of magnitude for our computations, namely $\nu \in (10^{-2}, 10^{-1})$. In many materials as described in [35], we have that the Flory interaction parameter $\chi \in (0, 1)$, with only some outside this range. We shall assume as reference that $\chi = \frac{1}{4}$, and then take a slightly higher value, for instance $\chi = \frac{1}{2}$, to see its effect.

Finally, we consider a specific range for the respective boundary conditions. On the one hand, we consider both compression and expansion, hence allowing for λ to be both smaller and larger than unity. On the other hand, the inner radius δ is assumed to be

small relative to the outer radius, that is $\delta \ll 1$. We shall consider $\delta = 0.1$ as an upper boundary, and subsequently decrease it by one order of magnitude to study its effect on the stress and the total free energy.

5.5.3 Results

We run a certain number of simulations for various material parameters and different boundary conditions and categorize the results according to the two types of boundary conditions, namely displacement and dead-load traction.

Displacement Boundary Conditions

We start with the displacement boundary conditions $r(1) = \lambda$. For different λ , corresponding to both compression and expansion, we compute the corresponding radial displacements $r(R)$ solving the Euler-Lagrange equation (5.2) and hence minimize the total free energy E_{tot} .

In Figure 5.1, we plot these deformations as well as the strains $\frac{dr(R)}{dR}$, corresponding to the first principle stretch. We observe that the strain around δ sharply increases

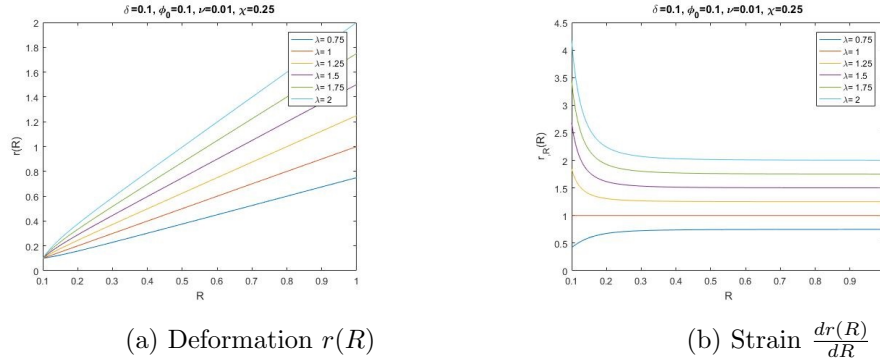


Figure 5.1: Reference Radial Deformations and Strains for Different Stretches

with the intensity of the expansion or the compression, and that we have a quasi-linear strain away from core. This expected, physical phenomenon confirms the validity of our results since more material moves near the point of attachment δ as the intensity of the stretch increases.

Furthermore, we may compare the deformation $r(R)$ obtained from the simulations to the explicit solution $r_1(R)$ of the linearized Euler-Lagrange equations. In Table 5.1, we summarize the differences between the two deformations in the \mathcal{L}^2 norm for different stretches λ and for the two inner boundary conditions $\delta_1 = 0.1$ and $\delta_2 = 0.01$. We

λ	1.0	1.25	1.5	2.0	5.0	10.0	100.0
$\ r - r_1\ _2^{\delta_1}$	0.0	0.0103	0.0197	0.0184	0.0017	1.90e-04	7.52e-08
$\ r - r_1\ _2^{\delta_2}$	0.0	5.19e-04	0.0016	0.0028	4.65e-04	4.53e-05	2.41e-05

Table 5.1: Error between r and r_1 for Different $\delta_1 = 0.1$ and $\delta_2 = 0.01$

observe that the linear and nonlinear solutions are, as expected, equal when we have no displacement. The difference spikes as we impose a displacement until a critical value at which it then continuously decreases to zero. Since the linearization is around the reference state $r(1) = 1$, it is not surprising that the difference increases as we move away from it. We note that we may use the explicit linearized result r_1 for large deformations as it converges to the nonlinear simulation.

From a different perspective, we may look at the stress fields related to the various stretches that we impose. Our main observation from Figure 5.2 is that we obtain the

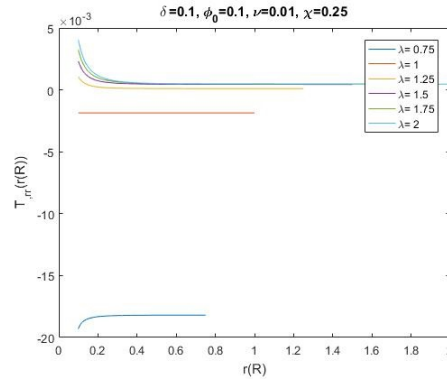


Figure 5.2: Reference Radial Stresses for Different Stretches

highest stress at the inner core. Moreover, we have an increase in stress at the core boundary as we increase the displacement. These results align with Ball's theory: On the one hand, the cavity always nucleates at the center since the stress is always highest there. On the other hand, the cavity nucleates after a critical stretch λ is attained.

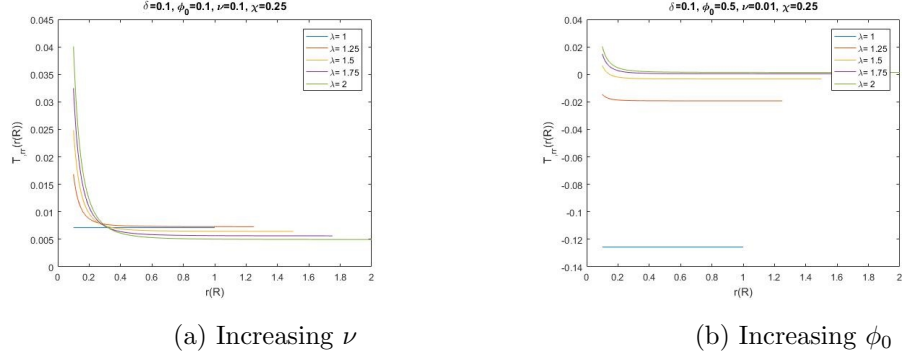


Figure 5.3: Radial Stresses with Modified Material Parameters for Different Stretches

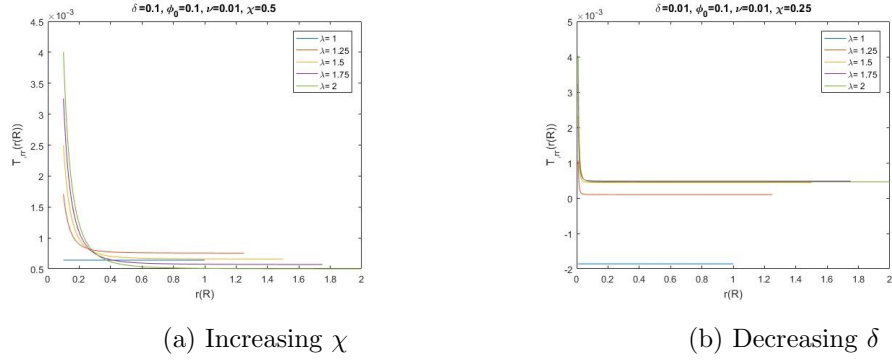


Figure 5.4: Radial Stresses with Modified Material Configuration for Different Stretches

Next, we change the material parameters to study the effects on the stress field. In Figure 5.3, we observe a spike in radial stresses as we increase both the polymer crosslink density ν and the polymer volume fraction ϕ_0 . We explain this by a restriction in material movement with a higher number of crosslinks, resulting in a stress increase. Similarly, there is more resistance with a higher value of ϕ_0 , which also leads to a significant increase in stress. The change of the Flory interaction parameter χ does not seem to have any obvious effects on the stress in Figure 5.4. However, we shall give an interpretation in the next section where the effect becomes more clear with the second type of boundary condition. Finally, we also observe from Figure 5.4 that the stress field is more abrupt as we decrease δ , which is due to a higher stress concentration at origin. However, the size of δ when $\delta \ll 1$ has no significant effect on the radial Cauchy stress $T_{rr}(\delta)$. This can also be shown analytically by using the linearized solution r_1

and explicitly computing the $T_{rr}(r_1(\delta))$.

Comparing Figures 5.2, 5.3 and 5.4 shows that the stress at the outer boundary is not monotonic with respect to the stretch. Indeed, by taking a closer look at our

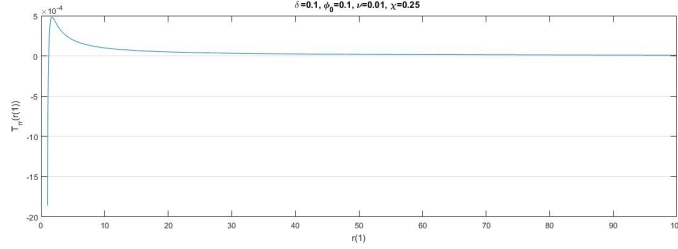


Figure 5.5: Reference Radial Stress at Outer Boundary for Different Stretches

reference state in Figure 5.5, we notice that the material is not relaxed in the reference configuration, that is $r(1) = 1$, but has a negative stress. As we increase the displacement, the material approaches its stress-free equilibrium, that is $T_{rr}(r(1)) = 0$. The stress initially increases as we continue expanding the material further. Finally, the stress decreases and asymptotically approaches zero again as the displacement goes to infinity. This is an artifact of the model at infinity as this behavior corresponds to the swelling of the gel by absorbing enough solvent to be saturated and attain a stress-free equilibrium. This occurs for a finite expansion, or compression depending on the material parameters. The notion of swelling equilibrium leads us now to the second type of boundary condition which is more appropriate for modeling gels.

Dead-load Traction Boundary Conditions

As explained above, the natural displacement of a gel occurs through swelling by absorbing solvent until the material reaches equilibrium, or through the inverse process, that is shrinking. This equilibrium corresponds to the stress-free state at the outer boundary, which we may characterize by the dead-load traction boundary condition $T_{rr}(r(1)) = 0$.

We start by pointing out that the stress-free equilibrium state of the gel corresponds to its lowest energy state, as shown in Figure 5.6. This physical equivalence follows from the theory and reaffirms the validity of our model. Furthermore, if the gel in the reference configuration Ω_0 is not already in equilibrium, the energy in the deformed configuration is always lower than in the reference configuration, as shown in Figure 5.7

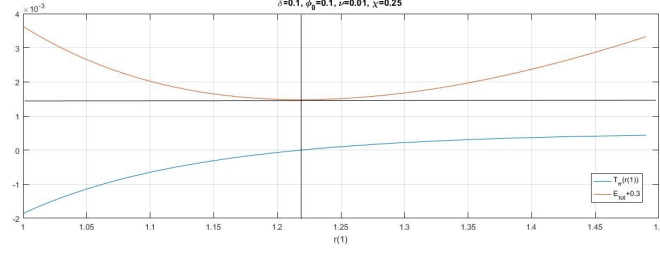


Figure 5.6: Reference Energy-Stress Relation for Different Stretches

In addition, a complete stress-free state, that is $T_{rr}(r(R)) = 0$ for any R , is attained when we do not fix the inner boundary and the material experiences a pure expansion $r_{pure} = \lambda R$. Therefore, the energy associated to r_{pure} is always lower than the energy for the deformation r with $r(\delta) = \delta$, which Figure 5.7 confirms.

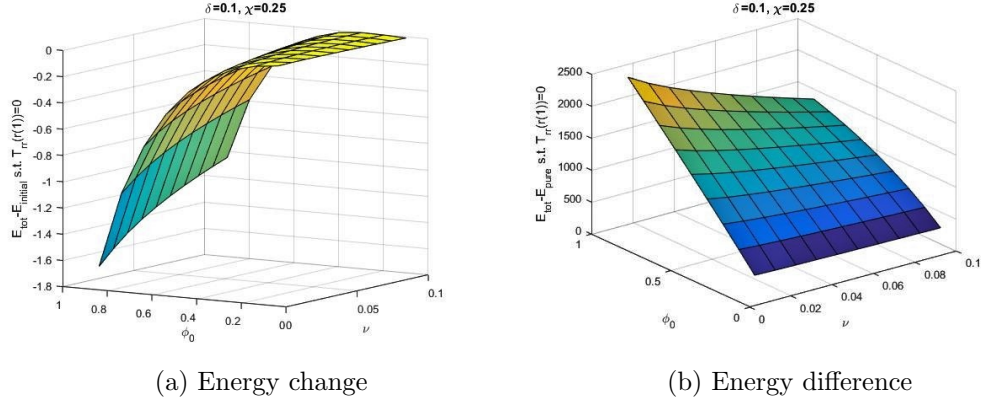


Figure 5.7: Reference Energy Compared to Initial and Radial Energies

When comparing Figures 5.7 and 5.8, we observe that the movement in displacement field and energy difference are correlated. Indeed, the pure expansion is increasingly favored the more displacement the material experiences as additional energy is created for the fixed core case.

As for the range of parameters, we observe from Figure 5.8 that the displacement, which corresponds to the swelling, is highest for large ϕ_0 and small ν , and vice-versa. Indeed, the gel absorbs most solvent when it is in its driest state, allowing it to swell more. Furthermore, the material wants to expand less when there are more crosslinks, that is for a higher ν . As for the stress field, we have the same phenomenon that we

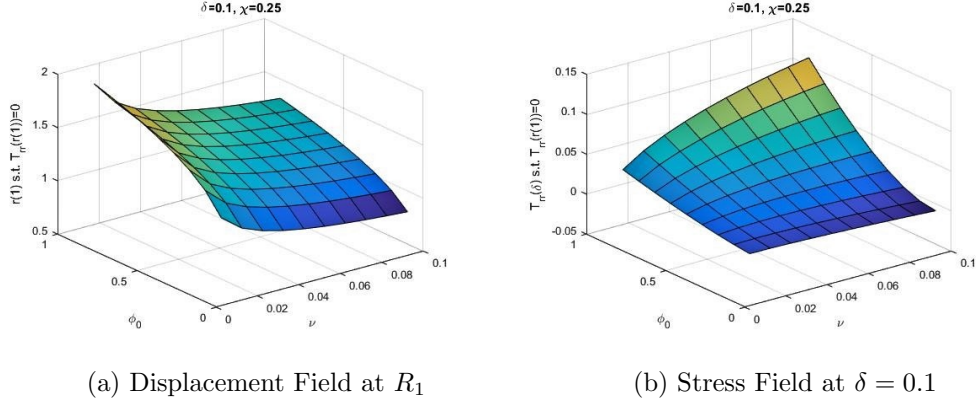


Figure 5.8: Reference Relaxed State with Stress-Free Outer Boundary

already observed for the displacement boundary conditions. The stress is highest at the core for a large ϕ_0 since this corresponds to a higher movement resistance. For the same reason, the stress also increases in absolute value, that is for both expansion and compression, for large polymer crosslink densities ν .

Finally, we again look at the outcome when we additionally change the remaining parameters of the problem. When we increase the Flory interaction parameter χ , we observe a lower stress field at the core in Figure 5.9. We have seen in the discussion on the Flory-Huggins energy that the χ term opposes the mixing of the polymer with the solvent, hence explaining a lower displacement field and less stress. As for the change in magnitude of the inner core δ , we again do not notice significant differences in Figure 5.10, as already observed in the previous section with displacement boundary conditions.

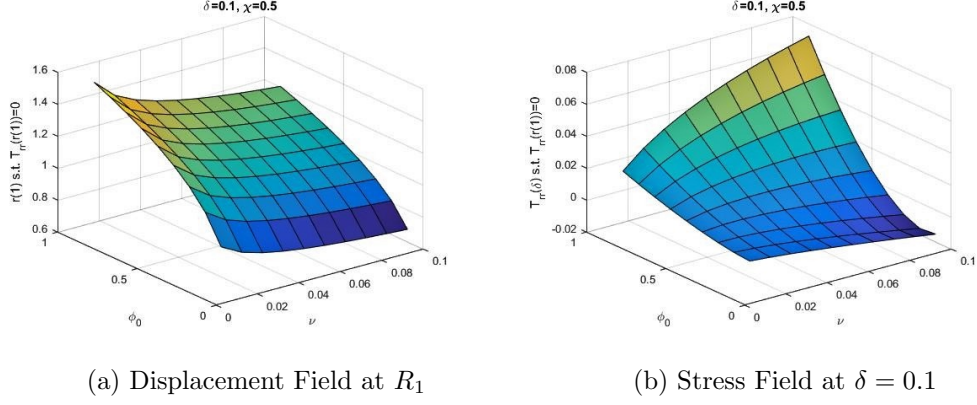


Figure 5.9: Relaxed State with Stress-Free Outer Boundary for Increasing χ

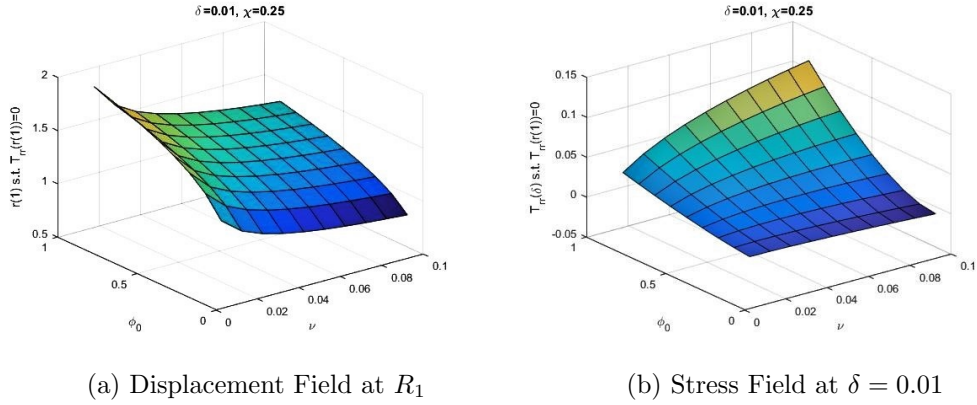


Figure 5.10: Relaxed State with Stress-Free Outer Boundary for Decreasing δ

5.6 Stresses in Spherical Caps

It is physically possible to have a gel occupying a spherical domain and constrained to radially symmetric deformations, the problem we have so far studied in this thesis. However, it is more unlikely to have such a setup in an experiment, let alone to have an appropriate application for it. Therefore, we switch gears in this final section and we consider a slightly different configuration. Namely, we assume that the gel occupies a spherical cap firmly attached to a substrate by its flat surface in the reference configuration. The gel may be subject to deformations through either displacement or traction boundary conditions.

5.6.1 Configuration

The gel occupies a spherical cap, a portion of a unit hemispherical domain given by

$$\Omega_0 = \{\mathbf{X} \in \mathbb{R}^3 \mid |\mathbf{X}| \leq 1; X_3 \geq k \text{ for } k \geq 0\},$$

in the reference configuration. We note that we do not need to consider a fixed core at the “center” given by $(0, 0, k)$, since we do not anticipate any singularities there. We again denote the deformation map by $\Phi : \Omega_0 \rightarrow \Omega; \mathbf{X} \mapsto \mathbf{x}(\mathbf{X})$, and it is appropriate to choose spherical coordinates, that is $\mathbf{X} = (R, \Theta, \Psi)$. However, the deformation is not

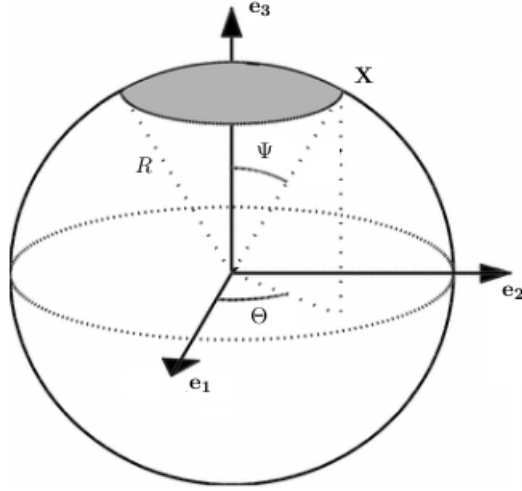


Figure 5.11: Spherical Cap (Source: geoweb.princeton.edu/people/simons/PIX)

restricted to radial symmetry anymore, meaning that we include an additional degree of freedom. Namely, we consider the angle Ψ to be a second variable, besides the radius R . This second variable is necessary since the cap is not able to conserve its radial symmetry. Indeed, the cap is firmly attached to a substrate, which does not allow for any movement along that surface. We call the deformation to be *rotationally symmetric* and define it by

$$r = r(R, \Psi), \quad \theta = \Theta, \quad \phi = \phi(\Psi).$$

where $\mathbf{x} = (r, \theta, \phi) \in \Omega$. Further details on rotational symmetry can be found in the appendix, such as the derivation of the deformation gradient $\underline{\mathbf{F}}$, which is given by

$$\underline{\mathbf{F}} = \frac{\partial \underline{\Phi}}{\partial \underline{\mathbf{X}}} = \begin{pmatrix} r_{,R} & 0 & \frac{r_{,\Psi}}{R} - \frac{\phi}{R} \\ 0 & \frac{r}{R} + \cot \Psi \frac{\phi}{R} & 0 \\ 0 & 0 & \frac{r}{R} + \frac{\phi_{,\Psi}}{R} \end{pmatrix}.$$

We assume the same total free energy as previously defined in (5.1), namely

$$\bar{E}_{tot} = \phi_0 \int_{\Omega_0} \frac{\nu}{2} |\underline{\mathbf{F}}|^2 + \ln \left(1 - \frac{\phi_0}{\det \underline{\mathbf{F}}} \right) + \chi \left(1 - \frac{\phi_0}{\det \underline{\mathbf{F}}} \right) d\underline{\mathbf{X}},$$

where we recall that ϕ_0 is the polymer volume fraction, ν the polymer crosslink number density and χ is the Flory interaction parameter.

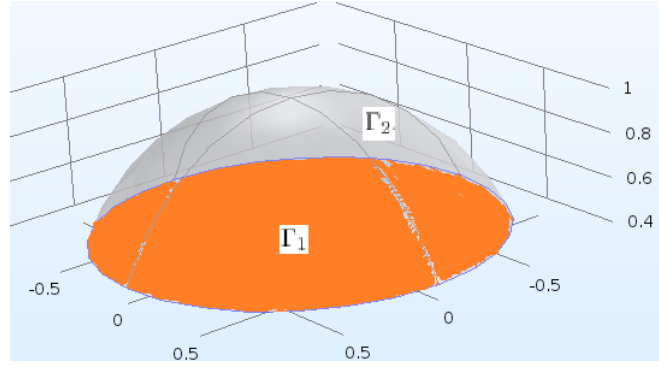


Figure 5.12: Spherical Cap Boundaries

We recall that the Cauchy stress tensor is given by $\underline{\mathbf{T}} = \hat{\underline{\mathbf{T}}}(\underline{\mathbf{F}}) := \frac{1}{\det \underline{\mathbf{F}}} \frac{\partial W}{\partial \underline{\mathbf{F}}} \underline{\mathbf{F}}^T$ and that the First Piola-Kirchhoff stress tensor is defined by $\underline{\mathbf{P}} = \hat{\underline{\mathbf{P}}}(\underline{\mathbf{F}}) := (\det \underline{\mathbf{F}}) \underline{\mathbf{T}} \underline{\mathbf{F}}^{-T} = \frac{\partial W}{\partial \underline{\mathbf{F}}}$. The boundary is divided into two portions, Γ_1 and Γ_2 , such that $\partial\Omega_0 = \Gamma_1 \cup \Gamma_2$. Hence, we define the boundary conditions by

1. No-slip boundary condition on the flat surface Γ_1 , that is $r(R, \frac{\pi}{2}) = 0$ for all $R \in (k, 1)$, where $k \geq 0$ is the height of the cap in the X_3 direction.
2. Either displacement boundary condition as before, namely $r(1, \Psi) = \lambda$ for $\lambda > 0$, or normal traction boundary conditions, that is $\mathbf{p}_1 \cdot \mathbf{N} = p_0$, with $p_0 \geq 0$, at the outer curved boundary Γ_2 . Here, we have that \mathbf{N} is the normal vector and $\mathbf{p}_1 = \underline{\mathbf{P}} \mathbf{N}$ is the stress vector, or contact force as previously defined.

Finally, we introduce a new notion for the stress used for our plots later.

Definition 5.6.1. We define the *von Mises* stress, denoted by T_{vm} , as the combination of the Cauchy stress tensor's coordinates. In 3D, the von Mises stress is given by

$$T_{vm} = \sqrt{\frac{1}{2} [(T_{11} - T_{22})^2 + (T_{22} - T_{33})^2 + (T_{33} - T_{11})^2 + 6(T_{12}^2 + T_{23}^2 + T_{31}^2)]} \quad (5.18)$$

The von Mises stress is an indicator of stress intensity at any given point in the domain, without the information on the direction of the stress.

5.6.2 Numerical Simulations

Problem Setup

For our setup, the strong form of the Euler-Lagrange equations given in (4.5) yields a system of two second order partial differential equations in r and ϕ . We do not develop a finite element method ourselves, but instead use COMSOL, a multiphysics modeling software, to explicitly solve this system. Moreover, we do not consider a range for the material properties, and we set $\phi_0 = 0.1$, $\nu = 0.01$ and $\chi = 0.25$ for the simulations. Indeed, a change in any of these properties has the same effect on the stress field as in the spherical case with radially symmetric deformations. Therefore, we omit the results from this work as they do not yield any new information.

Results

We note that we restrict ourselves to 2D deformations for the purpose of best illustrating our results. The plots below show the reference configuration with a black contour, the deformed configuration which is the colored shape as well as the von Mises stresses, which are described by the color itself.

First, we observe that the von Mises stresses are highest at the edge of Γ_1 for both displacement and traction boundary conditions. We assume that the gel may eventually start detaching at a critical stress since failure occurs where the concentration of stress is the highest, as we previously discussed. Hence, this setting yields a delamination rather than a cavitation, which is comparable to the phenomenon of debonding. At a closer look, we note that the material undergoes a larger displacement in Figure 5.14, compared to the one in Figure 5.13, and the stress concentration is consequently higher.

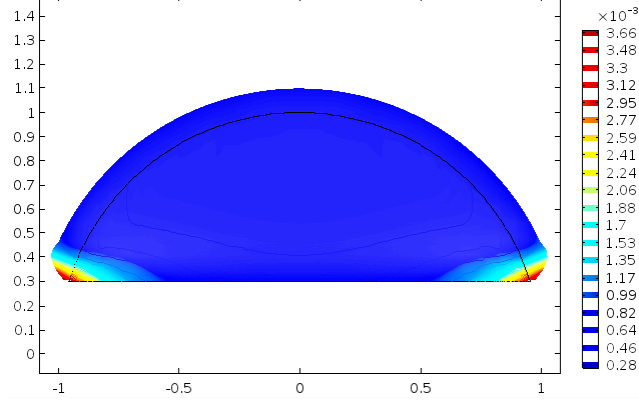


Figure 5.13: Spherical Cap, Displacement Boundary Condition $r(1, \Psi) = 1.1$

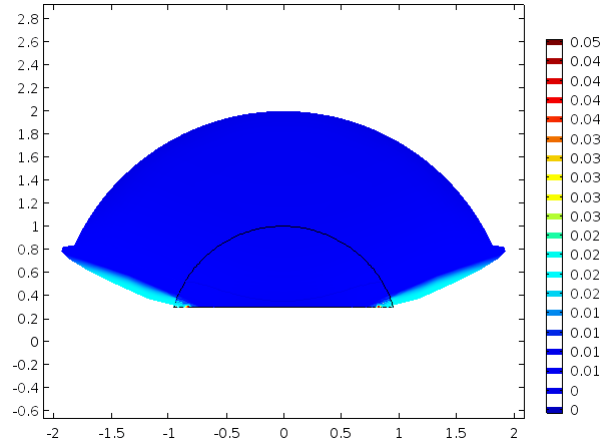


Figure 5.14: Spherical Cap, Displacement Boundary Condition $r(1, \Psi) = 2$

From a different perspective, we consider the traction boundary conditions in the reference configuration illustrated in Figures 5.15 and 5.16. We observe a considerably higher expansion by increasing the normal stress in the reference configuration. This also yields a higher stress concentration at the edge of Γ_1 , as stated above. On the other hand, the stress along the boundary Γ_2 decreases with an increased displacement, reflecting a complete relaxation of the body after the deformation.

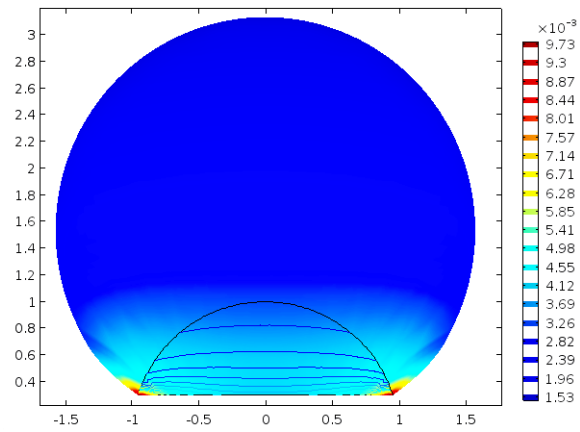


Figure 5.15: Spherical Cap, Traction Boundary Condition $\mathbf{p}_1 \cdot \mathbf{N} = 0.01$

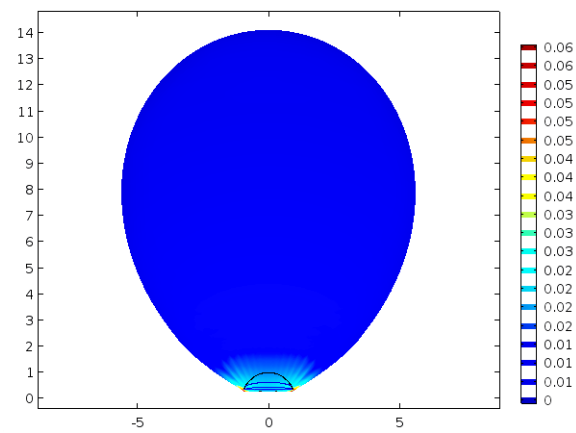


Figure 5.16: Spherical Cap, Traction Boundary Condition $\mathbf{p}_1 \cdot \mathbf{N} = 0.05$

Chapter 6

Conclusion and Discussion

We conclude the thesis with a final chapter that summarizes the main results and that gives an outlook on possible future directions.

6.1 Summary

The scope of this work is the study of cavity nucleation within a gel, a mixture of polymer and solvent, occupying a spherical domain Ω_0 . We define a dimensionless stored energy density W for the gel which accounts for the material's key properties, such as the polymer's elasticity and the interaction between the polymer and the solvent components. We look for deformations $\mathbf{x}(\mathbf{X})$, $\mathbf{X} \in \Omega_0$, that minimize the corresponding total free energy $E_{tot} = \int_{\Omega_0} W \, d\mathbf{X}$ over the domain, by restricting the search to purely radial solutions $\mathbf{x}(\mathbf{X}) = r(R)$ for $R \in (0, 1)$. The gel is subject to boundary conditions of two types: on the one hand, we impose a radial displacement boundary condition given by $r(1) = \lambda$ for $\lambda > 0$. On the other hand, we require a traction boundary condition $T_{rr}(r(1)) = p_0$, which ultimately allows to model the swelling of a gel. We recall that a gel may absorb additional solvent if it is initially dry enough. The gel swells until it reaches its equilibrium, which occurs at $p_0 = 0$.

6.2 Results

In a first attempt, we verify that Ball's main theorem on cavitation applies to a gel with a total free energy E_{tot} . Indeed, we show that there are two competing deformations that minimize E_{tot} . First, we have the purely radial expansion r_{pure} , with $r_{pure}(0) = 0$. Then, we have a second, cavitating deformation $r(R)$ such that $r(0) > 0$. We define the necessary conditions, based on balance of mass, that allow for this cavitating solution in the case of a gel. This is a new approach, which is not required in previous studies on cavitation in nonlinear elasticity as the materials were solid and not a mixture. We also know through Ball's work that there exists a critical radial displacement λ_{cr} beyond which $E_{tot}(r(R)) < E_{tot}(r_{pure}(R))$.

At the same time, we encounter the shortcoming that we are unable to explicitly derive this critical value. Indeed, authors in previous research focus on particular types of stored energy densities, namely special types of stored elastic energy densities, which are not applicable for the study of gels. This enables them to determine λ_{cr} without explicitly solving the minimization problem itself. The search for a minimizing solution to E_{tot} with $r(0) > 0$ requires to solve the corresponding Euler-Lagrange equations with a singularity at the origin.

To avoid this singular problem, we proceed by assuming a fix core of radius $\delta \ll 1$ at the center of the domain, that is $r(\delta) = \delta$. We impose the same boundary conditions as before and study their impact on the stress field accross the domain. In particular, we focus on the stress at the core boundary since we know through our previous analysis that the cavity nucleates at the center. The idea is the following: an increasing stress at the core eventually reaches a critical threshold at which the bonds in the mixture break and a cavity, filled with solvent, forms.

We numerically solve the Euler-Lagrange equations for deformations satisfying the inner and outer boundary conditions. We use the resulting minimizing deformations to compute the radial component $T_{rr}(r(R))$ of the Cauchy stress tensor T . We observe that the stress is indeed the highest at the inner core, that is $\max_r T_{rr}(r) = T_{rr}(r(\delta))$. Moreover, it appears that decreasing the size of the inner core does not have any major increasing impact on $T_{rr}(r(\delta))$. We also linearize the Euler-Lagrange equations to obtain an analytical approximation of the deformation, and conclude that it is close enough to

the numerical solution.

The main parameters of the problem have a more significant impact on the stress. To see this, we reduce our model to only include these essential parameters, namely: the polymer volume fraction ϕ_0 , the polymer crosslink density ν and the Flory interaction parameter χ . We consider different scales for these parameters to observe their effects on the stress $T_{rr}(r(\delta))$. The results not only give us important information, but also serve to benchmark the physical validity of our model. For instance, the gel swells most when it is the driest, that is when ϕ_0 is the largest. Furthermore, a high number of crosslinks in the polymer prevent the material of extensive swelling, which in return causes a higher intensity in stresses.

Finally, we compare the total free energy of the radial deformation $r(R)$, subject to the imposed boundary conditions, to the one of a pure expansion $r_{pure} = \lambda R$ where the core is “free”. Naturally, the latter energy is always the smallest, and increasingly so for larger deformations. Hence, it is intuitive that the energy is lowered when the stress reaches the critical value at the core to break the polymer and form a cavity.

We conclude that cavities do nucleate at the center of a gel occupying a spherical domain when only radial symmetric deformations are allowed. This may be a result of both an imposed radial displacement and a more natural free swelling, resulting in a stress-free outer boundary. Moreover, nucleation of a cavity also depends on the specific gel type, which is determined by its parameters. We note that this research does not give any insight to the exact instance of cavity formation. Therefore, further work needs to be conducted in future and we discuss certain possible avenues that may be taken in this direction and beyond.

6.3 Outlook

6.3.1 Experiments

First, it would be beneficial to investigate gel characteristics from an experimental point of view. It is necessary to exactly understand how the mixture breaks down and how the components may separate. This would not only serve as a possible benchmark but may also be incorporated in the mathematical model, either directly into the total free energy, or even as a constraint.

6.3.2 Total Free Energy

Following the lead from the previous point, we may penalize material properties beyond elasticity and component interactions in the gel by adding more terms to the total free energy of the gel.

One possible avenue would be to account for the polymer chain length. Indeed, the length of a polymer chain is correlated to the deformation it can sustain. Given a fixed imposed displacement, a shorter polymer chain breaks before a longer one. Therefore, we may account for the chain size in the total energy and possibly even for the location of each chain.

Bearing a similar mindset, we may incorporate the surface energy into the energy minimization. The surface energy would measure the work required to break the material and to force a cavity nucleation. As mentioned in the literature review, recent work is heading in this direction, for instance done by the authors in [16] or [17].

For instance, we may compare the energy associated to a pure expansion with a cavitating energy at the expansion where the gel reaches its critical stress around the core to break the mixture.

6.3.3 Geometry

We may also pursue the avenue of considering more complex geometries. The case of a spherical domain with an admissible set of only radially symmetric deformations is very particular, as already indicated in the work of [16]. It is also a very unique configuration for actual applications involving gels.

In this thesis, we initiate the process and consider a gel occupying a spherical cap firmly attached to a substrate by its flat surface $\partial_D \Omega_0 \subset \partial \Omega_0$. This requires two major updates to our preexisting model. On the one hand, we need to widen the constraint of only radially symmetric deformation to $r = r(R, \Psi)$ and $\phi = \phi(\Psi)$. On the other hand, we impose a no-slip Dirichlet boundary condition $\mathbf{x}(\mathbf{X}) = 0$ on $\partial_D \Omega_0$, which describes the firm attachment.

The minimizing solutions to the total free energy yield that the stress concentration is focused around the edge of $\partial_D \Omega_0$. A critical stress may then lead to the delamination of the gel from the substrate. This is closely related to the phenomenon of debonding

mentioned in the introduction

In future work, we may consider unconstrained deformations or different domains, for instance a rectangular. We observe that new domains also give rise to imposing further boundary conditions. We may look at new problems where the settings enable us to connect cavitation to debonding in gels.

6.3.4 Time-dependence

From a different perspective, the static analysis of cavities is already a challenging endeavor in mathematics. However, we would propose to also pursue a time-dependent study of cavitation in gels in future. The current setting with a spherical domain and radially symmetric deformations $r = r(R, t)$ for $t \in (0, \infty)$ would be the simplest case.

A time-dependent model would also enable us to an extensive stability analysis of the cavity. Indeed, we could determine if a cavity is stable or unstable after nucleation. The latter case may be of most relevance as it is essential to understand if the cavity grows or collapses after nucleation.

References

- [1] M. E. Rognes, M.C. Calderer and C. A. Micek. *Modelling of and Mixed Finite Element Methods for Gels in Biomedical Applications*. SIAM J. Appl. Math., Vol. 70, No. 4, pp. 1305-1329, 2009.
- [2] M.C. Calderer and H. Zhang. *Incipient Dynamics of Swelling of Gels*. SIAM J. Appl. Math., Vol.68, No. 6, pp. 1641-1664, 2008.
- [3] M.C. Calderer, H. Chen, C. Micek and Y. Mori. *A Dynamic Model of Polyelectrolyte Gels*. SIAM J. Appl. Math., Vol. 73, No. 1, pp. 104-133, 2013.
- [4] M.C. Calderer and B. Chabaud. *Effects of Permeability and Viscosity in Linear Polymeric Gels*. SIAM J. Appl. Math., 2013.
- [5] T. Tanaka and D. Fillmore. *Kinetics of swelling of gels*. J. Chem. Phys. 70(03), pp.1214-1218, 1979.
- [6] T. Tomari and M. Doi. *Swelling Dynamics of a Gel Undergoing Volume Transition*. J. Phys. Soc. Japan, Vol. 63, No. 6, pp.2093-2101, 1994.
- [7] Y. Hu and Z. Suo. *Viscoelasticity and Poroelasticity in Elastomeric Gels*. Acta Mech. Sol. Sin., Vol. 25, No. 5, pp. 441-457, 2012.
- [8] J. Nase, A. Lindner and C. Creton. *Pattern Formation during Deformation of a Confined Viscoelastic Layer: From a Viscous Liquid to a Soft Elastic Solid*. Phys. Rev. Lett., Vol. 101, No. 7, 074503, 2008.
- [9] J. M. Ball. *Discontinuous Equilibrium Solutions and Cavitation in Nonlinear Elasticity*. Phil. Trans. Roy. Soc. Lond. Math. Phys. Sci., Vol. 306, No. 1496, pp. 557-611, 1982.

- [10] A. N. Gent and D. A. Tompkins. *Nucleation and Growth of Gas Bubbles in Elastomers*. J. of Appl. Phys., Vol. 40, No. 6, pp. 2520-2525, 1969.
- [11] J. Sivaloganathan and S. J. Spector. *Myriad Radial Cavitating Equilibria in Nonlinear Elasticity*. SIAM J. Appl. Math., Vol. 63, No. 4, pp. 1461-1473, 2003.
- [12] C. O. Horgan and T. J. Pence. *Cavity Formation at the Center of a Composite Incompressible Nonlinearly Elastic Sphere*. ASME J. Appl. Mech., Vol. 56, pp. 302-308, 1989.
- [13] D. A. Polignone and C. O. Horgan. *Cavitation for Incompressible Anisotropic Nonlinearly Elastic Spheres*. Kluwer J. Elas., Vol. 33, pp.27-65, 1993.
- [14] T. J. Pence and H. Tsai. *Bulk Cavitation and the Possibility of Localized Interface Deformation due to Surface Layer Swelling*. J. Elast., Vol. 87:, pp. 161185, 2007.
- [15] C. O. Horgan. *Void Nucleation and Growth for Compressible Nonlinearly Elastic Materials: an Example*. Int. J. Sol. Struct., Vol. 29, No. 3, pp.279-291, 1992.
- [16] S. Mueller and S. Spector. *An Existence Theory for Nonlinear Elasticity that Allows for Cavitation*. Arch. Rat. Mech. and Anal., Vol. 131, No. 1, pp. 1-66, 1995.
- [17] D. Henao and C. Mora-Corral, *Invertibility and Weak Continuity of the Determinant for the Modelling of Cavitation and Fracture in Nonlinear Elasticity*. Arch. Rat. Mech. and Anal., Vol. 197, No. 2, pp. 619-655, 2010.
- [18] K. A. Pericak-Spector and S. J. Spector. *Nonuniqueness for a Hyperbolic System: Cavitation in Nonlinear Elastodynamics*. Arch. Rational Mech. Anal., Vol. 101, Issue 4, pp. 293-317, 1988.
- [19] D. Henao and S. Serfaty. *Energy Estimates and Cavity Interaction for a Critical-Exponent Cavitation Model*. Comm. Pure Appl. Math., Vol. 66, Issue 7, pp. 1028-1101, 2013.
- [20] T. Yamaguchi and M. Doi. *Debonding Dynamics of Pressure-Sensitive Adhesives*. Eur. Phys. J.E, 21, pp. 331-339, 2006.

- [21] F. Tanguy, M. Nicoli, A. Lindner and C. Creton. *Quantitative Analysis of the Debonding Structure of Soft Adhesives*. arXiv, 2013.
- [22] A. A. L. Baldelli, B. Bourdin, J.-J. Marigo and C. Maurini. *Fracture and debonding of a thin film on a stiff substrate: analytical and numerical solutions of a one-dimensional variational model*. Cont. Mech. Thermodyn., 25, pp. 243268, 2013.
- [23] M. E. Gurtin, E. Fried and L. Anand. *The Mechanics and Thermodynamics of Continua*.
- [24] E. Tadmor, R. Miller and R. Elliott. *Continuum Mechanics and Thermodynamics*.
- [25] C. Evans. *Partial Differential Equations*. Grad. Stud. in Math., Vol. 19, pp.454-456.
- [26] B. Dacorogna, *Introduction to the Calculus of Variations*. Imperial College Press, pp.53-54.
- [27] P. Olver, *Introduction to Calculus of Variations*. Lecture Notes, pp.18-22.
- [28] I. Gelfand and S. Fomin, *Calculus of Variations*. Prentice Hall, pp.97-129.
- [29] J. Li, Y. Hu, J. J. Vlassak and Z. Suo. *Experimental determination of equations of state for ideal elastomeric gels*. Roy. Soc. of Chem., Soft Matter 8, pp.8121-8128, 2012.
- [30] M. Rubinstein and R. Colby. *Polymer Physics*. Oxford, pp.137-143.
- [31] M. Doi. *Soft Matter Physics*. Oxford University Press, 2013.
- [32] J. Ball. *Constitutive inequalities and existence theorems in nonlinear elastostatics*. Nonlin. Anal. Mech., Heriot-Watt Symposium, Vol. 1., 1977.
- [33] D. Liberzon *Calculus of Variations and Optimal Control Theory: A Concise Introduction*. <http://liberzon.csl.illinois.edu/teaching/cvoc/cvoc.html>
- [34] T. Yamaue, T. Taniguchic and M. Doi. *The simulation of the swelling and deswelling dynamics of gels*. Molecular Physics, Vol. 102, No. 2, pp. 167-172, 2004.
- [35] R. A. Orwoll and P. A. Arnold “*Polymer-Solvent Interaction Parameter*” in *Physical Properties of Polymers Handbook*. Springer, Chapter 14, pp.233-257.

Appendix A

The appendix serves as a reference for some relevant operations and elementary calculations needed in some keys steps for the work of the thesis.

A.1 Operations on Determinants and Traces

The first section is devoted to identities involving determinants and traces, namely identities related to the differentiation of these operators. Let us start with the following proposition:

Proposition A.1.1. *Let $\underline{\mathbf{A}}, \underline{\mathbf{B}} \in \mathbb{M}^{n \times n}$ be two matrices, with $\underline{\mathbf{A}}$ invertible, $\alpha \in \mathbb{R}$, we have*

$$\left. \frac{d}{d\alpha} \right|_{\alpha=0} \det(\underline{\mathbf{A}} + \alpha \underline{\mathbf{B}}) = (\det \underline{\mathbf{A}}) \operatorname{tr}(\underline{\mathbf{B}} \underline{\mathbf{A}}^{-1}).$$

Proof. We first note that

$$\det(\underline{\mathbf{A}} + \alpha \underline{\mathbf{B}}) = \det((\underline{\mathbf{I}} + \alpha \underline{\mathbf{B}} \underline{\mathbf{A}}^{-1}) \underline{\mathbf{A}}) = (\det \underline{\mathbf{A}}) (\det(\underline{\mathbf{I}} + \alpha \underline{\mathbf{B}} \underline{\mathbf{A}}^{-1})). \quad (\text{A.1})$$

Next, let $\{\mathbf{e}_i\}_{i=1, \dots, n}$ of \mathbb{R}^n be an orthonormal basis and let $\underline{\mathbf{C}} := \underline{\mathbf{B}} \underline{\mathbf{A}}^{-1}$. Then we have

$$\begin{aligned} \det(\underline{\mathbf{I}} + \alpha \underline{\mathbf{C}}) &= \det(\mathbf{e}_1 + \alpha \mathbf{C}_1, \dots, \mathbf{e}_n + \alpha \mathbf{C}_n) \\ &= 1 + \alpha \sum_{i=1}^n C_{ii} + \mathcal{O}(\alpha^2) \\ &= 1 + \alpha \operatorname{tr} \underline{\mathbf{C}} + \mathcal{O}(\alpha^2). \end{aligned}$$

Taking the derivative with respect to α at $\alpha = 0$, we obtain

$$\left. \frac{d}{d\alpha} \right|_{\alpha=0} \det(\underline{\mathbf{I}} + \alpha \underline{\mathbf{C}}) = \operatorname{tr} \underline{\mathbf{C}}.$$

The result follows immediately from combining equations (A.1) and (A.1). \square

The next two results yield the derivative of the determinant of a matrix $\underline{\mathbf{A}}$.

Proposition A.1.2. Jacoby's Formula *Let $t \in \mathbb{R}$ be a scalar and let $\underline{\mathbf{A}} = \underline{\mathbf{A}}(t) \in \mathbb{M}^{n \times n}$ be an invertible matrix. Then*

$$\frac{d}{dt} \det(\underline{\mathbf{A}}) = \det(\underline{\mathbf{A}}) \operatorname{tr} \left(\underline{\mathbf{A}}^{-1} \frac{d\underline{\mathbf{A}}}{dt} \right).$$

Corollary A.1.3. *For $\underline{\mathbf{A}} \in \mathbb{M}^{n \times n}$ an invertible matrix, we have*

$$\frac{d}{d\underline{\mathbf{A}}} (\det \underline{\mathbf{A}}) = (\det \underline{\mathbf{A}}) \underline{\mathbf{A}}^{-T}.$$

The final proposition covers the derivative of the trace of a matrix $\underline{\mathbf{A}}$.

Proposition A.1.4. *Let $t \in \mathbb{R}$ be a scalar and let $\underline{\mathbf{A}} = \underline{\mathbf{A}}(t) \in \mathbb{M}^{n \times n}$ be a matrix. Then*

$$\frac{d}{dt} \operatorname{tr} \underline{\mathbf{A}}(t) = \operatorname{tr} \frac{d}{dt} \underline{\mathbf{A}}(t).$$

A.2 Deformation Mapping

In this section, we first work through the transformations between Cartesian and spherical coordinates, then formally define the deformation gradient in spherical coordinates. Finally, we derive the main operators in spherical coordinates and we provide computations used for derivating the Euler-Lagrange equations.

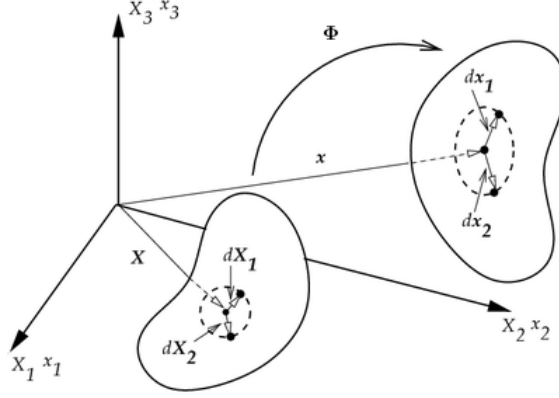


Figure A.1: General Constellation (Source: Wikiversity)

A.2.1 Deformation Gradient

We consider a point $\mathbf{X} = (X_1, X_2, X_3)$ in spherical coordinates by $\hat{\mathbf{X}} = (R, \Theta, \Psi)$, i.e.

$$X_1 = R \cos \Theta \sin \Psi, \quad X_2 = R \sin \Theta \sin \Psi, \quad X_3 = R \cos \Psi.$$

From this definition, we express (R, Θ, Ψ) in terms of $\mathbf{X} = (X_1, X_2, X_3)$. We get

$$R = \sqrt{X_1^2 + X_2^2 + X_3^2}, \quad \Theta = \tan^{-1} \frac{X_2}{X_1}, \quad \Psi = \cos^{-1} \frac{X_3}{\sqrt{X_1^2 + X_2^2 + X_3^2}}. \quad (\text{A.2})$$

Next, we express the orthonormal set associated to the spherical coordinates, given by \mathbf{J}_R , \mathbf{J}_Θ and \mathbf{J}_Ψ , in terms of Θ and Ψ . This gives us

$$\mathbf{J}_R := \mathbf{J}_1 = \frac{\frac{dr}{dR}}{\left| \frac{dr}{dR} \right|} = \cos \Theta \sin \Psi \mathbf{e}_1 + \sin \Theta \sin \Psi \mathbf{e}_2 + \cos \Psi \mathbf{e}_3,$$

$$\mathbf{J}_\Theta := \mathbf{J}_2 = \frac{\frac{dr}{d\Theta}}{\left| \frac{dr}{d\Theta} \right|} = -\sin \Theta \mathbf{e}_1 + \cos \Theta \mathbf{e}_2,$$

$$\mathbf{J}_\Psi := \mathbf{J}_3 = \frac{\frac{dr}{d\Psi}}{\left|\frac{dr}{d\Psi}\right|} = \cos \Theta \cos \Psi \mathbf{e}_1 + \sin \Theta \cos \Psi \mathbf{e}_2 - \sin \Psi \mathbf{e}_3.$$

There is a corresponding orthonormal set $\{\mathbf{j}_1, \mathbf{j}_2, \mathbf{j}_3\}$ for \mathbf{x} in the deformed configuration. Since in our study, we consider the coordinate system to be invariant under the deformation, we have that $\mathbf{j}_i = \mathbf{J}_i$ for $i = 1, 2, 3$. We can now compute the deformation tensor $\underline{\mathbf{F}}$ defined by the deformation map Φ :

$$\underline{\mathbf{F}} := \frac{\partial \Phi(\mathbf{X})}{\partial \mathbf{X}} = \frac{\partial \Phi}{\partial \hat{\mathbf{X}}} \frac{\partial \hat{\mathbf{X}}}{\partial \mathbf{X}} = \frac{\partial \Phi}{\partial \hat{X}_i} \frac{\partial \hat{X}_i}{\partial \mathbf{X}} = \frac{\partial \Phi}{\partial \hat{X}_i} \frac{\partial \hat{X}_i}{\partial X_j} \frac{\partial X_j}{\partial \mathbf{X}} = \frac{\partial \Phi}{\partial \hat{X}_i} \frac{\partial \hat{X}_i}{\partial X_j} e_j.$$

Hence, it remains to determine $\frac{\partial \Phi}{\partial \hat{X}_i}$ and $\frac{\partial \hat{X}_i}{\partial X_j}$. Let us first formally compute $\frac{\partial \hat{X}_i}{\partial X_j}$. We have that $\frac{\partial \hat{X}_1}{\partial X_j} = \frac{\partial R}{\partial X_j}$, $\frac{\partial \hat{X}_2}{\partial X_j} = \frac{\partial \Theta}{\partial X_j}$ and $\frac{\partial \hat{X}_3}{\partial X_j} = \frac{\partial \Psi}{\partial X_j}$. By using Equation (A.2), we obtain

$$\frac{\partial R}{\partial X_j} = \frac{1}{\sqrt{X_1^2 + X_2^2 + X_3^2}} (X_1, X_2, X_3) = (\cos \Theta \sin \Psi, \sin \Theta \sin \Psi, \cos \Psi) = \mathbf{J}_1,$$

$$\frac{\partial \Theta}{\partial X_j} = \frac{1}{X_1^2 + X_2^2} (-X_2, X_1, 0) = \frac{1}{R \sin \Psi} (-\sin \Theta, \cos \Theta, 0) = \frac{1}{R \sin \Psi} \mathbf{J}_2.$$

$$\begin{aligned} \frac{\partial \Psi}{\partial X_j} &= \frac{-1}{\sqrt{X_1^2 + X_2^2} (X_1^2 + X_2^2 + X_3^2)} (-X_1 X_3, -X_2 X_3, X_1^2 + X_2^2) \\ &= \frac{1}{R \sin \Psi} (\cos \Theta \cos \Psi \sin \Psi, \sin \Theta \cos \Psi \sin \Psi, -\sin^2 \Psi) \\ &= \frac{1}{R} \mathbf{J}_3, \end{aligned}$$

On the other hand, it remains to compute

$$\frac{\partial \Phi}{\partial \hat{X}_i} = \left(\frac{\partial \Phi}{\partial R}, \frac{\partial \Phi}{\partial \Theta}, \frac{\partial \Phi}{\partial \Psi} \right). \quad (\text{A.3})$$

These quantities depend on the type of deformation we impose, and we consider two types relevant to our study.

Radial Symmetry

First, the main deformations we are interested in are purely radially symmetric ones, so that $r = f(R)$, $\theta = \Theta$ and $\phi = \Psi$. This implies that for $\mathbf{X} \in \Omega_0$, we have $\mathbf{X} = R \mathbf{J}_1$ and that after the deformation $\mathbf{x} = r \mathbf{j}_1$, for $\mathbf{x} \in \Omega$. Hence, it follows that (A.3) yields

$$\frac{\partial \Phi}{\partial R} = \frac{\partial}{\partial R} (r \mathbf{j}_1) = \frac{\partial r}{\partial R} \mathbf{j}_1 + r \frac{\partial}{\partial R} \mathbf{j}_1 = \frac{\partial r}{\partial R} \mathbf{j}_1 = \frac{\partial r}{\partial R} \mathbf{J}_1,$$

$$\begin{aligned}\frac{\partial \Phi}{\partial \Theta} &= \frac{\partial}{\partial \Theta}(r\mathbf{j}_1) = r \frac{\partial}{\partial \Theta} \mathbf{j}_1 = r \sin \Psi \mathbf{j}_2 = r \sin \Psi \mathbf{j}_2 = r \sin \Psi \mathbf{J}_2, \\ \frac{\partial \Phi}{\partial \Psi} &= \frac{\partial}{\partial \Psi}(r\mathbf{j}_1) = r \frac{\partial}{\partial \Psi} \mathbf{j}_1 = r\mathbf{j}_3 = r\mathbf{j}_3 = r\mathbf{J}_3.\end{aligned}$$

Finally, we have that the deformation gradient with radial symmetry is

$$\underline{\mathbf{F}} = \frac{\partial \Phi}{\partial \mathbf{X}} = \frac{\partial r}{\partial R} \mathbf{J}_1 \otimes \mathbf{J}_1 + r \sin \Psi \mathbf{J}_2 \otimes \frac{1}{R \sin \Psi} \mathbf{J}_2 + r \mathbf{J}_3 \otimes \left(\frac{1}{R} \mathbf{J}_3 \right) = \begin{pmatrix} r_{,R} & 0 & 0 \\ 0 & \frac{r}{R} & 0 \\ 0 & 0 & \frac{r}{R} \end{pmatrix}. \quad (\text{A.4})$$

Rotational Symmetry

Finally, we also consider deformations that are only rotationally symmetric meaning that $r = f(R, \Psi)$, $\theta = \Theta$ and $\phi = h(\Psi)$. It follows that for $\mathbf{X} \in \Omega_0$, we have $\mathbf{X} = R\mathbf{J}_1$ and that after the deformation $\mathbf{x} = r\mathbf{j}_1 + \phi\mathbf{j}_3$, for $\mathbf{x} \in \Omega$. Hence, (A.3) yields

$$\begin{aligned}\frac{\partial \Phi}{\partial R} &= \frac{\partial}{\partial R}(r\mathbf{j}_1 + \phi\mathbf{j}_3) = \frac{\partial}{\partial R}(r\mathbf{j}_1) = \frac{\partial r}{\partial R} \mathbf{J}_1, \\ \frac{\partial \Phi}{\partial \Theta} &= \frac{\partial}{\partial \Theta}(r\mathbf{j}_1 + \phi\mathbf{j}_3) = r \frac{\partial \mathbf{j}_1}{\partial \Theta} + \phi \frac{\partial \mathbf{j}_3}{\partial \Theta} = (r \sin \Psi + \phi \cos \Psi) \mathbf{J}_2, \\ \frac{\partial \Phi}{\partial \Psi} &= \frac{\partial}{\partial \Psi}(r\mathbf{j}_1 + \phi\mathbf{j}_3) = \frac{\partial r}{\partial \Psi} \mathbf{j}_1 + r \frac{\partial \mathbf{j}_1}{\partial \Psi} + \frac{\partial \phi}{\partial \Psi} \mathbf{j}_3 + \phi \frac{\partial \mathbf{j}_3}{\partial \Psi} = \left(\frac{\partial r}{\partial \Psi} - \phi \right) \mathbf{J}_1 + \left(r + \frac{\partial \phi}{\partial \Psi} \right) \mathbf{J}_3.\end{aligned}$$

Therefore, the deformation gradient with rotational symmetry becomes

$$\underline{\mathbf{F}} = \frac{\partial \Phi}{\partial \mathbf{X}} = \begin{pmatrix} r_{,R} & 0 & \frac{r_{,\Psi}}{R} - \frac{\phi}{R} \\ 0 & \frac{r}{R} + \cot \Psi \frac{\phi}{R} & 0 \\ 0 & 0 & \frac{r}{R} + \frac{\phi_{,\Psi}}{R} \end{pmatrix}. \quad (\text{A.5})$$

A.2.2 Operations in Spherical Coordinates

Next, we aim to define operations key to our work in spherical coordinates, namely the divergence and the gradient operators. We reference the reader to the section on tensors in [24] for more details on the derivation of the expressions below. Note: the authors in [24] use the “physical” notation for spherical coordinates (R, Θ_1, Ψ_1) whereas we use the “mathematical” notation (R, Θ, Ψ) , with $\Theta_1 = \Psi$ and $\Psi_1 = \Theta$.

Divergence Operator

Let $\mathbf{v} \in \mathbb{R}^3$ be a vector and let $\underline{\mathbf{S}} \in \mathbb{R}^{3 \times 3}$ be a tensor.

$$\begin{aligned} \nabla \cdot \mathbf{v} &= v_{R,R} + 2 \frac{v_R}{R} + \frac{v_{\Psi,\Psi}}{R} + \frac{v_{\Theta,\Theta}}{R \sin \Psi} + \cot \Psi \frac{v_{\Psi}}{R}, \\ \nabla \cdot \underline{\mathbf{S}} &= \begin{bmatrix} S_{RR,R} + 2 \frac{S_{RR}}{R} + \frac{S_{\Psi R,\Psi}}{R} + \cot \Psi \frac{S_{\Psi R}}{R} + \frac{S_{\Theta R,\Theta}}{R \sin \Psi} - \frac{S_{\Psi\Psi} + S_{\Theta\Theta}}{R} \\ S_{R\Theta,R} + 2 \frac{S_{R\Theta}}{R} + \frac{S_{\Psi\Theta,\Psi}}{R} + \cot \Psi \frac{S_{\Psi\Theta}}{R} + \frac{S_{\Theta\Theta,\Theta}}{R \sin \Psi} + \frac{S_{\Theta R}}{R} + \cot \Psi \frac{S_{\Theta\Psi}}{R} \\ S_{R\Psi,R} + 2 \frac{S_{R\Psi}}{R} + \frac{S_{\Psi\Psi,\Psi}}{R} + \cot \Psi \frac{S_{\Psi\Psi}}{R} + \frac{S_{\Theta\Psi,\Theta}}{R \sin \Psi} + \frac{S_{\Psi R}}{R} - \cot \Psi \frac{S_{\Theta\Theta}}{R} \end{bmatrix}. \end{aligned}$$

Gradient Operator

Let $f \in \mathbb{R}$ be a scalar and let $\mathbf{v} \in \mathbb{R}^3$ be a vector. We have that

$$\begin{aligned} \nabla f &= \begin{bmatrix} f_{,R} & \frac{f_{,\Theta}}{R \sin \Psi} & \frac{f_{,\Psi}}{R} \end{bmatrix}^T, \\ \nabla \mathbf{v} &= \begin{bmatrix} v_{R,R} & \frac{v_{R,\Theta}}{R \sin \Psi} - \frac{v_{\Theta}}{R} & \frac{v_{R,\Psi}}{R} - \frac{v_{\Psi}}{R} \\ v_{\Theta,R} & \frac{v_{\Theta,\Theta}}{R \sin \Psi} + \cot \Psi \frac{v_{\Psi}}{R} + \frac{v_R}{R} & \frac{v_{\Theta,\Psi}}{R} \\ v_{\Psi,R} & \frac{v_{\Psi,\Theta}}{R \sin \Psi} - \cot \Psi \frac{v_{\Theta}}{R} & \frac{v_{\Psi,\Psi}}{R} + \frac{v_R}{R} \end{bmatrix}. \end{aligned}$$

A.2.3 Computations in the Reference Configuration

Finally, we give the results of computations in spherical coordinates needed to express the Euler-Lagrange equations for a gel explicitly.

Radial Symmetry

First, we consider the radial symmetric case and compute each term in the Euler-Lagrange equation explicitly. From Section A.2.1, we obtain $|\underline{\mathbf{F}}| = r_{,R}^2 + 2 \frac{r^2}{R^2}$ and $\det \underline{\mathbf{F}} = \frac{r_{,R} r^2}{R^2}$.

$$\begin{aligned} \nabla \left(|\nabla \mathbf{x}|^{2(s-1)} \right) &= 2(s-1) \left(r_{,R}^2 + 2 \frac{r^2}{R^2} \right)^{s-2} \begin{bmatrix} r_{,R} r_{,RR} + 2r \frac{r_{,R} R - r}{R^3} \\ 0 \\ 0 \end{bmatrix}, \\ \nabla \left[(\det \nabla \mathbf{x})^{2q} \right] &= 2q \left(r_{,R} \frac{r^2}{R^2} \right)^{2q-1} \begin{bmatrix} r \frac{R(r_{,RR} r + 2r_{,R}^2) - 2r_{,R} r}{R^3} \\ 0 \\ 0 \end{bmatrix}, \end{aligned}$$

$$\nabla \cdot (\nabla \mathbf{x}) = \begin{bmatrix} r_{,RR} + 2\frac{r_{,R}}{R} - 2\frac{r}{R^2} \\ 0 \\ 0 \end{bmatrix}, \quad \nabla \cdot (\nabla \mathbf{x}^{-1}) = \begin{bmatrix} \frac{-r_{,RR}}{r_{,R}^2} + \frac{2}{Rr_{,R}} - \frac{2}{r} \\ 0 \\ 0 \end{bmatrix},$$

$$\nabla[\phi_0(R)] = \begin{bmatrix} \phi_{0,R} \\ 0 \\ 0 \end{bmatrix}, \quad \nabla \left[\frac{\phi_0^2}{\det \nabla \mathbf{x}} \right] = \begin{bmatrix} R \frac{2(\phi_0^2 + R\phi_0\phi_{0,R})r_{,R}r - \phi_0^2 R(r_{,RR}r + 2r_{,R}^2)}{r_{,R}^2 r^3} \\ 0 \\ 0 \end{bmatrix},$$

$$\begin{aligned} & \nabla \left[\det \nabla \mathbf{x} \ln \left(1 - \frac{\phi_0}{\det \nabla \mathbf{x}} \right) \right] \\ &= \begin{bmatrix} \frac{r[(r_{,RR}r + 2r_{,R}^2)R - 2r_{,R}r]}{R^3} \left[\frac{\phi_0 R^2}{r_{,R}r^2 - \phi_0 R^2} + \ln \left(1 - \frac{\phi_0 R^2}{r_{,R}r^2} \right) \right] - \frac{\phi_{0,R}r_{,R}r^2}{r_{,R}r^2 - \phi_0 R^2} \\ 0 \\ 0 \end{bmatrix}. \end{aligned}$$

Rotational Symmetry

Lastly, we consider the slightly more general case of rotational symmetry. We restrict ourselves to the Neo-Hookean case $s = 1$ with the polymer volume fraction ϕ_0 constant and only consider the terms $\bar{\mu}$, \bar{b} and \bar{c} . Therefore, we only compute the related terms from the Euler-Lagrange equations as opposed to all the terms as above.

$$\begin{aligned}
\nabla \cdot (\nabla \mathbf{x}) &= \frac{1}{R^2} \begin{bmatrix} R^2 r_{,RR} + 2Rr_{,R} - 2r - (\cot \Psi \phi + \phi_{,\Psi}) \\ 0 \\ Rr_{,\Psi R} + 2r_{,\Psi} + \phi_{,\Psi\Psi} + \cot \Psi \phi_{,\Psi} - \frac{\phi}{\sin^2 \Psi} \end{bmatrix}, \\
\nabla \cdot (\nabla \mathbf{x}^{-1}) &= \begin{bmatrix} \frac{-r_{,RR}}{r_{,R}^2} + \frac{2}{Rr_{,R}} - \left(\frac{1}{r + \cot \Psi \phi} + \frac{1}{r + \phi_{,\Psi}} \right) \\ 0 \\ \frac{r_{,\Psi} - \phi - Rr_{,\Psi R}}{(r_{,\Psi} - \phi)^2} + \frac{2}{r_{,\Psi} - \phi} - \frac{\phi_{,\Psi\Psi} + r_{,\Psi}}{(r + \phi_{,\Psi})^2} + \frac{\cot \Psi}{r + \phi_{,\Psi}} - \frac{\cot \Psi}{r + \cot \Psi \phi} \end{bmatrix}, \\
\nabla [\det \nabla \mathbf{x}] &= \begin{bmatrix} \frac{(Rr_{,RR} - 2r_{,R})(r + \cot \Psi \phi)(r + \phi_{,\Psi}) + Rr_{,R}^2(2r + \phi_{,\Psi} + \cot \Psi \phi)}{R^3} \\ 0 \\ \frac{r_{,R\Psi}(r + \cot \Psi \phi)(r + \phi_{,\Psi}) + r_{,R} \left[\left(r_{,\Psi} - \frac{\phi}{\sin^2 \Psi} + \cot \Psi \phi_{,\Psi} \right) (r + \phi_{,\Psi}) + (r + \cot \Psi \phi)(r_{,\Psi} + \phi_{,\Psi\Psi}) \right]}{R^3} \end{bmatrix}, \\
\nabla \left[\frac{1}{\det \nabla \mathbf{x}} \right] &= \begin{bmatrix} -R \frac{(Rr_{,RR} - 2r_{,R})(r + \cot \Psi \phi)(r + \phi_{,\Psi}) + Rr_{,R}^2(2r + \phi_{,\Psi} + \cot \Psi \phi)}{r_{,R}^2(r + \cot \Psi \phi)^2(r + \phi_{,\Psi})^2} \\ 0 \\ -R \frac{r_{,R\Psi}(r + \cot \Psi \phi)(r + \phi_{,\Psi}) + r_{,R} \left[\left(r_{,\Psi} - \frac{\phi}{\sin^2 \Psi} + \cot \Psi \phi_{,\Psi} \right) (r + \phi_{,\Psi}) + (r + \cot \Psi \phi)(r_{,\Psi} + \phi_{,\Psi\Psi}) \right]}{r_{,R}^2(r + \cot \Psi \phi)^2(r + \phi_{,\Psi})^2} \end{bmatrix}, \\
\nabla \left[\det \nabla \mathbf{x} \ln \left(1 - \frac{\phi_0}{\det \nabla \mathbf{x}} \right) \right] &= \nabla (\det \nabla \mathbf{x}) \left(\frac{\phi_0}{\det \nabla \mathbf{x} - \phi_0} + \ln \frac{\det \nabla \mathbf{x} - \phi_0}{\det \nabla \mathbf{x}} \right).
\end{aligned}$$

A.3 Set of Parameters

The following table includes a summary of algebraic characters used to describe the most essential parameters of this work, and their definition.

n_1	# of lattice sites occupied by one monomer
n_2	# of lattice sites occupied by one solvent
n	# of monomers in a polymer chain
N_1	# of polymers in gel
N_2	# of solvent molecules in gel
$N = nn_1N_1 + n_2N_2$	# of lattice sites
v_0	volume of one lattice site
$v_1 = nn_1v_0$	volume of one polymer
$v_2 = n_2v_0$	volume of one solvent molecule
V_1	volume of the polymer
V_2	volume of the solvent
$V = V_1 + V_2$	total volume of the mixture
ϕ_0	volume fraction of polymer in the reference configuration
$\phi_1 = \frac{V_1}{V_1+V_2}$	volume fraction of polymer in the deformed configuration
$\phi_2 = 1 - \phi_1 = \frac{V_2}{V_1+V_2}$	volume fraction of fluid in the deformed configuration
T	temperature of the gel
Δw	change in the energy per monomer-solvent interaction
$\chi = \frac{\Delta w}{2k_B T}$	Flory interaction parameter
ν	# of crosslink density in the reference configuration
$\mu = \frac{k_B T}{v_0} \nu$	elastic stiffness modulus

Table A.1: List of Essential Parameters in Thesis

We also note that the Boltzmann constant is $k_B = 1.3806488 \times 10^{-23} \frac{\text{m}^2 \text{kg}}{\text{s}^2 \text{K}}$.